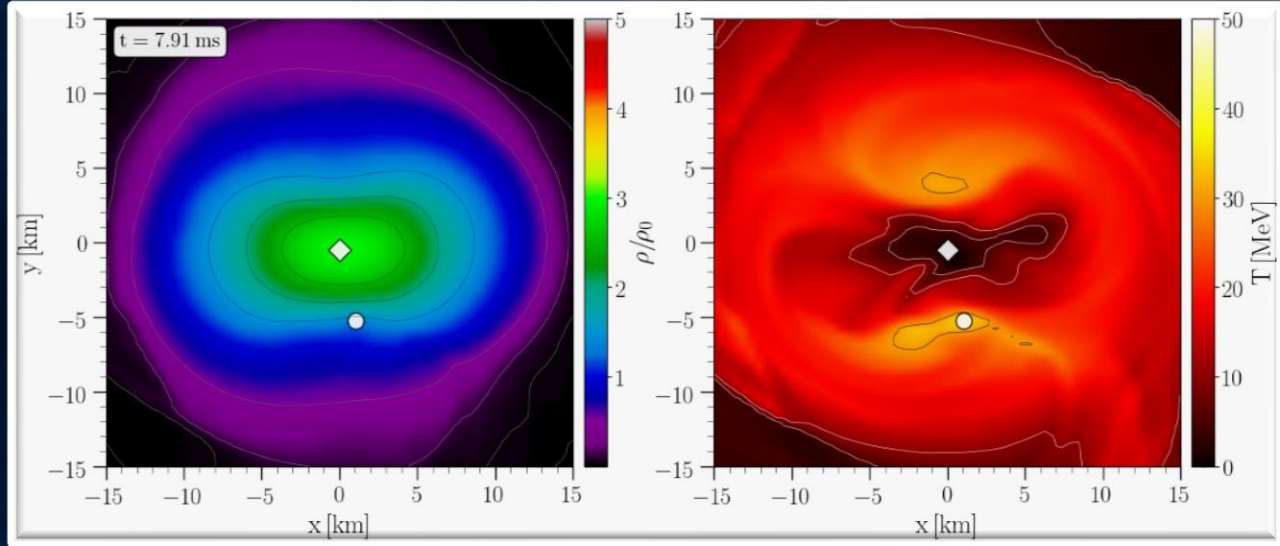


# Hypermassive Hybrid Stars

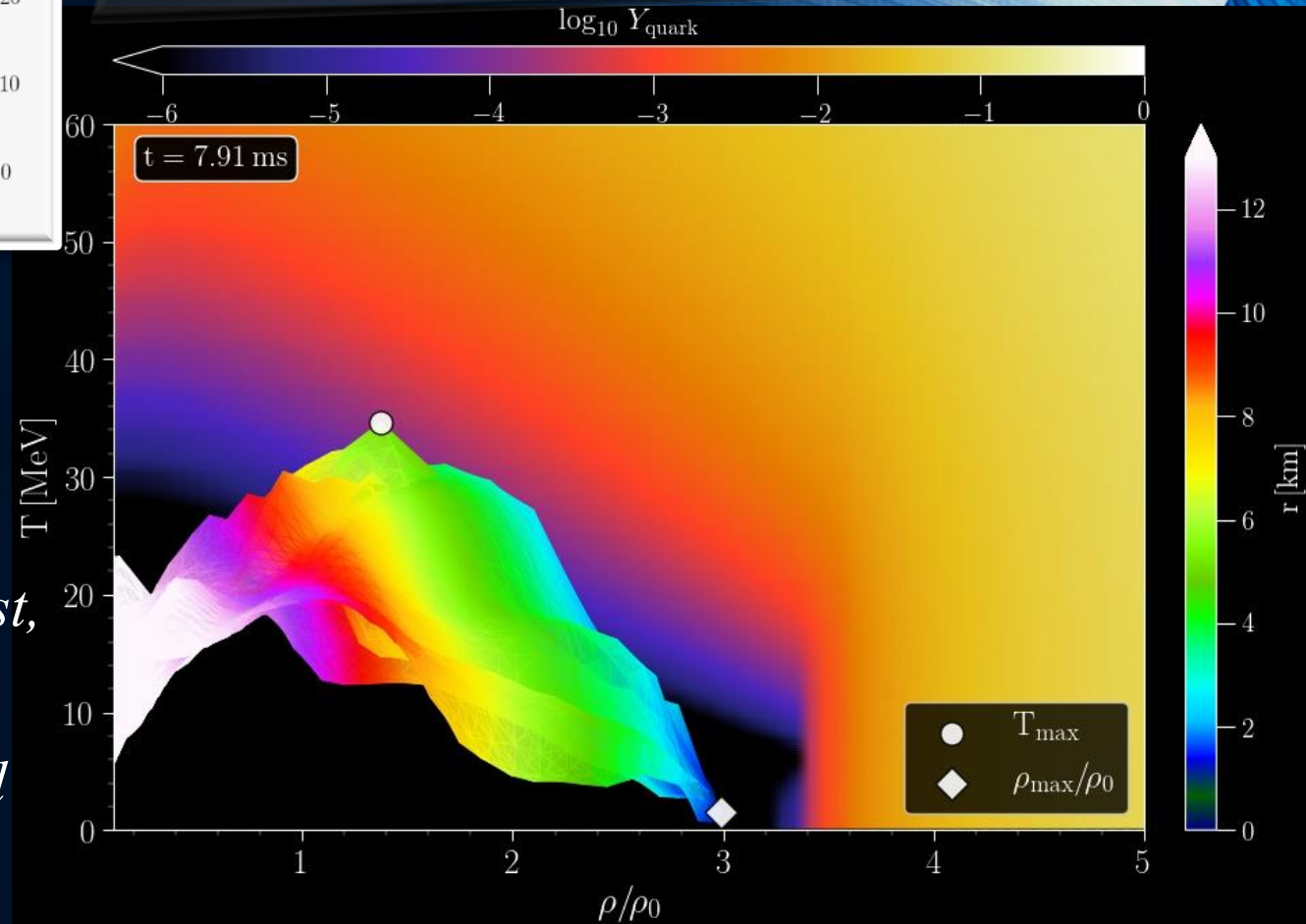
30TH TEXAS SYMPOSIUM  
PORTSMOUTH, 16 DEZEMBER 2019

within  
the  
Phase Diagram of  
Quantum Chromodynamics



MATTHIAS HANAUSKE  
FRANKFURT INSTITUTE FOR ADVANCED STUDIES  
JOHANN WOLFGANG GOETHE UNIVERSITÄT  
INSTITUT FÜR THEORETISCHE PHYSIK  
ARBEITSGRUPPE RELATIVISTISCHE ASTROPHYSIK  
D-60438 FRANKFURT AM MAIN

In collaboration with Luke Bovard, Elias R. Most,  
L. Jens Papenfort, Jan Steinheimer, Veronica  
Dexheimer, Stefan Schramm, Horst Stöcker and  
Luciano Rezzolla



# The Einstein Equation and the EOS of Compact Stars

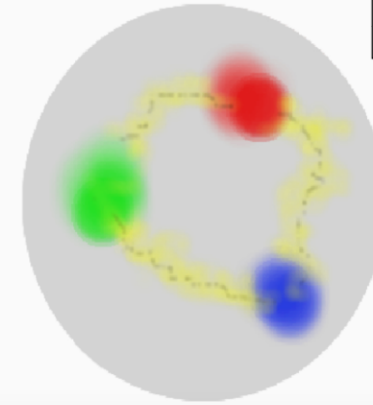
ART	<u>Yang-Mills-Theories</u>
$D_\beta v^\alpha = \partial_\beta v^\alpha + \Gamma_{\sigma\beta}^\alpha v^\sigma$	$D_{\beta a}{}^b = \partial_\beta 1_a{}^b + ig A_{\beta a}{}^b$
$R^\delta{}_{\mu\alpha\beta} v^\mu = [D_\alpha, D_\beta] v^\delta$	$F_{\alpha\beta a}{}^b = \frac{1}{ig} [D_{\alpha a}{}^c, D_{\beta c}{}^b]$
$R^\delta{}_{\mu\alpha\beta} = \Gamma_{\mu\alpha \beta}^\delta - \Gamma_{\mu\beta \alpha}^\delta$ $+ \Gamma_{\nu\beta}^\delta \Gamma_{\mu\alpha}^\nu + \Gamma_{\nu\alpha}^\delta \Gamma_{\mu\beta}^\nu$	$= A_{\beta a}{}^b _\alpha - A_{\alpha a}{}^b _\beta$ $+ \frac{1}{ig} [A_{\alpha a}{}^c, A_{\beta c}{}^b]$
$\mathcal{L}_G = R + \underbrace{(c_1 R_{\mu\nu} R^{\mu\nu} + \dots)}_{\equiv 0 \text{ for ART}}$	$\mathcal{L}_{YM} = \frac{1}{4} F_{\mu\nu a}{}^b F^{\mu\nu}{}_a{}^b$

Quantum ChromoDynamic:

( $SU(3)_{(c)}$ - Color Yang-Mills-Gauge Theory)

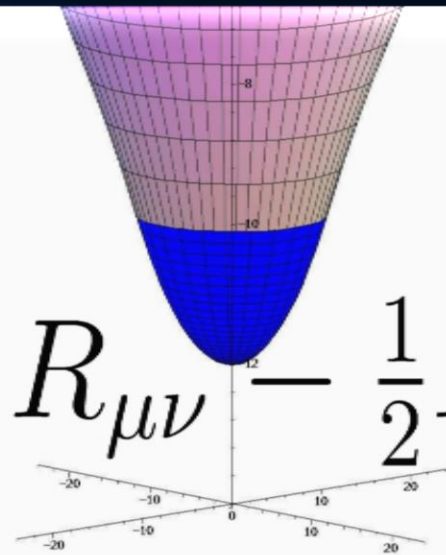
$$D_{\beta A}{}^B = \partial_\beta 1_A{}^B + ig G_{\beta A}{}^B$$

$A, B = \text{red, green, blue}$



$$\psi_A^f = \begin{pmatrix} \psi_r^f \\ \psi_g^f \\ \psi_b^f \end{pmatrix}$$

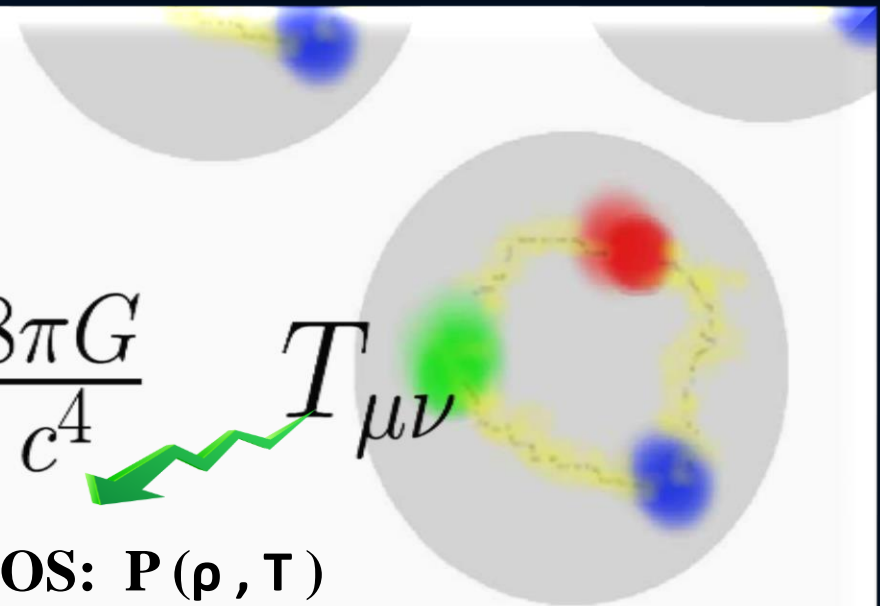
Confinement  
chiral symmetry, ...



$$R_{\mu\nu} - \frac{1}{2} R g_{\mu\nu} =$$

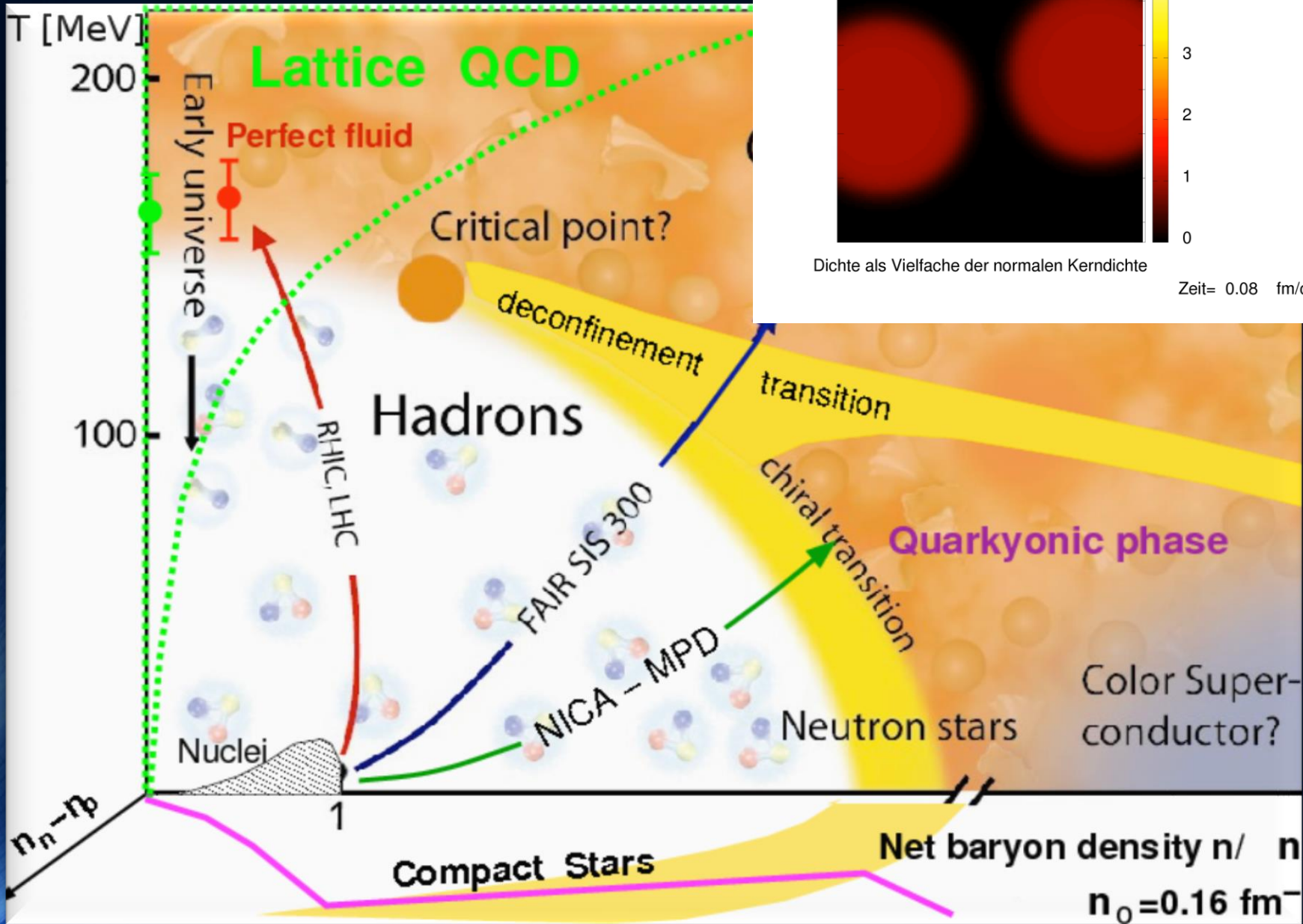
$$\frac{8\pi G}{c^4} T_{\mu\nu}$$

EOS:  $P(\rho, T)$

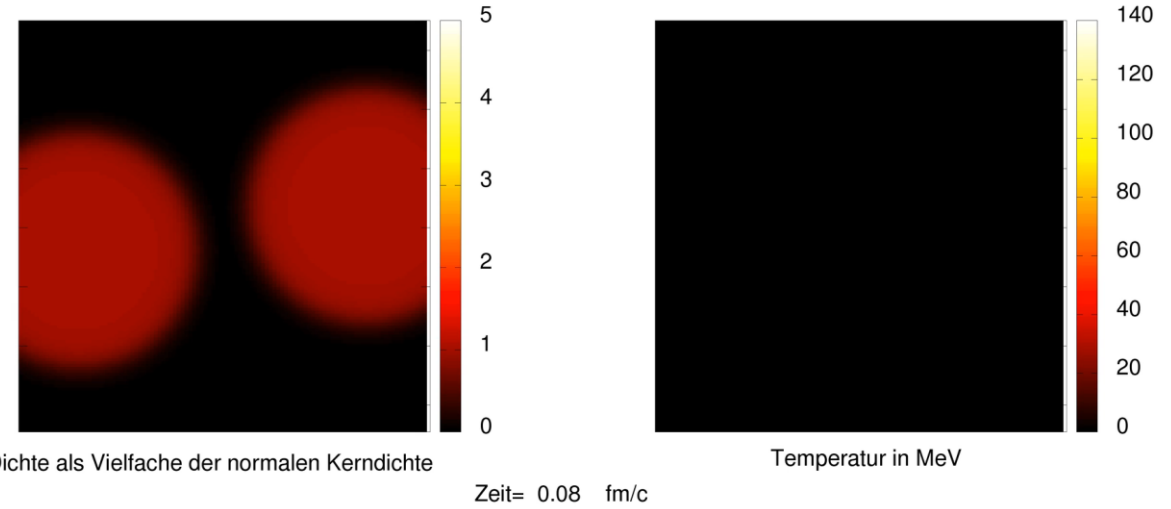


# The Hadron-Quark Phase Transition

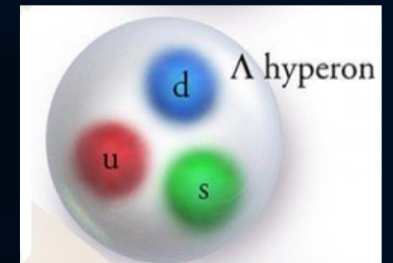
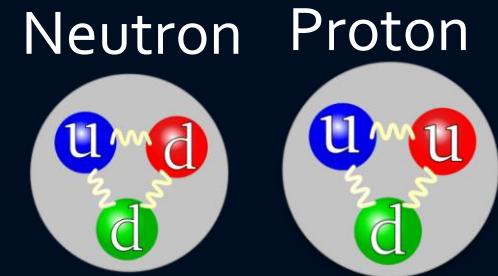
The QCD Phase Diagram



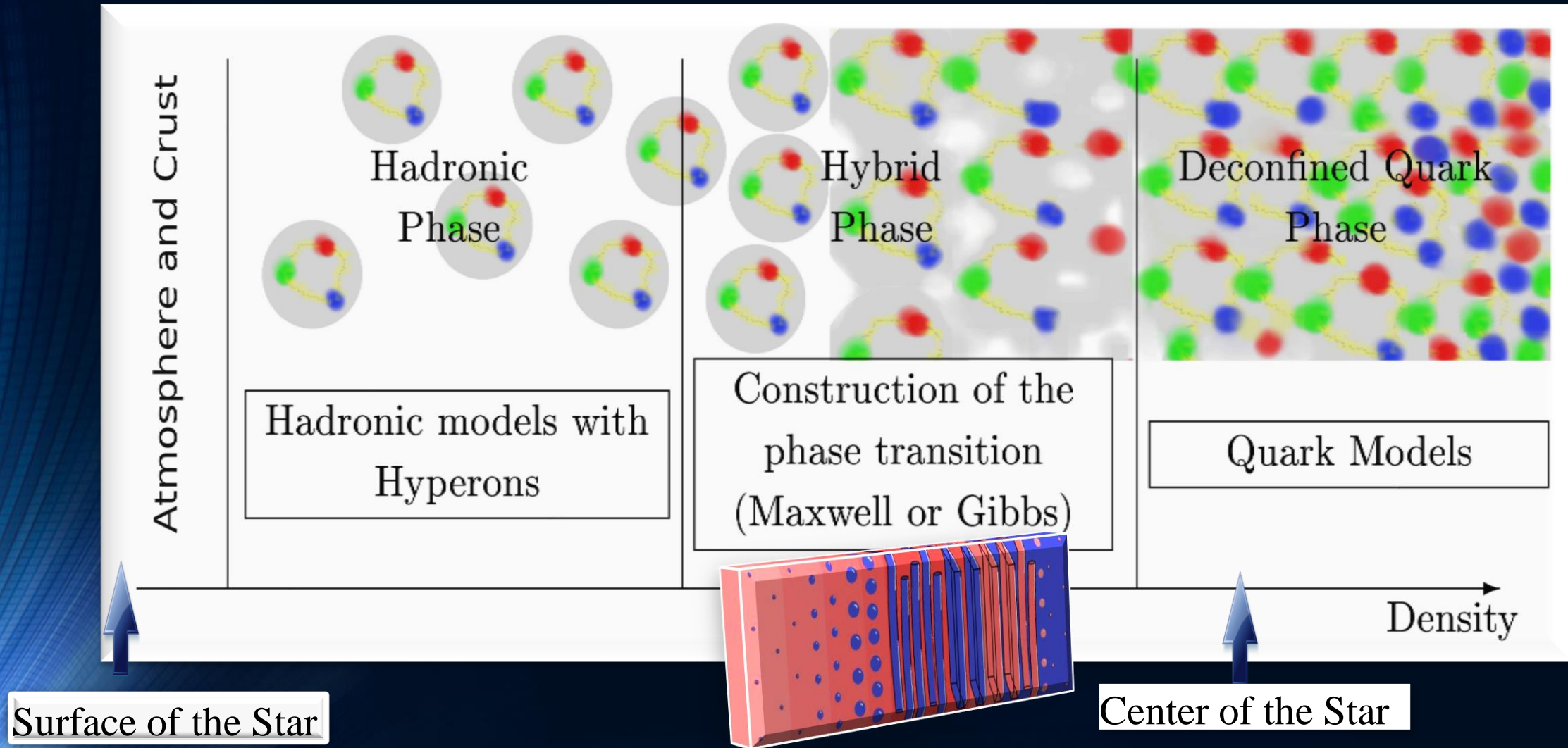
Gold+Gold Kollision am GSI: Helmholtz Zentrum für Schwerionenforschung / HADES Experiment  
Am FAIR Beschleuniger: noch höhere Strahlintensität



Credits:  
Jan Steinheimer



# The QCD – Phase Transition and the Interior of a Hybrid Star

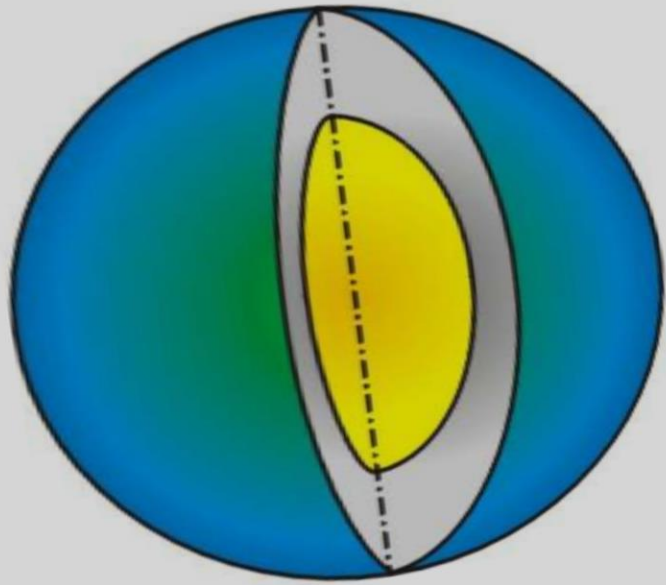


*Matthias Hanauske; Doctoral Thesis:*

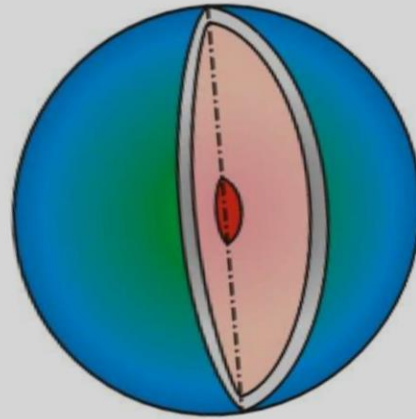
*Properties of Compact Stars within QCD-motivated Models; University Library Publication Frankfurt (2004)*

# Neutron Stars, Hybrid Stars, Quark Stars and Black Holes

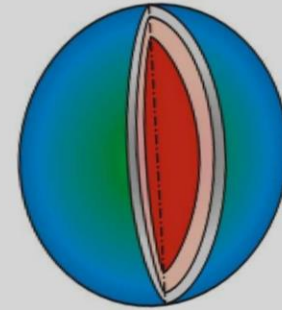
Neutron Stars



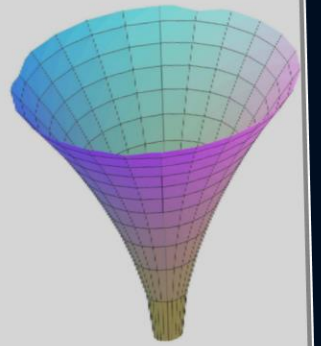
Hybrid Stars



Quark Stars



Black Holes



$\rho_c = \rho_0$   
Central density  $\rho_c$  in the star  
( $\rho_0 := 0.15/\text{fm}^3$ )

$\approx 2 \rho_0$

$\approx 5 \rho_0$

...  $\infty$

# Numerical Relativity and Relativistic Hydrodynamics of Binary Neutron Star Mergers

Einstein's theory of general relativity and the resulting general relativistic conservation laws for energy-momentum in connection with the rest-mass conservation are the theoretical groundings of neutron star binary mergers:

$$R_{\mu\nu} - \frac{1}{2}g_{\mu\nu}R = 8\pi T_{\mu\nu}$$

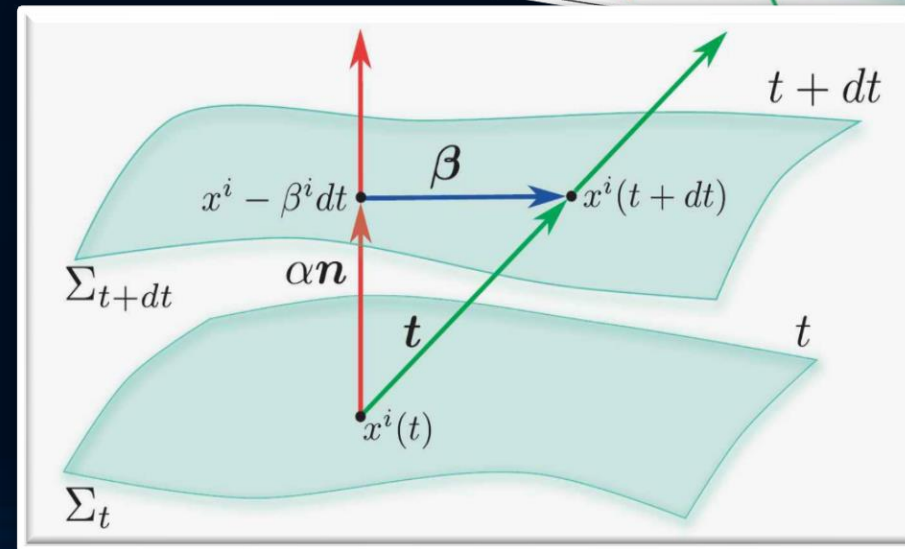
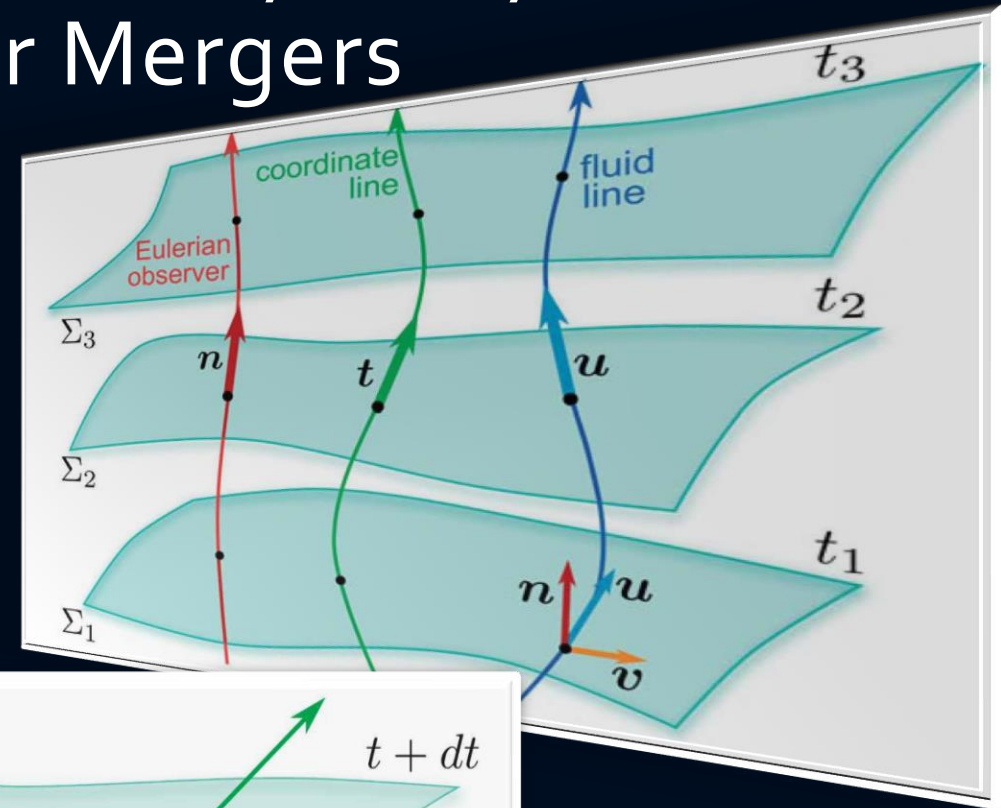
$$\begin{aligned}\nabla_{\mu}(\rho u^{\mu}) &= 0, \\ \nabla_{\nu}T^{\mu\nu} &= 0.\end{aligned}$$

(3+1) decomposition of spacetime

$$g_{\mu\nu} = \begin{pmatrix} -\alpha^2 + \beta_i\beta^i & \beta_i \\ \beta_i & \gamma_{ij} \end{pmatrix}$$

$$d\tau^2 = \alpha^2(t, x^j)dt^2$$

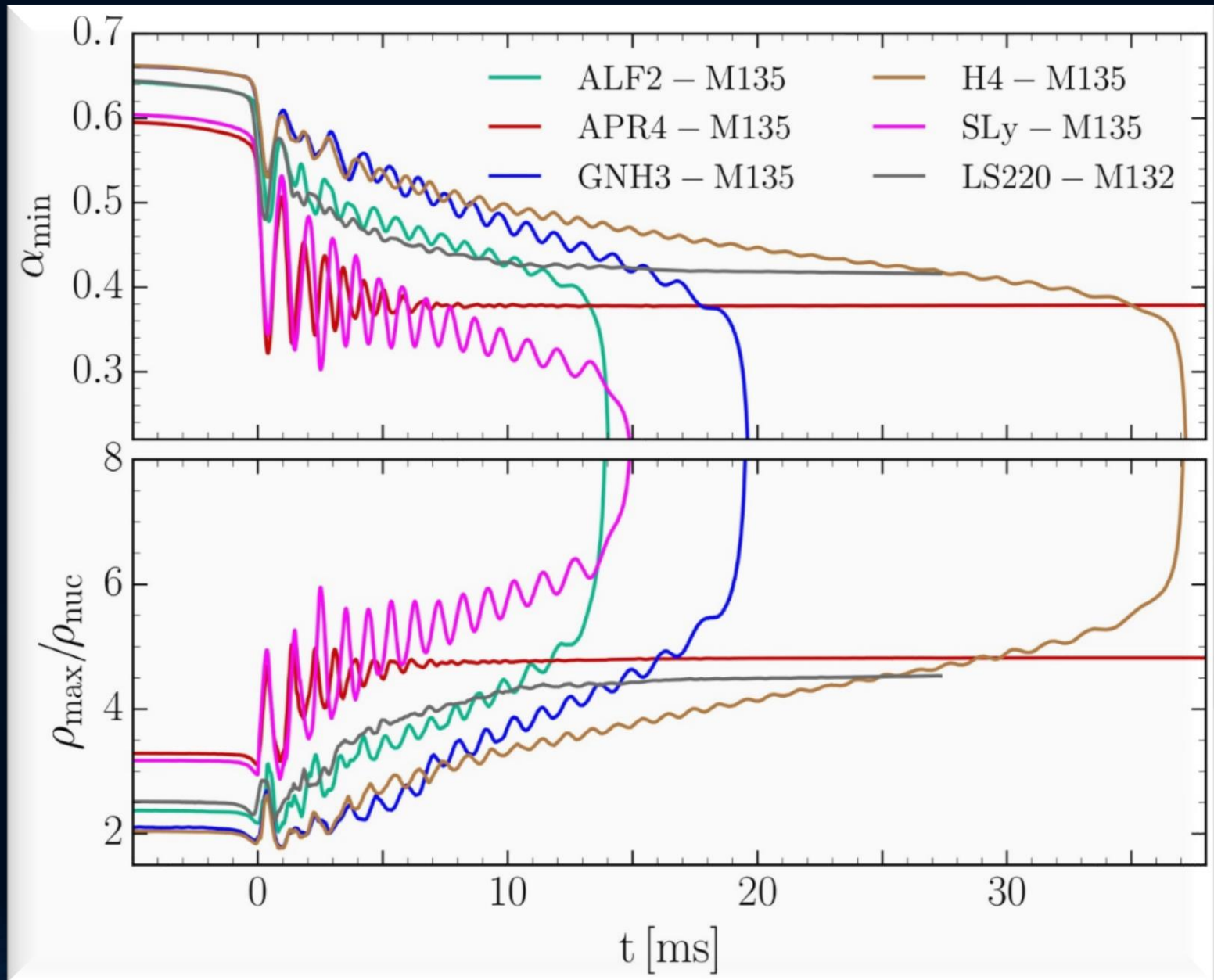
$$x^i_{t+dt} = x^i_t - \beta^i(t, x^j)dt$$



# Binary Merger of two Neutron Stars for different EoSs

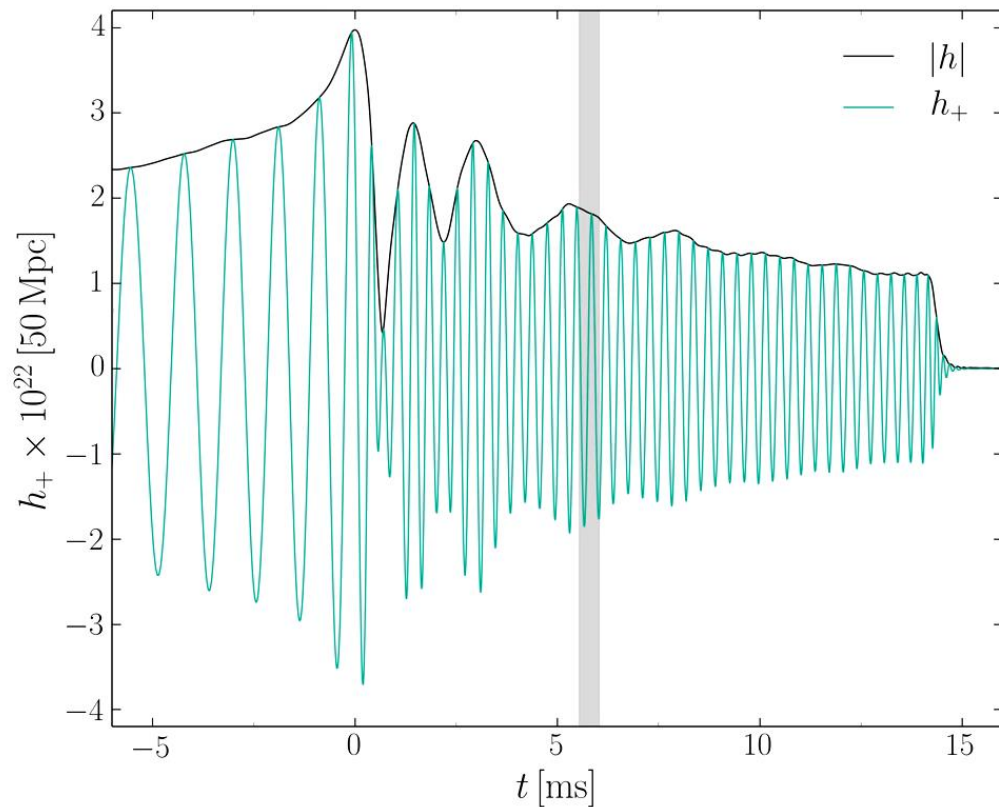
High mass simulations  
( $M=1.35 M_{\text{solar}}$ )

Central value of the lapse function  $\alpha_c$  (upper panel) and maximum of the rest mass density  $\rho_{\text{max}}$  in units of  $\rho_0$  (lower panel) versus time for the high mass simulations.

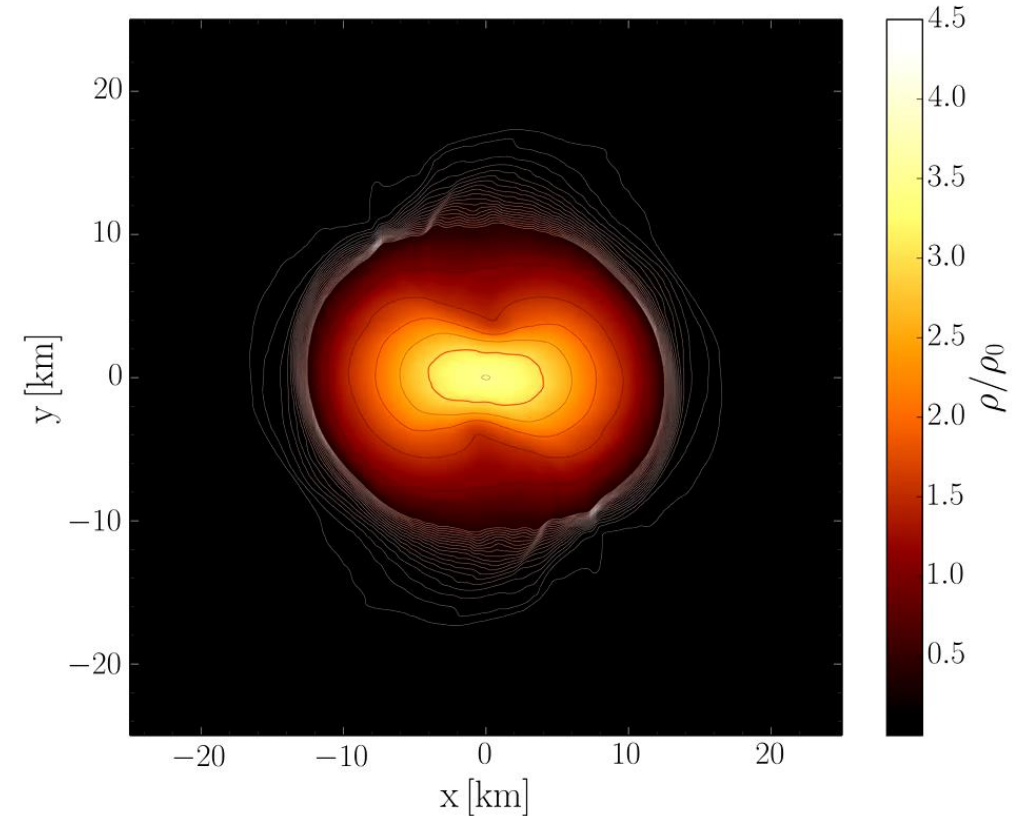


# Evolution of the density in the post merger phase

ALF2-EOS: Mixed phase region starts at  $3\rho_0$  (see red curve), initial NS mass:  $1.35 M_{\text{solar}}$



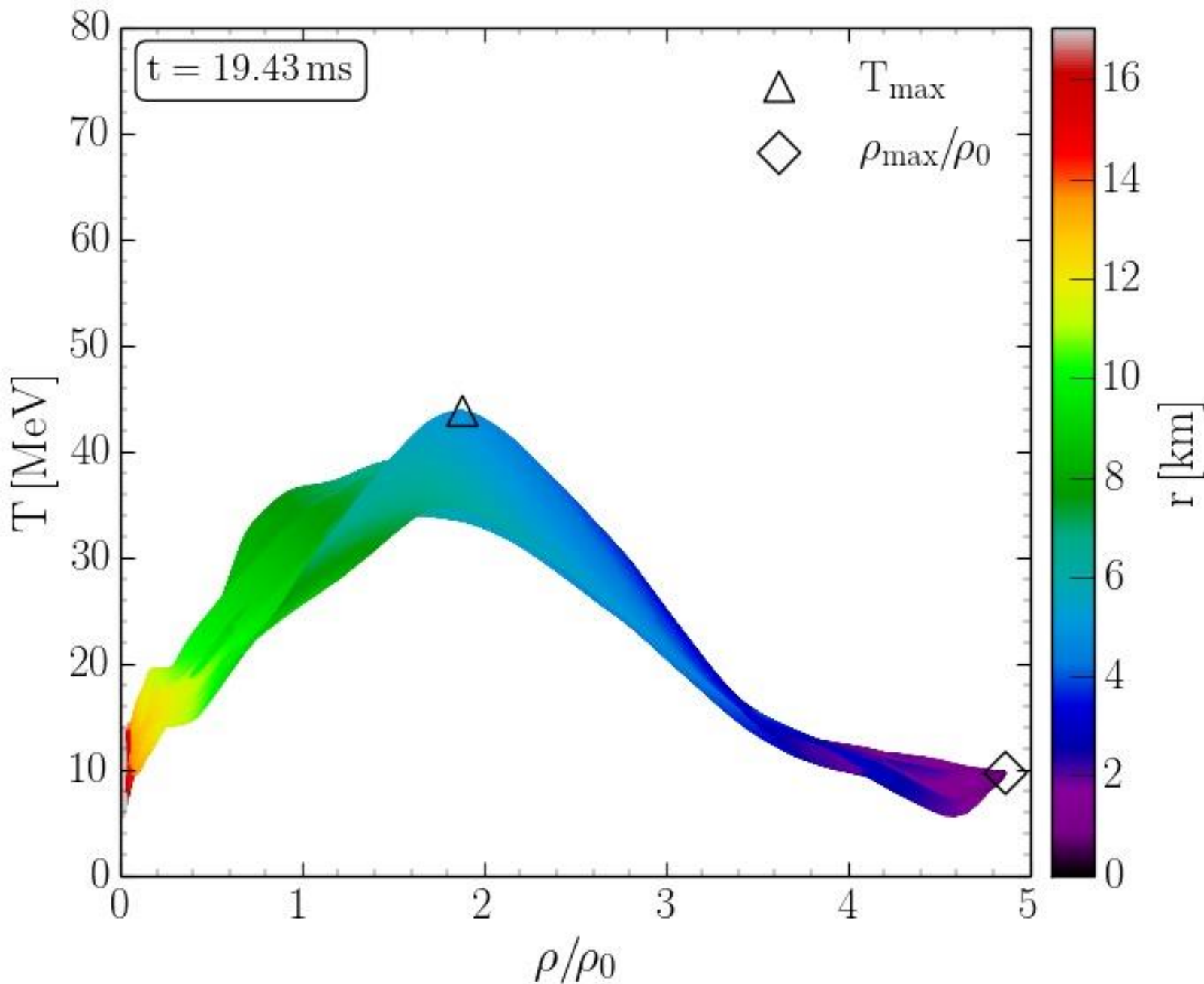
Gravitational wave amplitude  
at a distance of 50 Mpc



Rest mass density distribution  $\rho(x,y)$   
in the equatorial plane  
in units of the nuclear matter density  $\rho_0$



# Hypermassive Neutron Stars in the QCD Phase Diagram

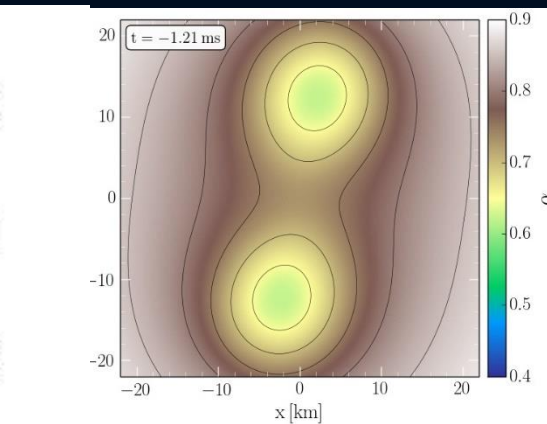
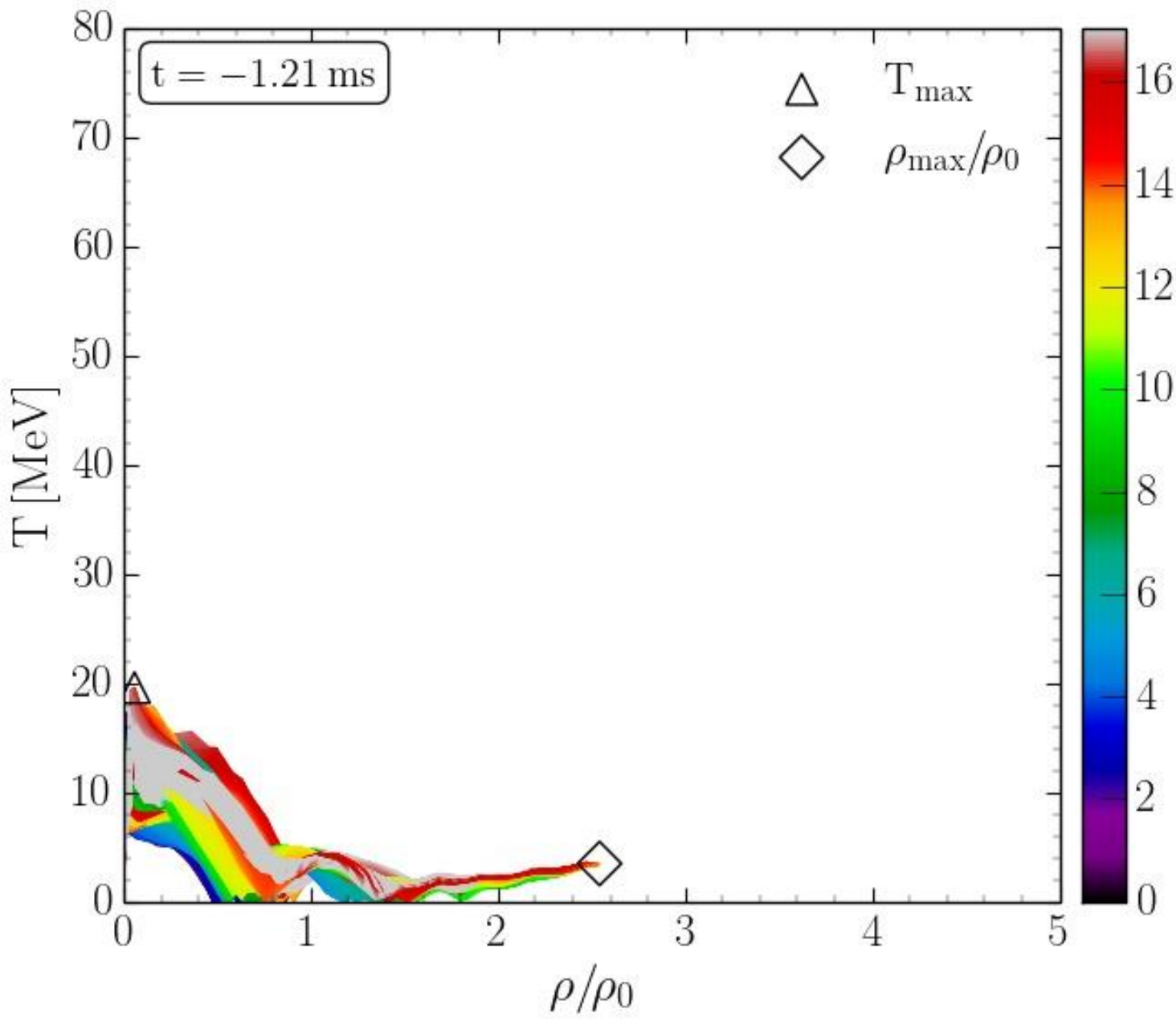


Density-temperature profiles inside the inner area of a hypermassive neutron star simulated within the LS220 EOS with a total mass of  $M_{\text{total}}=2.7 M_{\text{solar}}$  in the style of a  $(T-\rho)$  QCD phase diagram plot at  $t=19.43$  ms after the merger.

The color-coding indicates the radial position  $r$  of the corresponding  $(T-\rho)$  fluid element measured from the origin of the simulation  $(x, y) = (0, 0)$  on the equatorial plane at  $z = 0$ .

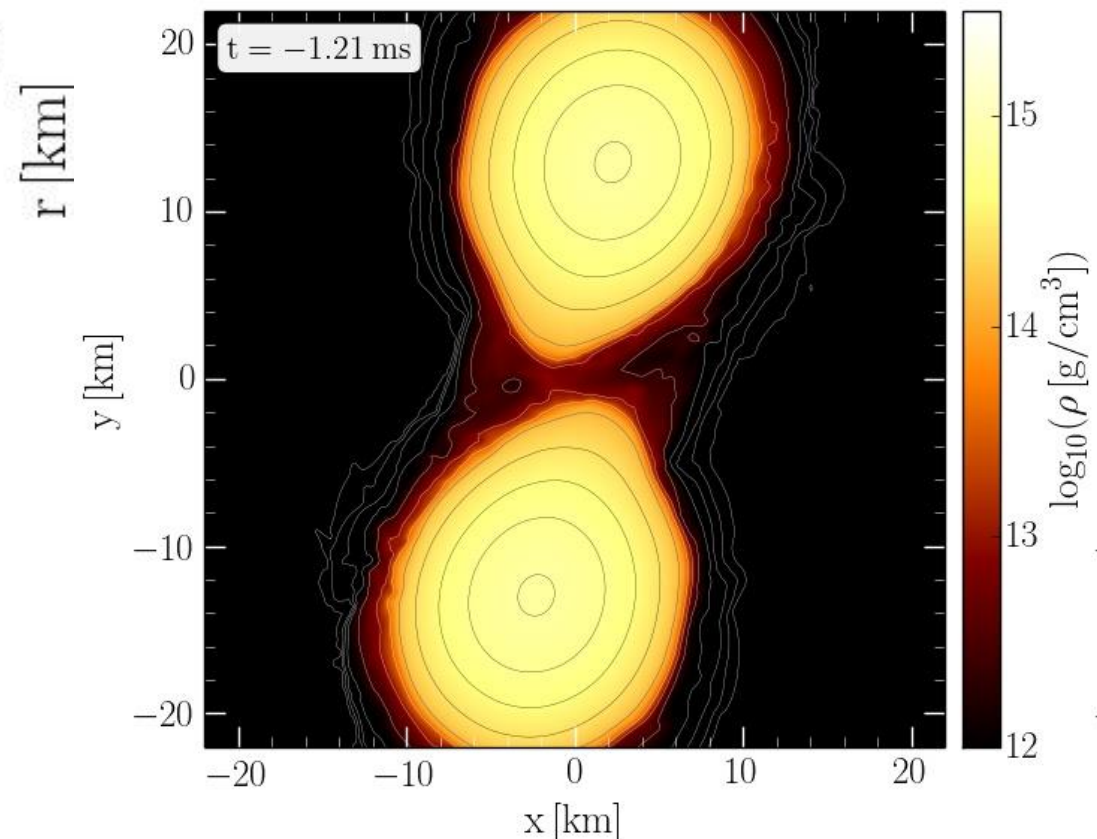
The open triangle marks the maximum value of the temperature while the open diamond indicates the maximum of the density.

# QCD Phase Diagram: The Late Inspiral Phase

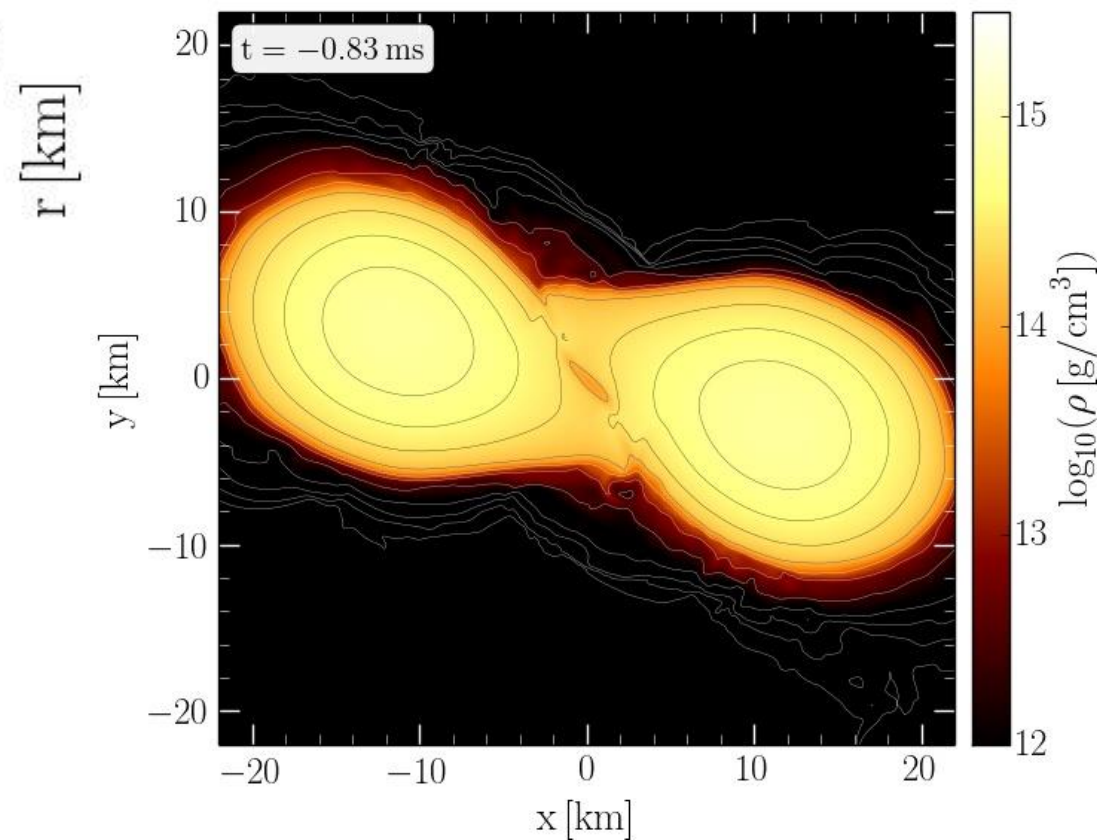
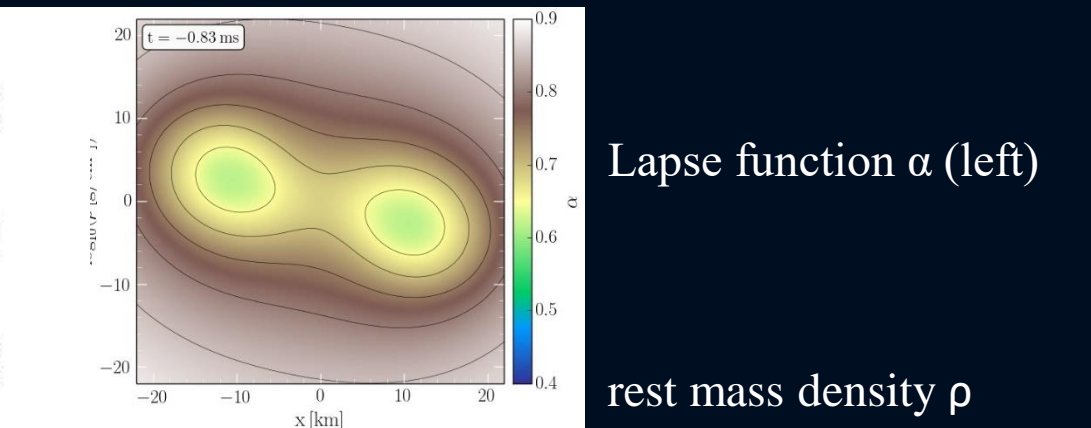
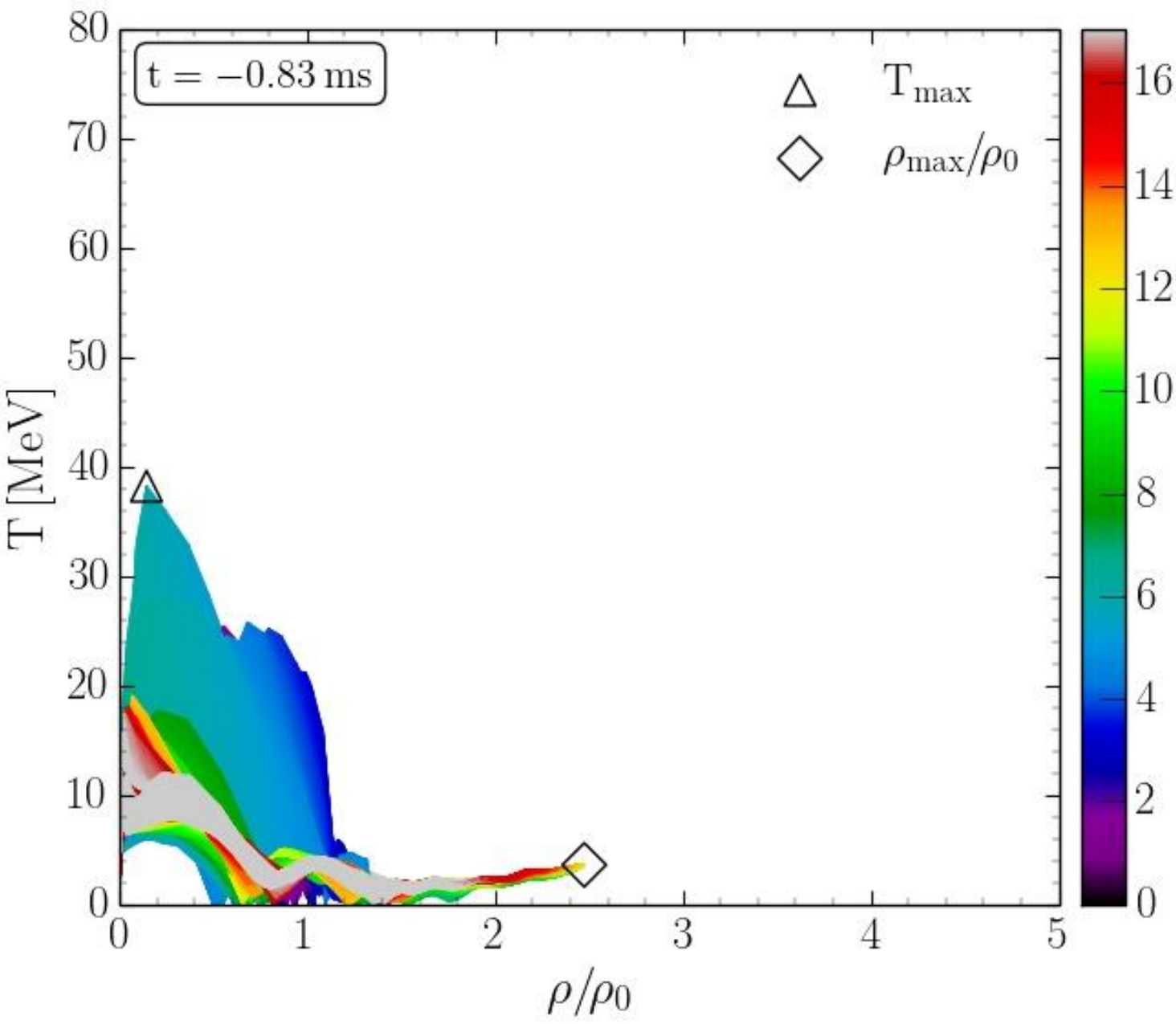


Lapse function  $\alpha$  (left)

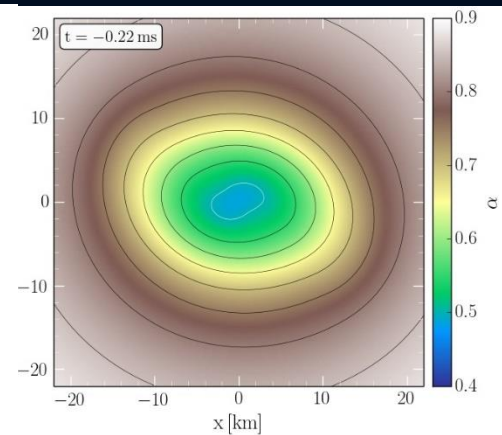
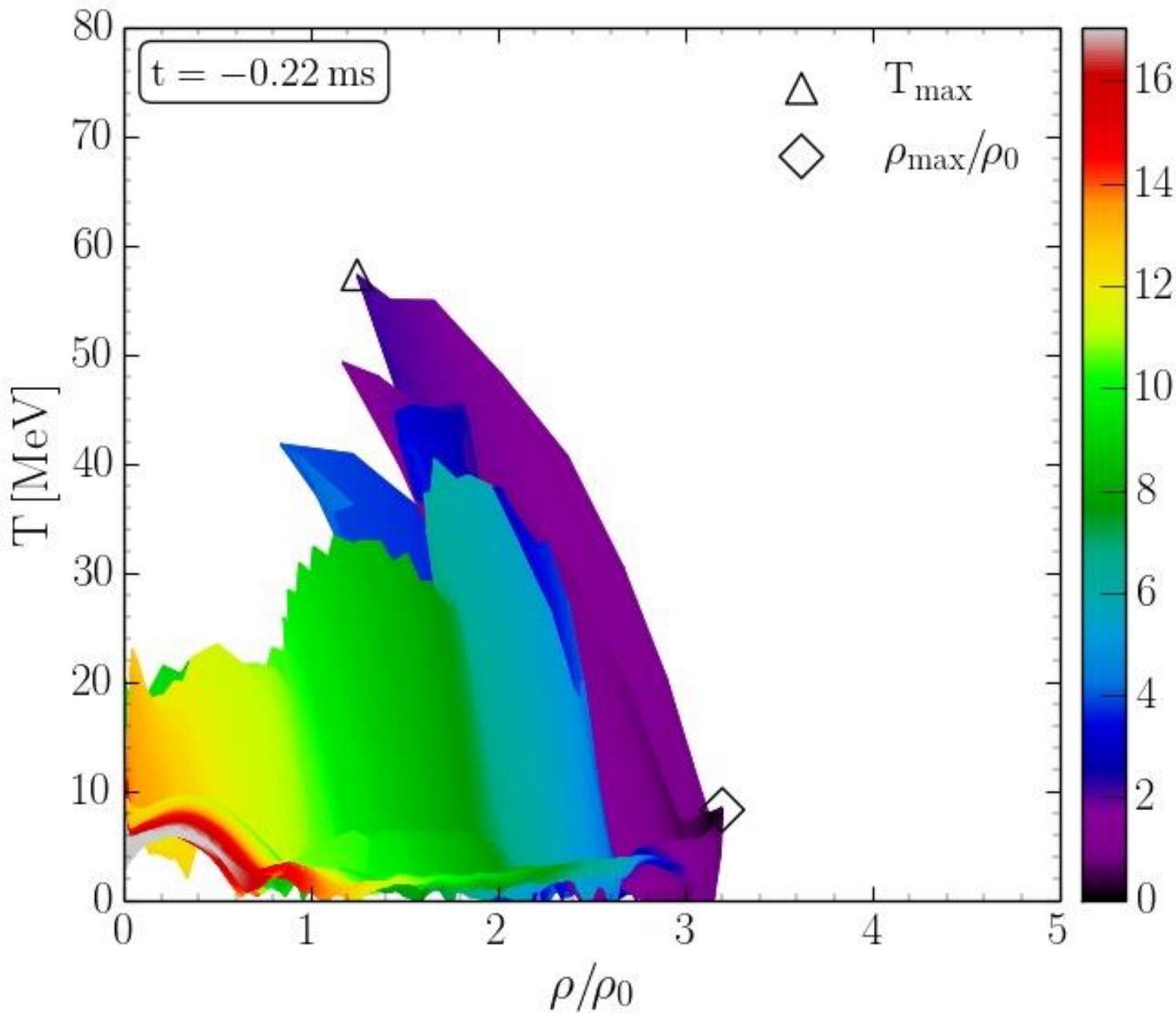
rest mass density  $\rho$



# QCD Phase Diagram: The Late Inspiral Phase

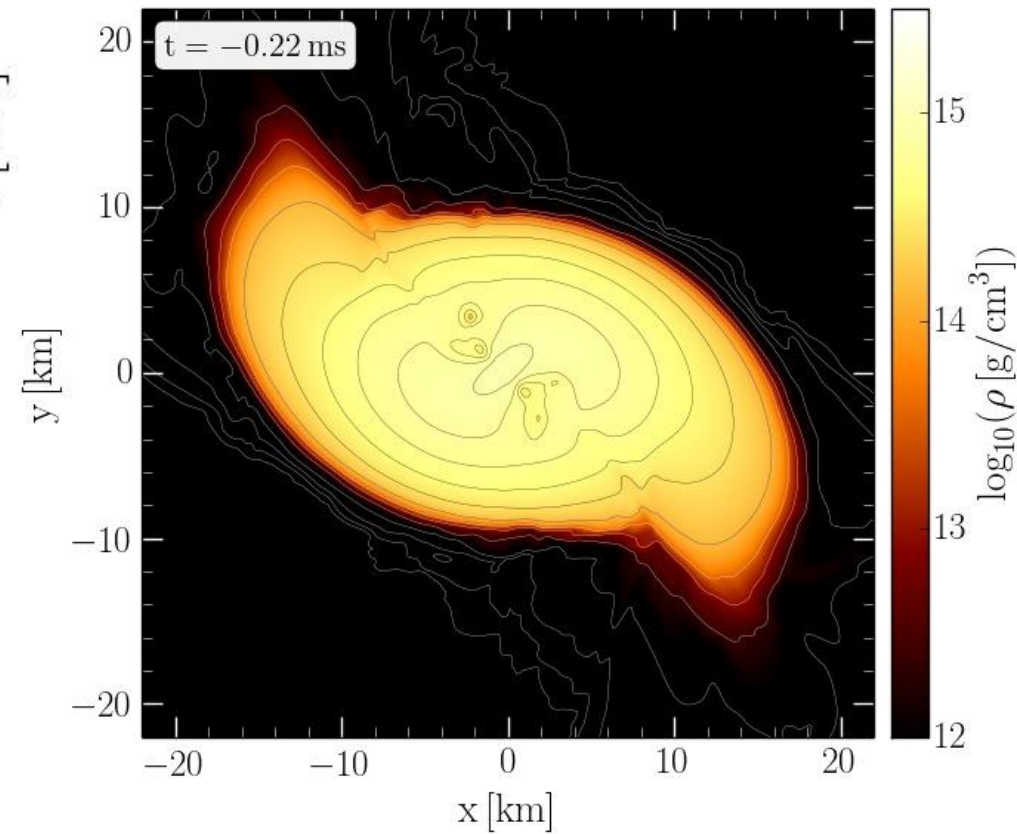


# QCD Phase Diagram: The Late Inspiral Phase

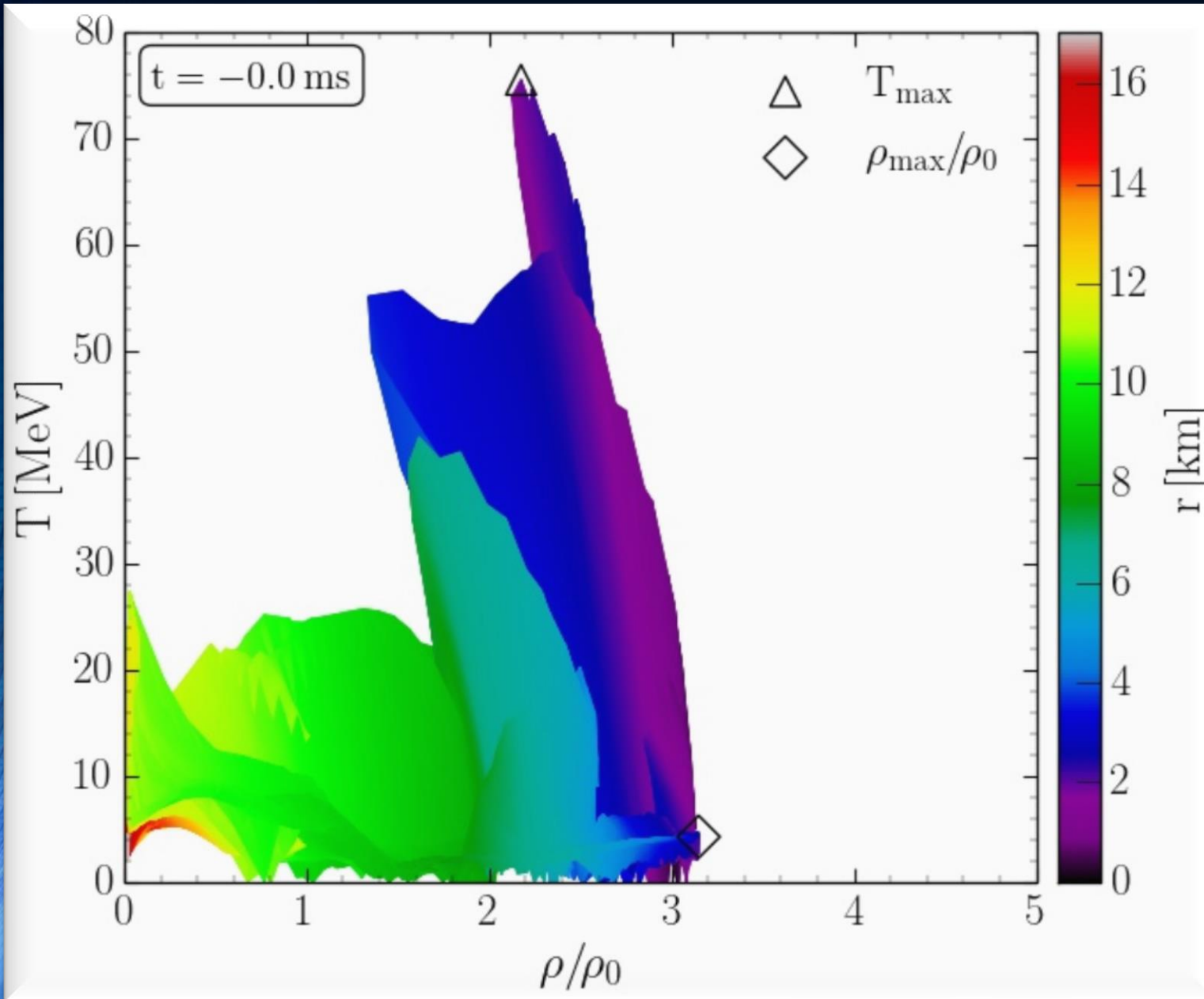


Lapse function  $\alpha$  (left)

rest mass density  $\rho$



# Binary Neutron Star Mergers in the QCD Phase Diagram

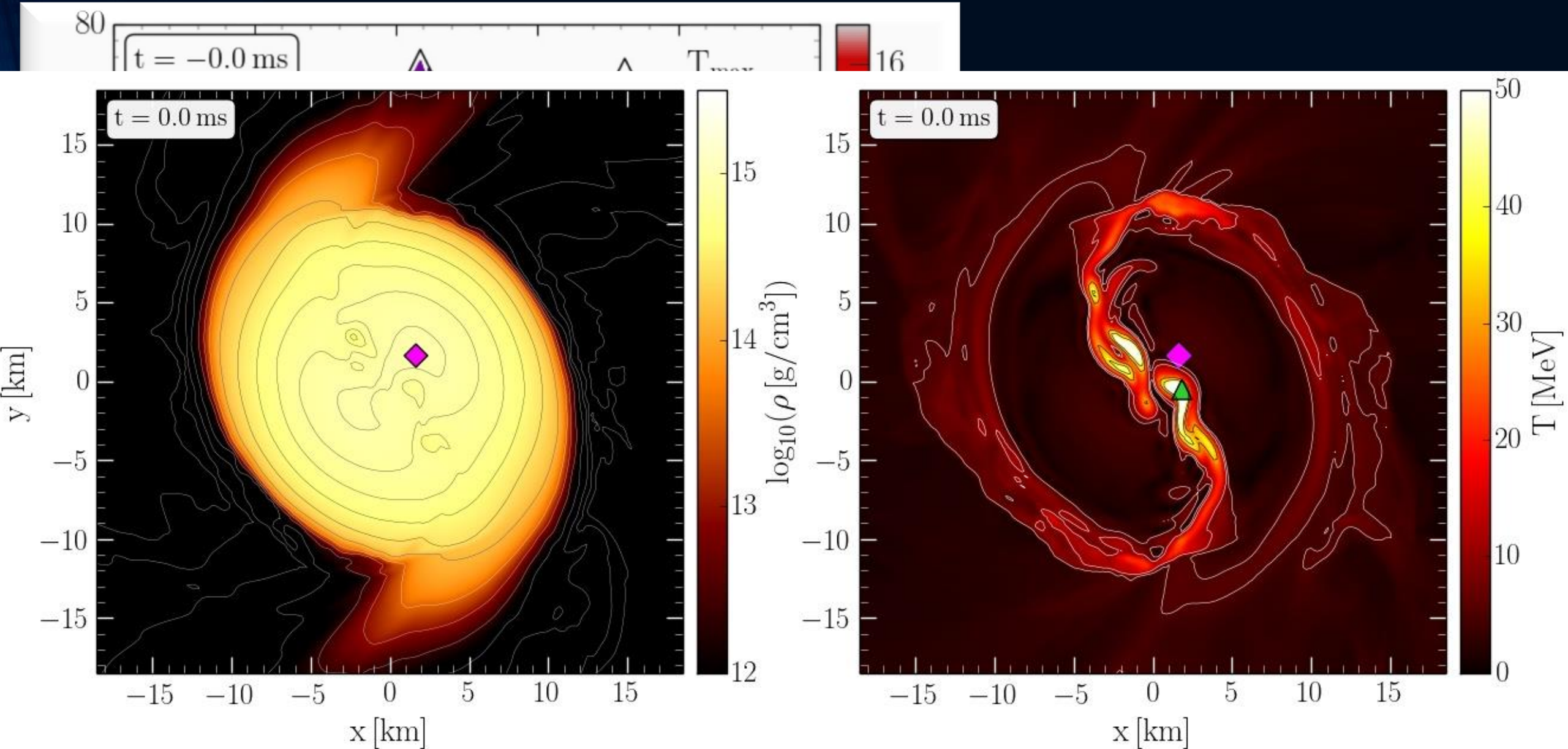


Density-temperature profiles inside the inner area of the LS220-M135 simulation in the style of a  $(T-\rho)$  QCD phase diagram plot at merger time ( $t=0$  ms).

The color-coding indicates the radial position  $r$  of the corresponding  $(T-\rho)$  fluid element measured from the origin of the simulation  $(x,y) = (0,0)$  on the equatorial plane ( $z = 0$ ).

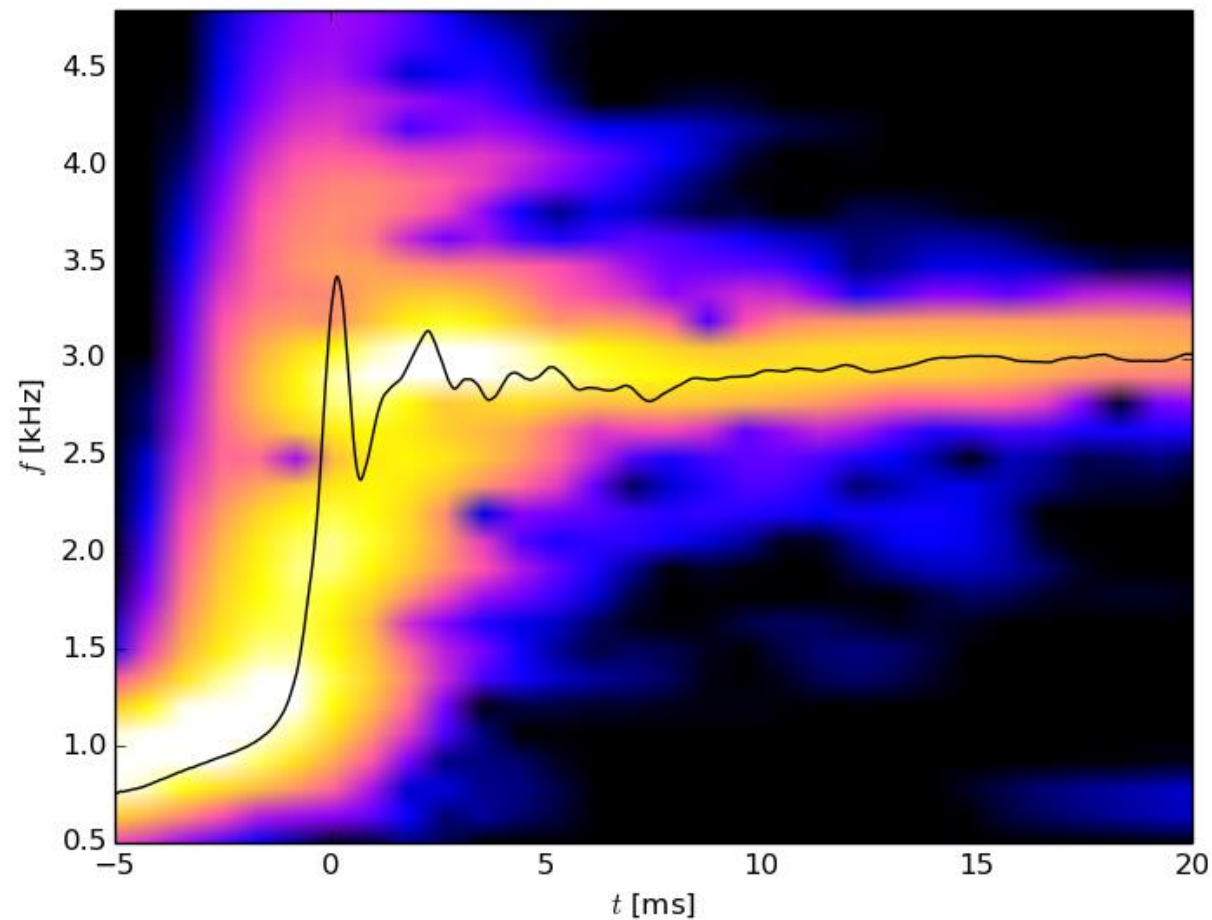
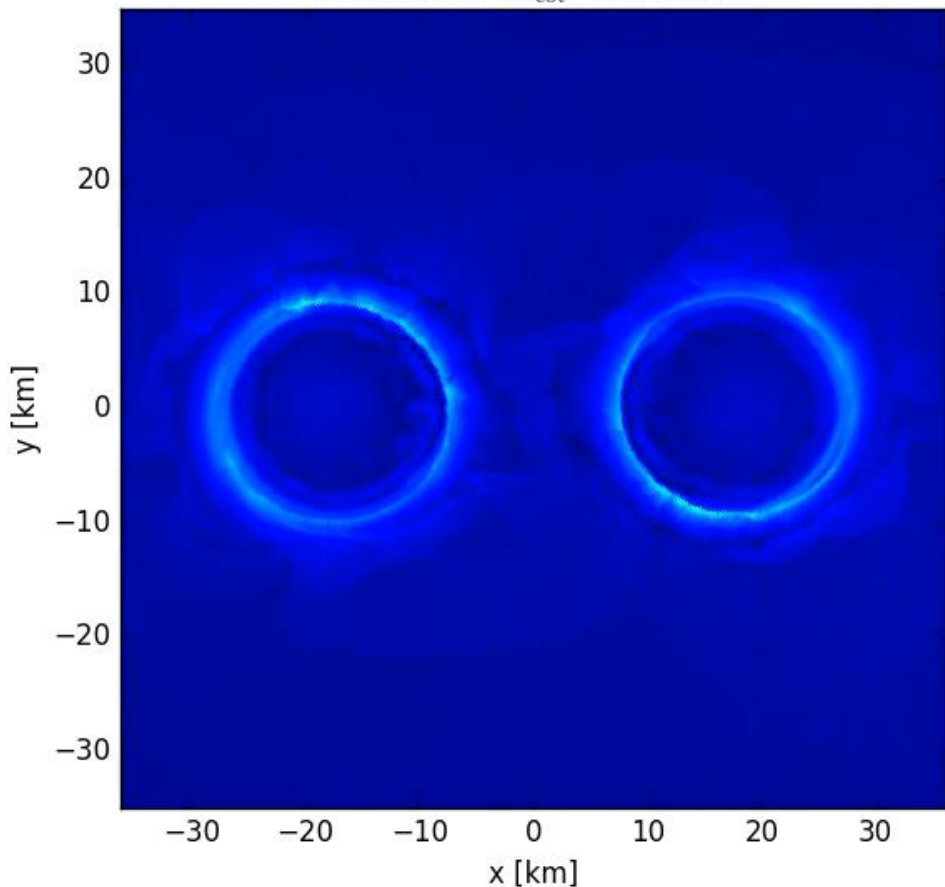
The open triangle marks the maximum value of the temperature while the open diamond indicates the maximum of the density.

# Binary Neutron Star Mergers in the QCD Phase Diagram



# The Co-Rotating Frame

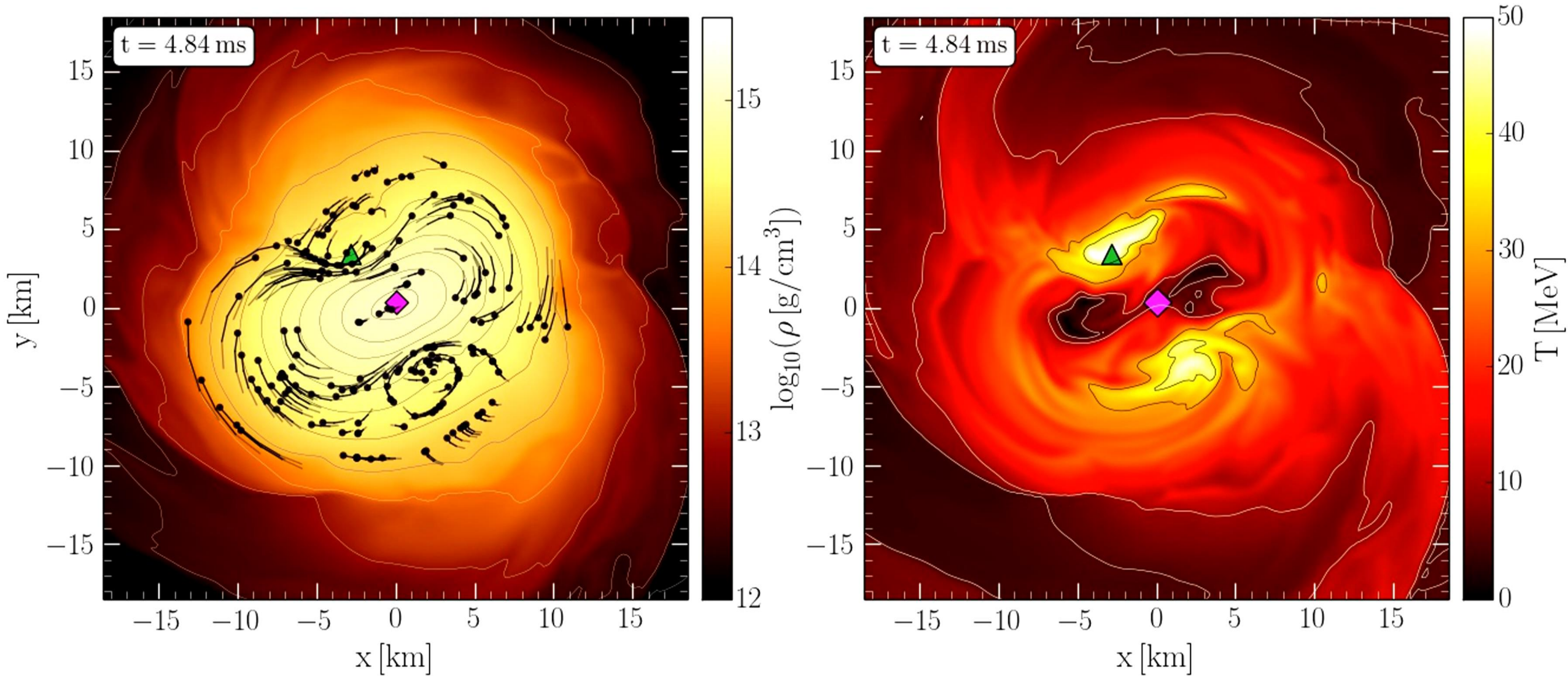
$t = 9.58\text{ms}$   $\Omega_{\text{cot}} = 387.20\text{Hz}$



- <sup>2</sup> Note that the angular-velocity distribution in the lower central panel of Fig. 10 refers to the corotating frame and that this frame is rotating at half the angular frequency of the emitted gravitational waves,  $\Omega_{\text{GW}}$ . Because the maximum of the angular velocity  $\Omega_{\text{max}}$  is of the order of  $\Omega_{\text{GW}}/2$  (cf. left panel of Fig. 12), the ring structure in this panel is approximately at zero angular velocity.

Simulation and movie has been produced by Luke Bovard

# Density and Temperature Evolution inside the HMNS

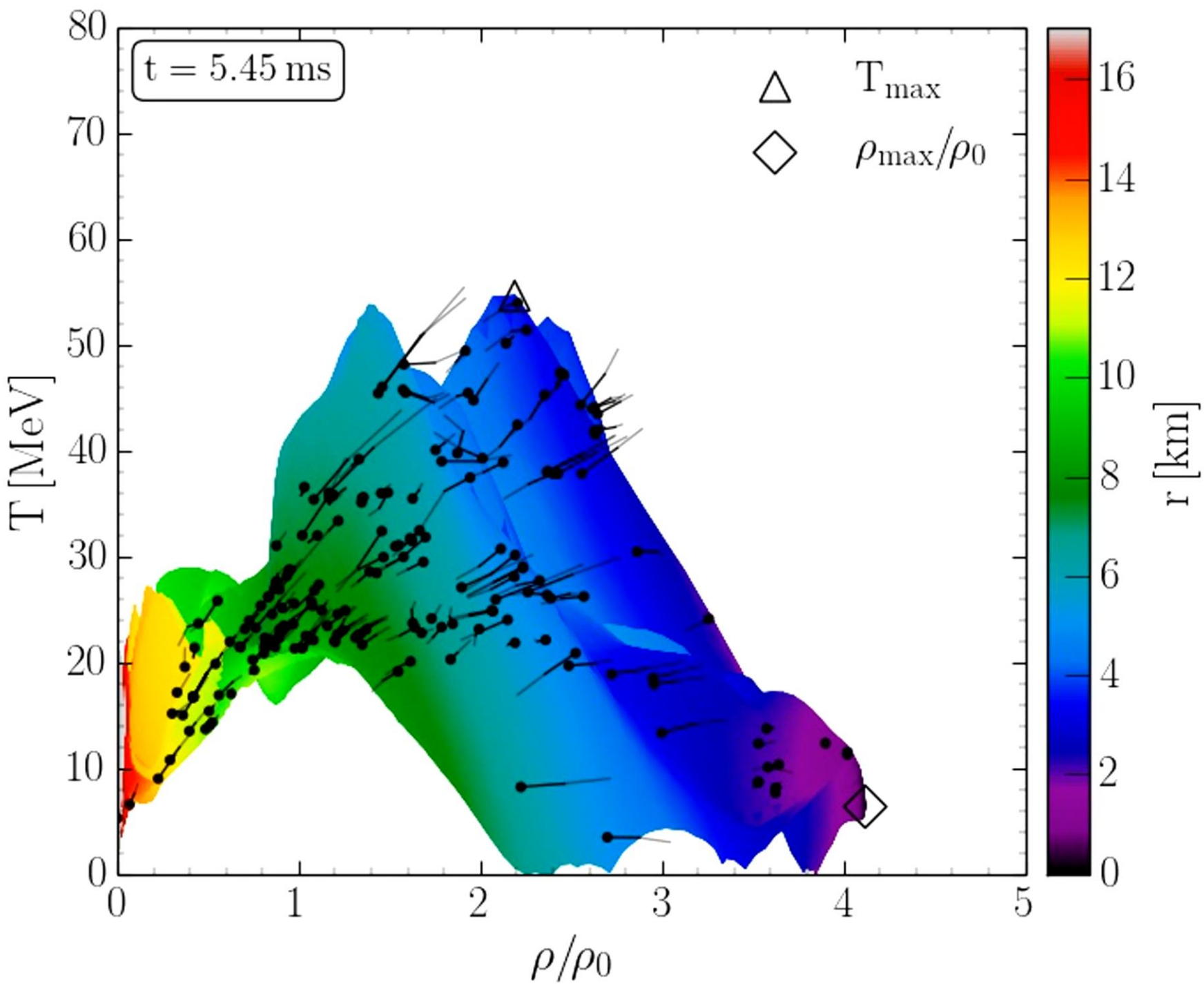


Rest mass density on the equatorial plane

Temperature on the equatorial plane



# Binary Neutron Star Mergers in the QCD Phase Diagram



Evolution of hot and dense matter inside the inner area of a hypermassive neutron star simulated within the LS220 EOS with a total mass of  $M_{\text{total}}=2.7 M_{\text{solar}}$  in the style of a  $(T-\rho)$  QCD phase diagram plot

The color-coding indicates the radial position  $r$  of the corresponding  $(T-\rho)$  fluid element measured from the origin of the simulation  $(x, y) = (0, 0)$  on the equatorial plane at  $z = 0$ .

The open triangle marks the maximum value of the temperature while the open diamond indicates the maximum of the density.

# The Angular Velocity in the (3+1)-Split

The angular velocity  $\Omega$  in the (3+1)-Split is a combination of the lapse function  $\alpha$ , the  $\phi$ -component of the shift vector  $\beta^\phi$  and the 3-velocity  $v^\phi$  of the fluid (spatial projection of the 4-velocity  $\mathbf{u}$ ):

**(3+1)-decomposition  
of spacetime:**

$$\Omega(x, y, z, t) = \frac{u^\phi}{u^t} = \alpha v^\phi - \beta^\phi$$

$$g_{\mu\nu} = \begin{pmatrix} -\alpha^2 + \beta_i \beta^i & \beta_i \\ \beta_i & \gamma_{ij} \end{pmatrix}$$

Angular velocity  
 $\Omega$

Lapse function  
 $\alpha$

$\Phi$ -component of  
3-velocity  $v^\phi$

Frame-dragging  
 $\beta^\phi$

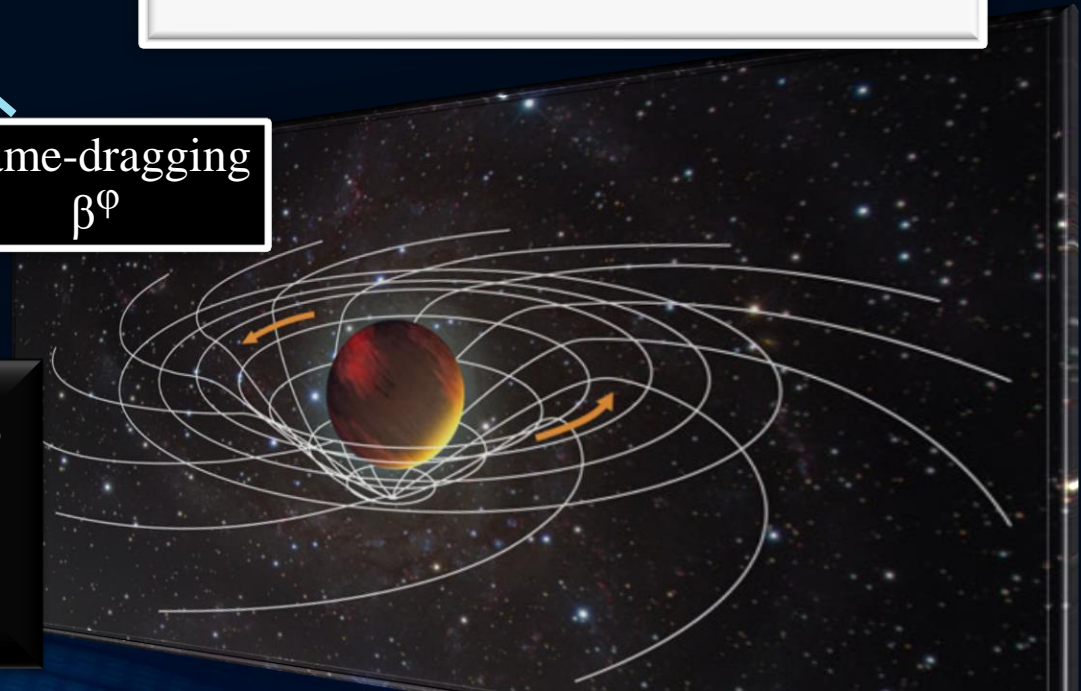
**Focus: Inner core of the differentially rotating HMNS**

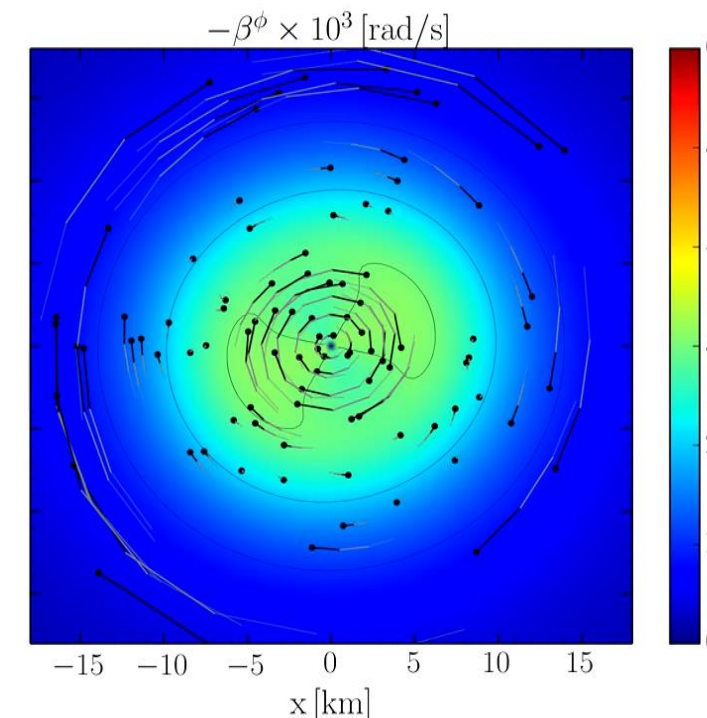
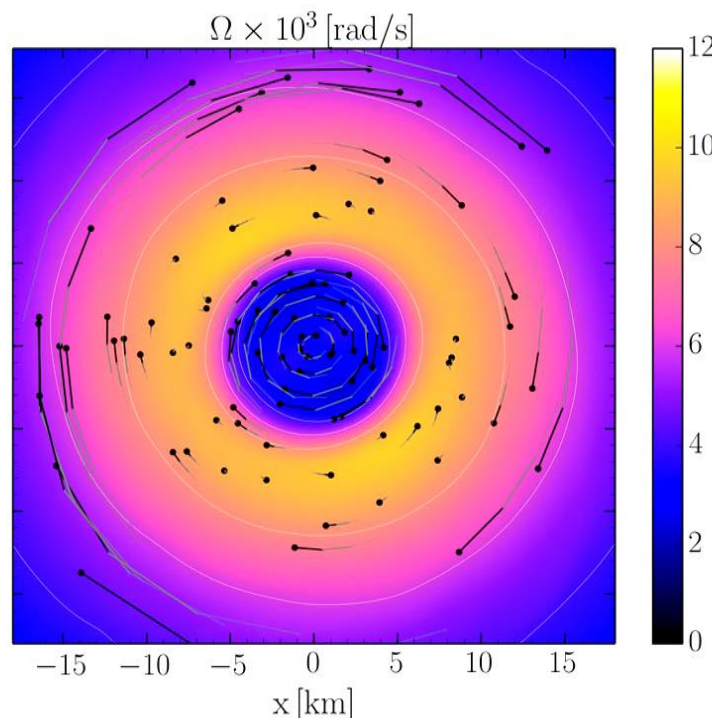
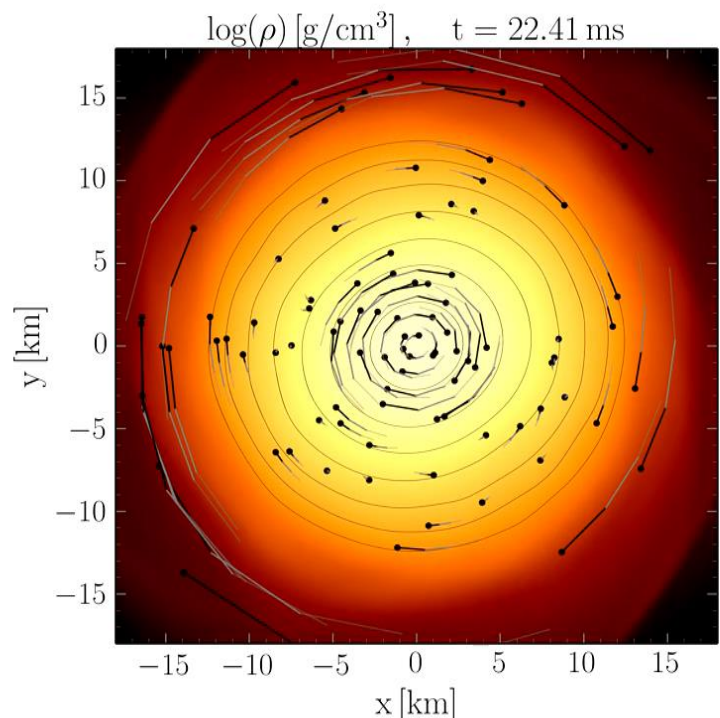
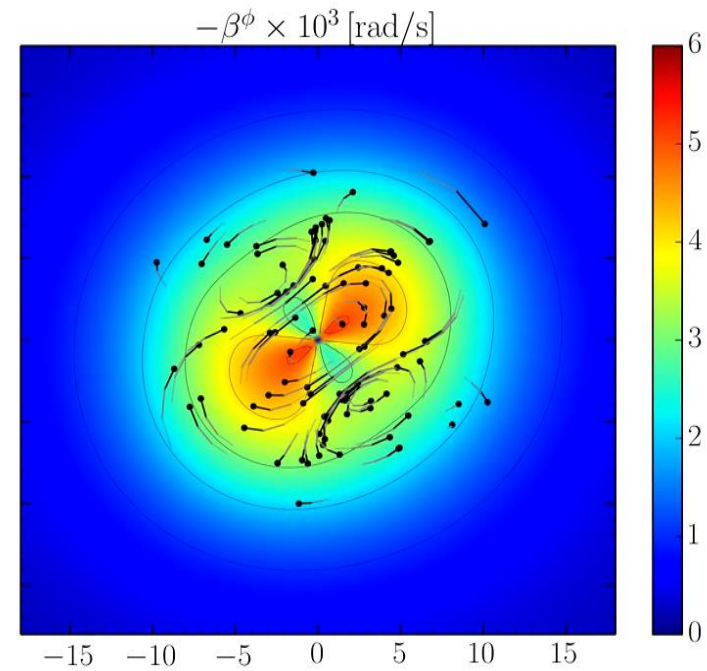
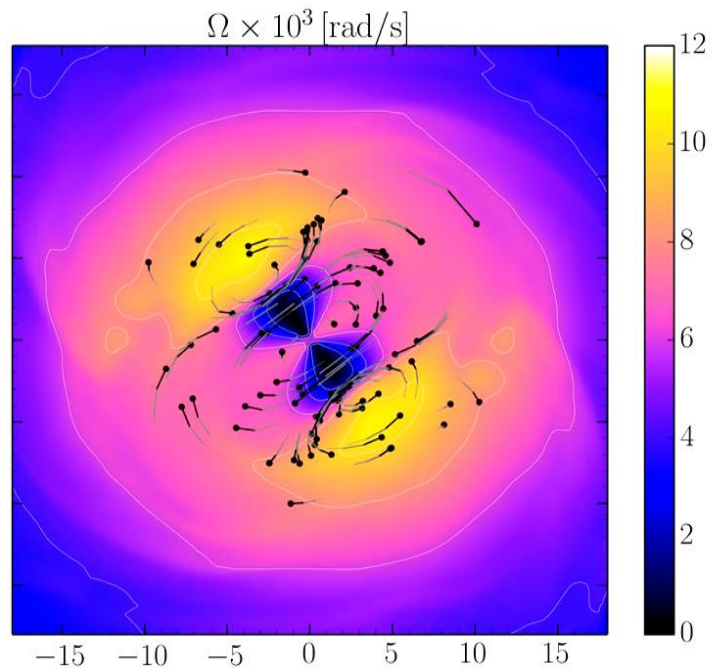
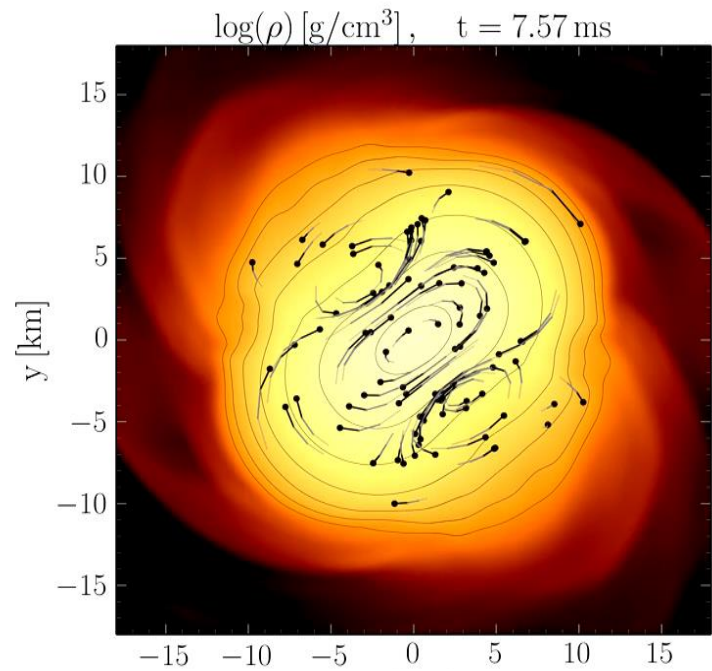
M. Shibata, K. Taniguchi, and K. Uryu, Phys. Rev. D 71, 084021 (2005)

M. Shibata and K. Taniguchi, Phys. Rev. D 73, 064027 (2006)

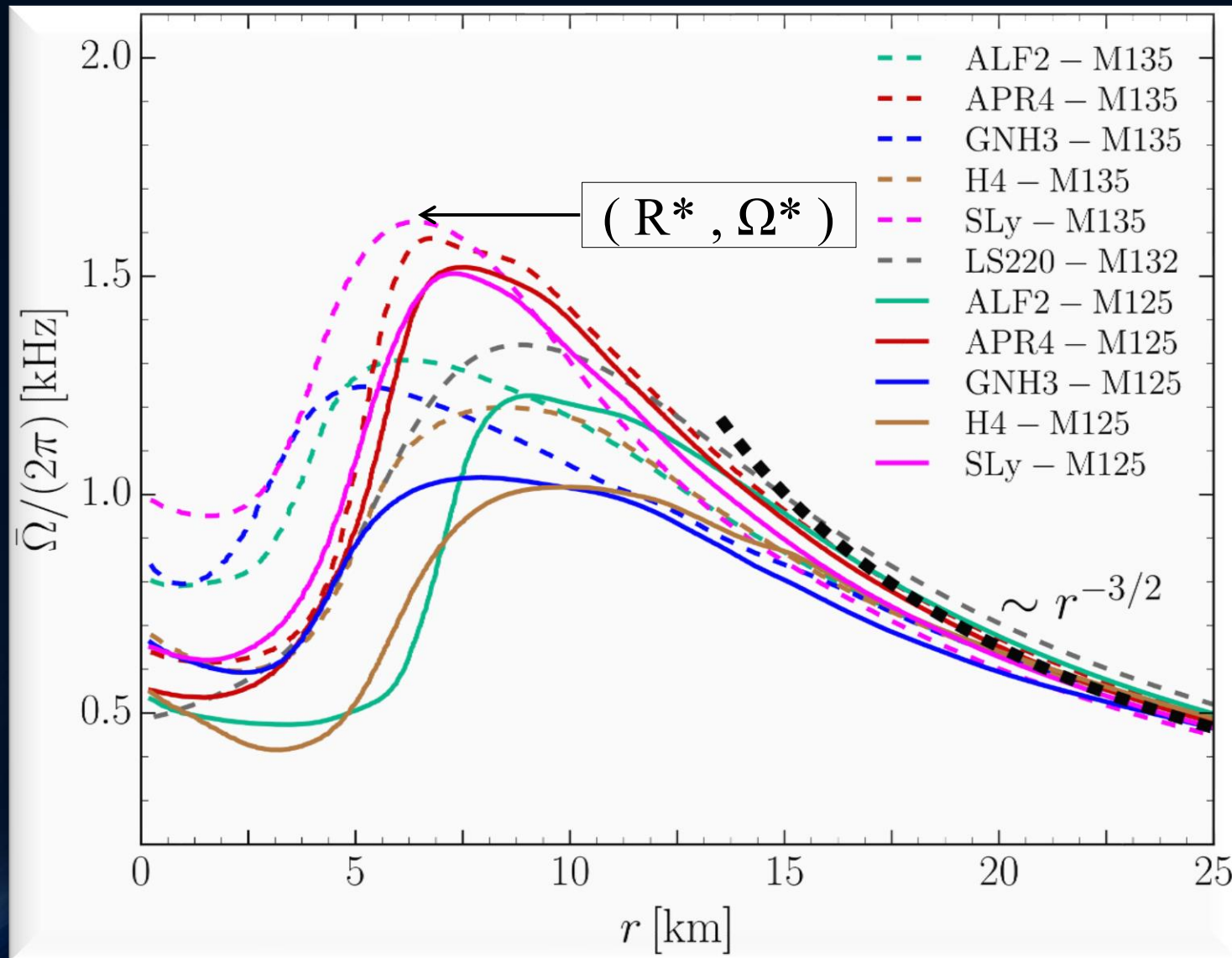
F. Galeazzi, S. Yoshida and Y. Eriguchi, A&A 541, p. A156 (2012)

W. Kastaun and F. Galeazzi, Phys. Rev. D 91, p. 064027 (2015)





# Time-averaged Rotation Profiles of the HMNSs



Soft EoSs:

Sly  
APR4

Stiff EoSs:

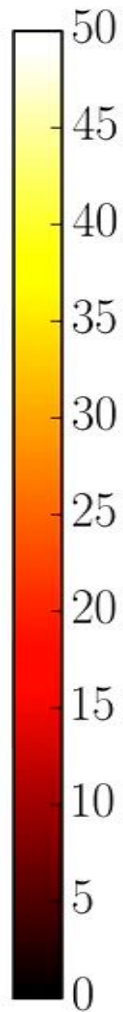
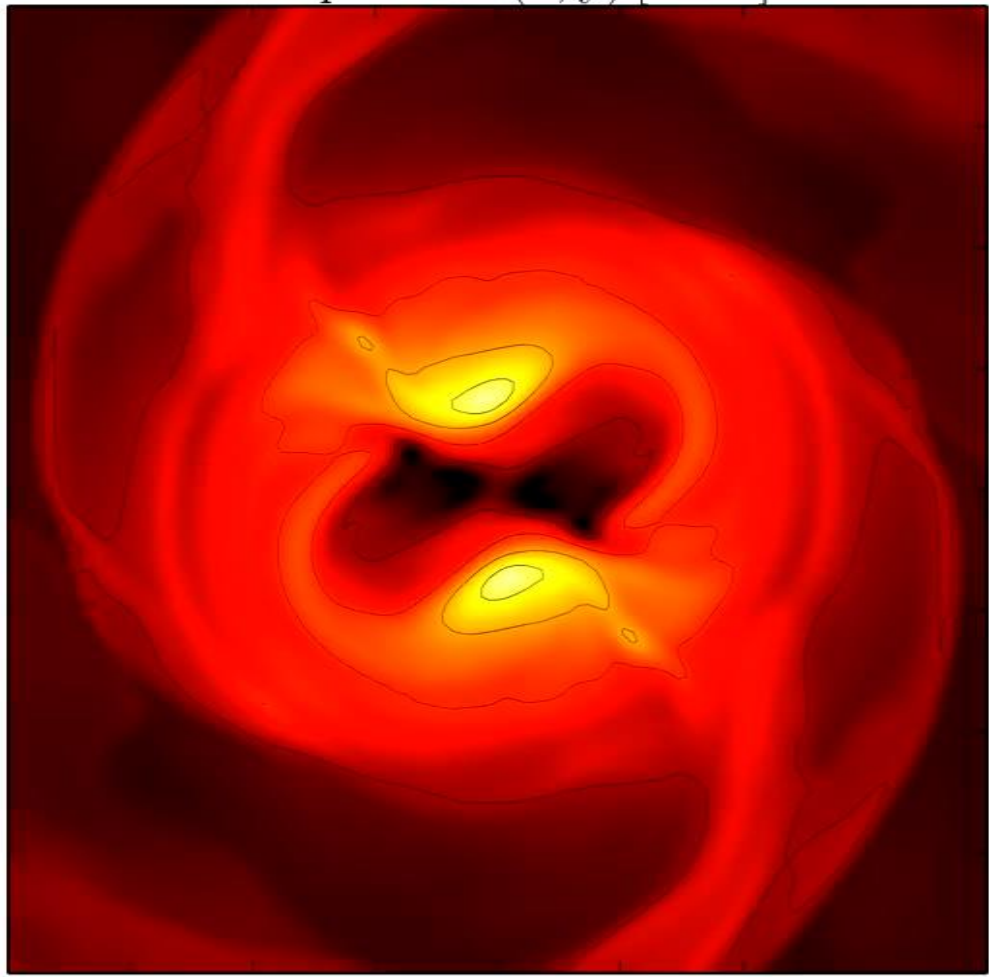
GNH3  
H4

Time-averaged rotation profiles for different EoS  
Low mass runs (solid curves), high mass runs (dashed curves).

Hanauske, et.al. PRD, 96(4), 043004 (2017)

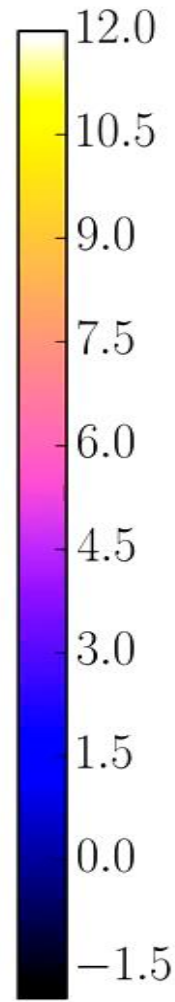
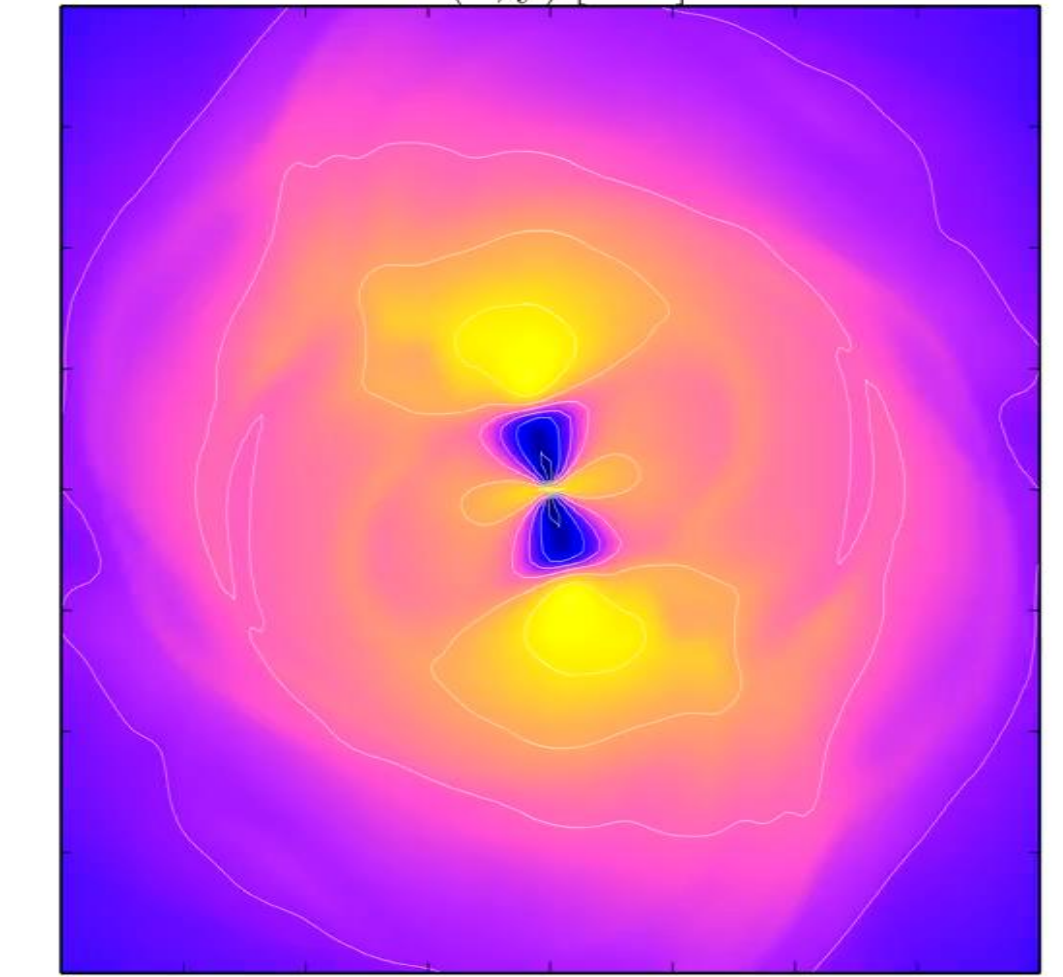
# Temperature

Temperature(x, y) [MeV]



# Angular Velocity

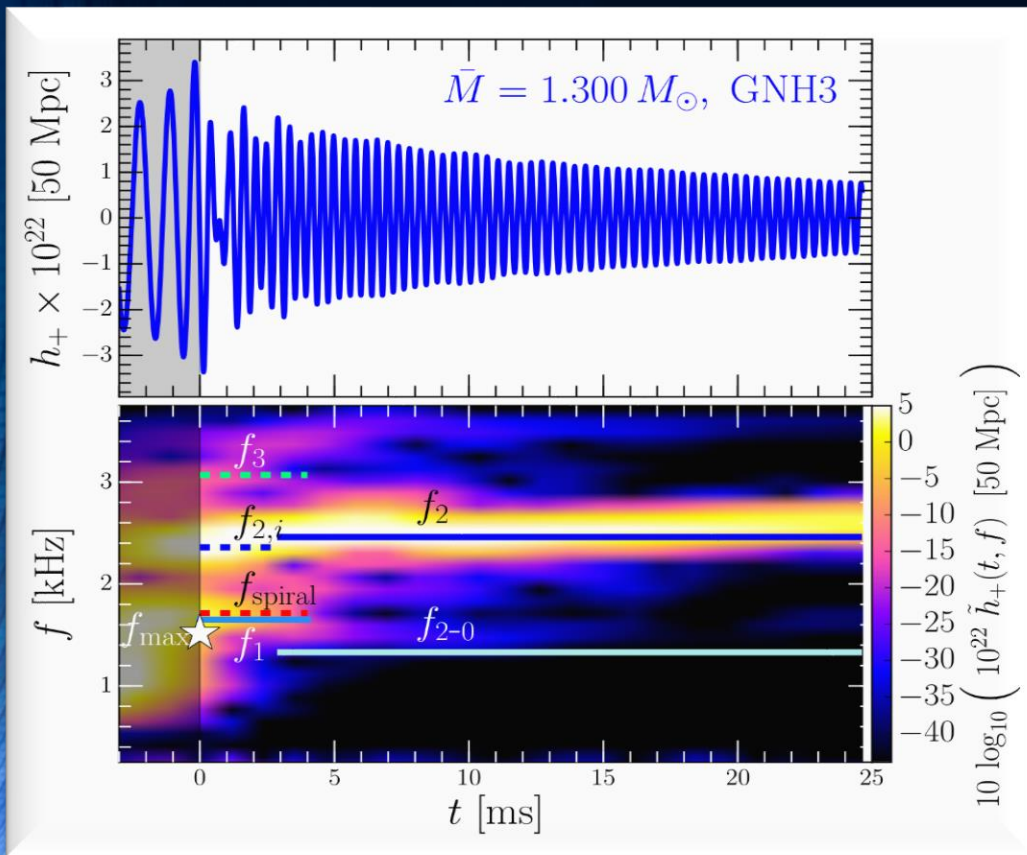
$\Omega(x, y)$  [kHz]



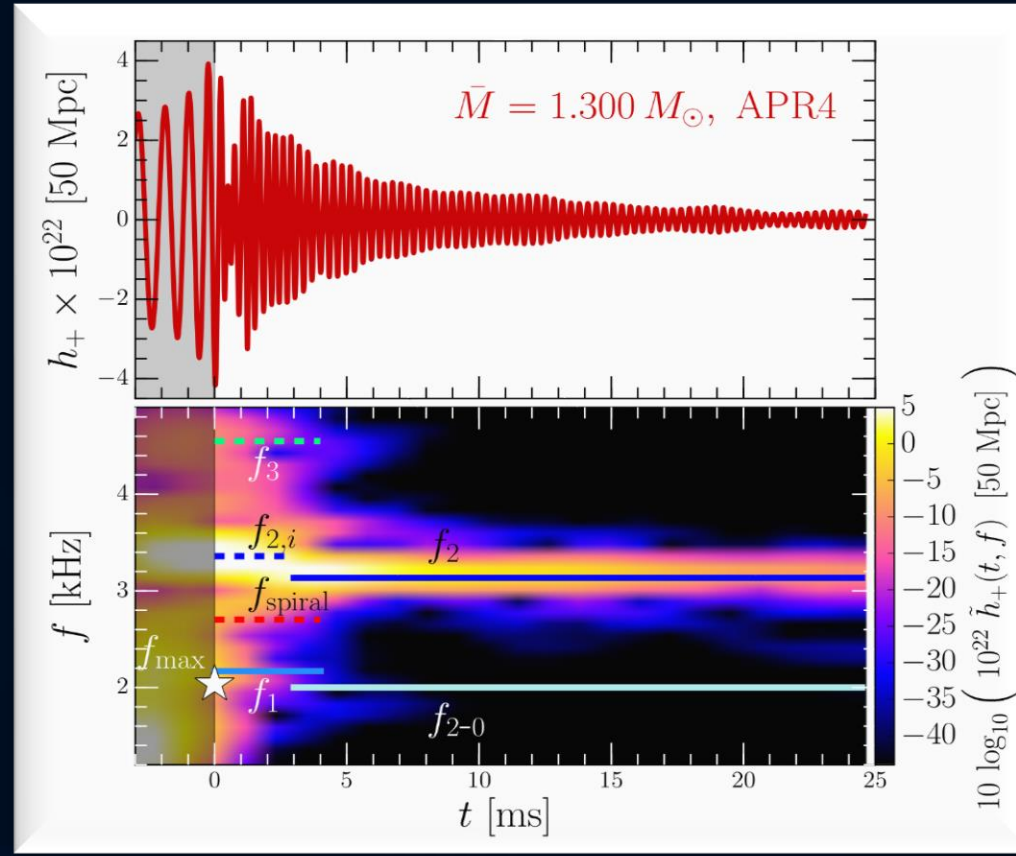
EOS: LS200 , Mass:  $1.32 M_{\text{solar}}$  , simulation with Pi-symmetry

# Time Evolution of the GW-Spectrum

The power spectral density profile of the post-merger emission is characterized by several distinct frequencies. Approximately 5 ms after merger, the only remaining dominant frequency is the  $f_2$ -frequency (see e.g. L.Rezzolla and K.Takami, PRD, 93(12), 124051 (2016))



Stiff EOS



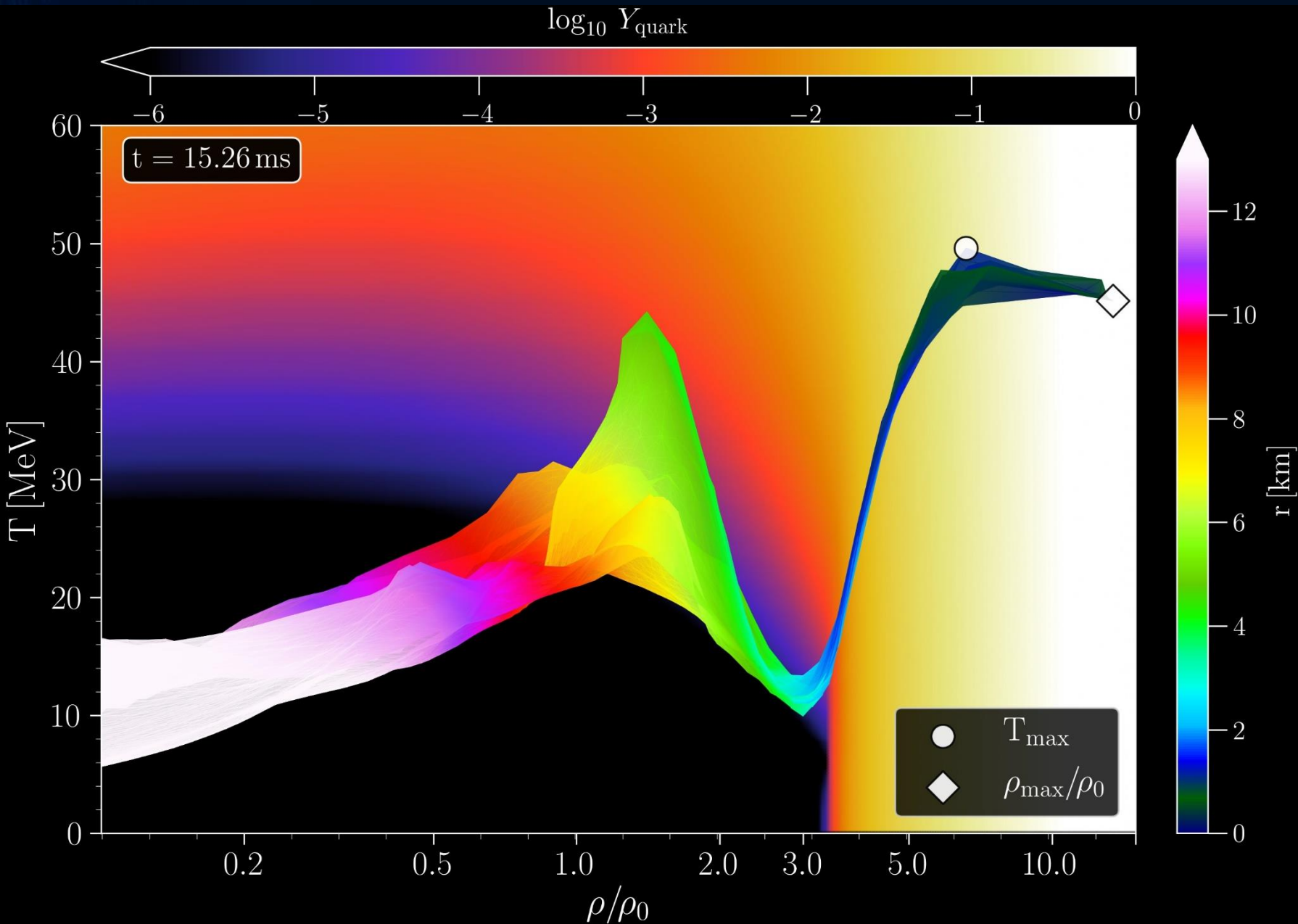
Soft EOS

Unfortunately, due to the low sensitivity at high gravitational wave frequencies, no post-merger signal has been found in GW170817.

But advanced detectors / next-generation detectors might be able to detect!!?

Evolution of the frequency spectrum of the emitted gravitational waves for the stiff GNH3 (left) and soft APR4 (right) EOS.

# Binary Hybrid Star Mergers and the QCD Phase Diagram

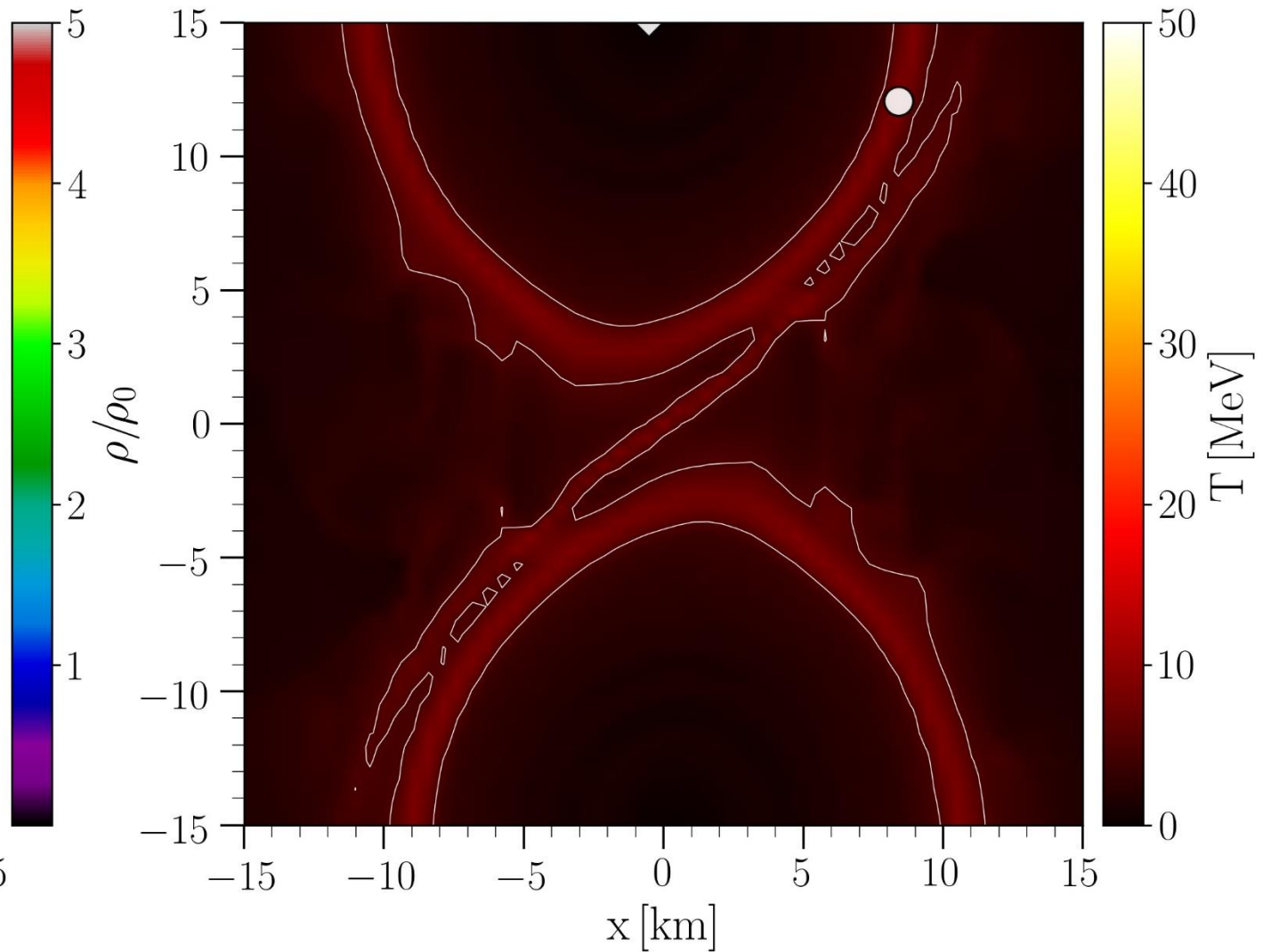
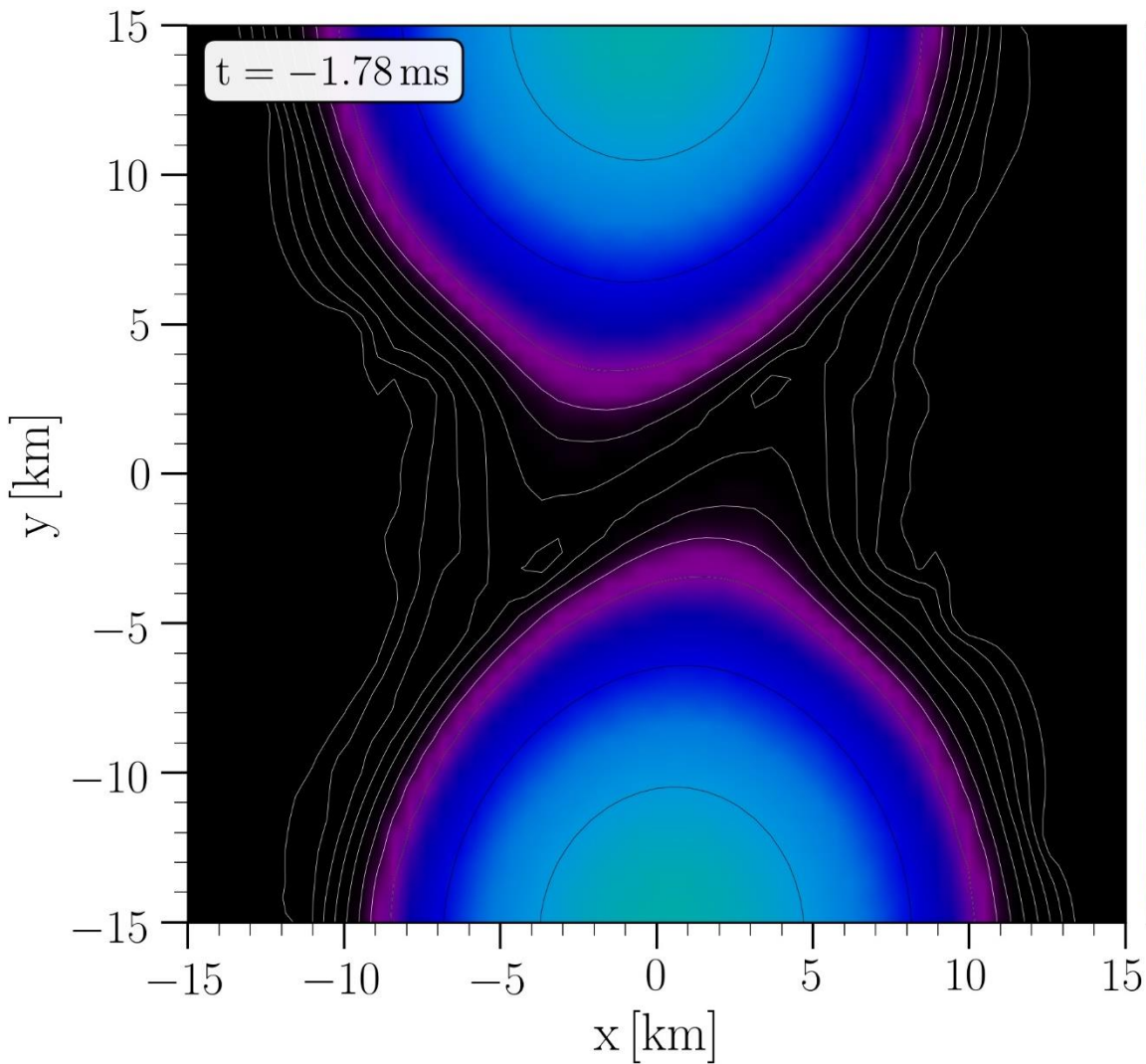


Hot and dense matter inside the inner area of a collapsing hypermassive hybrid star in the style of a  $(T-\rho)$  QCD phase diagram plot at a time right before the apparent horizon is formed in its center

The color-coding (right side) indicate the radial position  $r$  of the corresponding  $(T-\rho)$  fluid element measured from the origin of the simulation  $(x, y) = (0, 0)$  on the equatorial plane at  $z = 0$ . The color-coding (top) indicates the fraction of deconfined quarks.

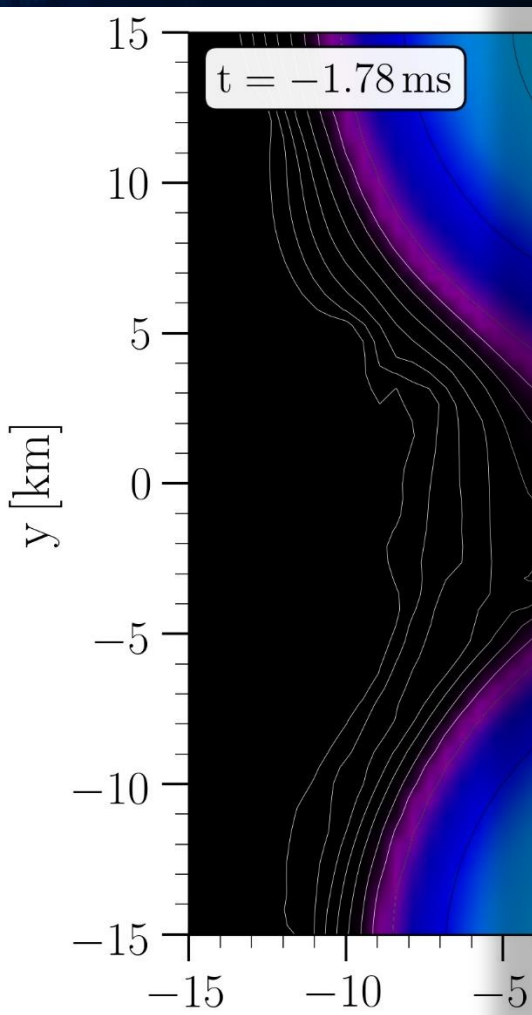
The open triangle marks the maximum value of the temperature while the open diamond indicates the maximum of the density.

# Late Inspiral Phase

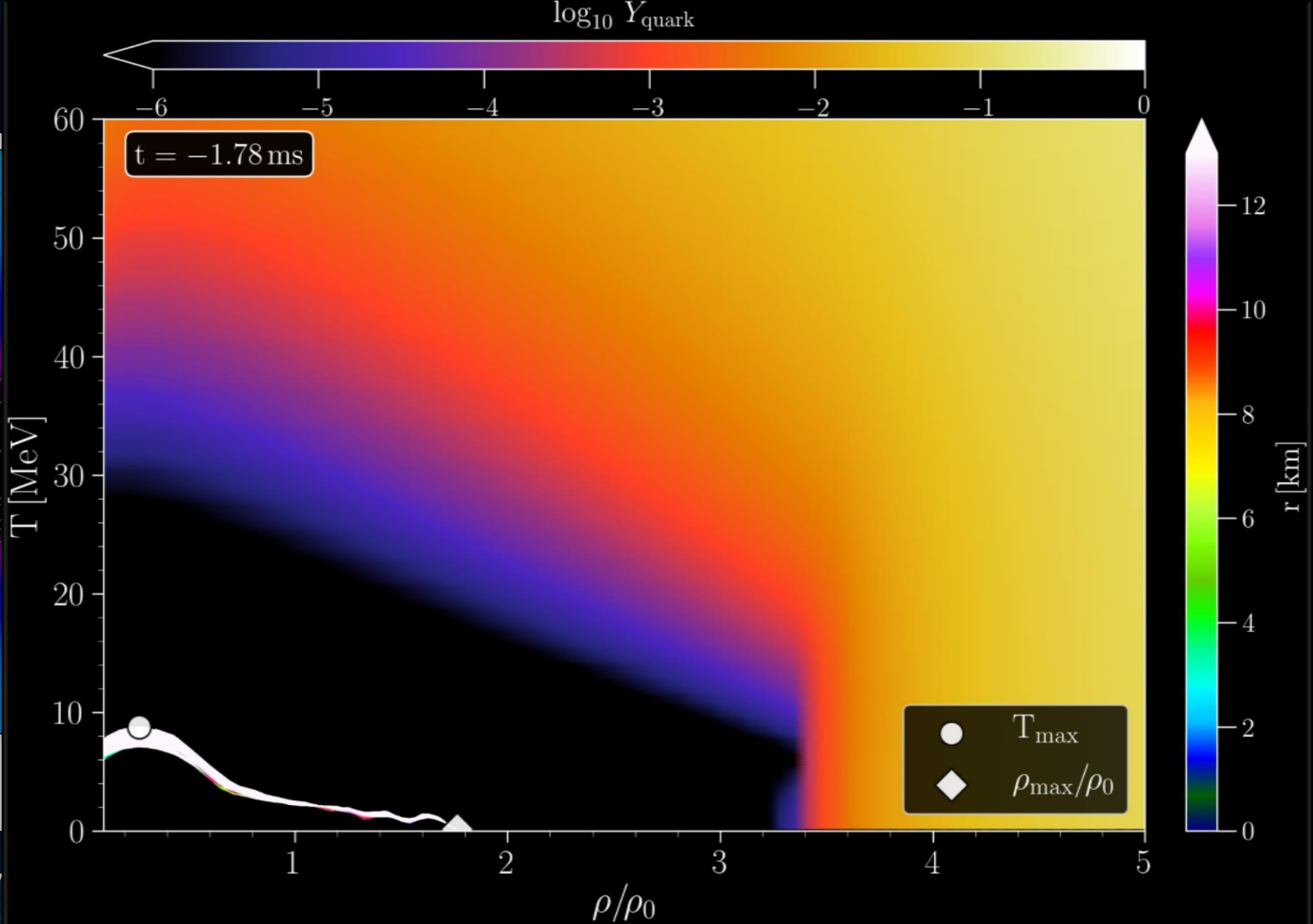




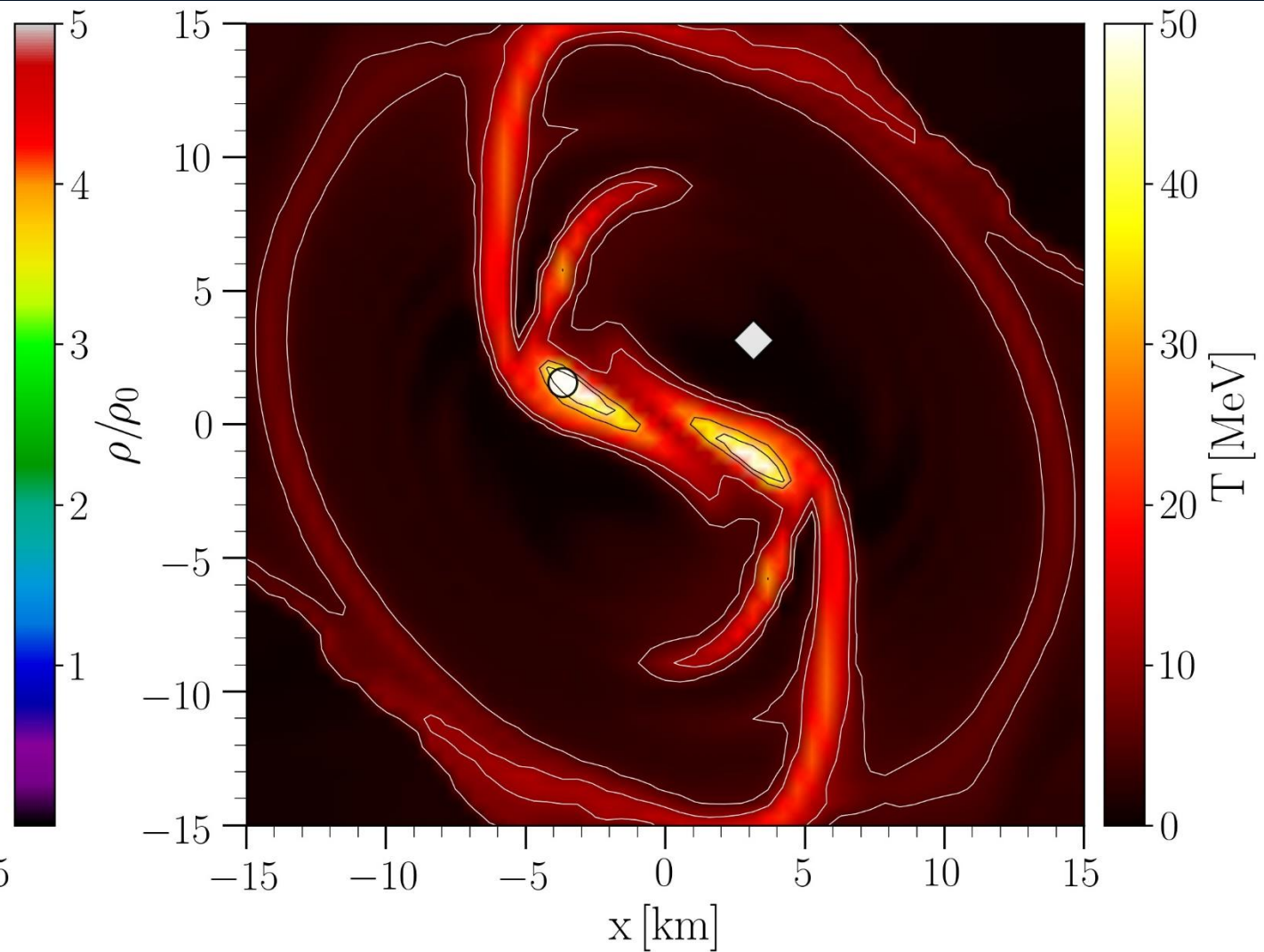
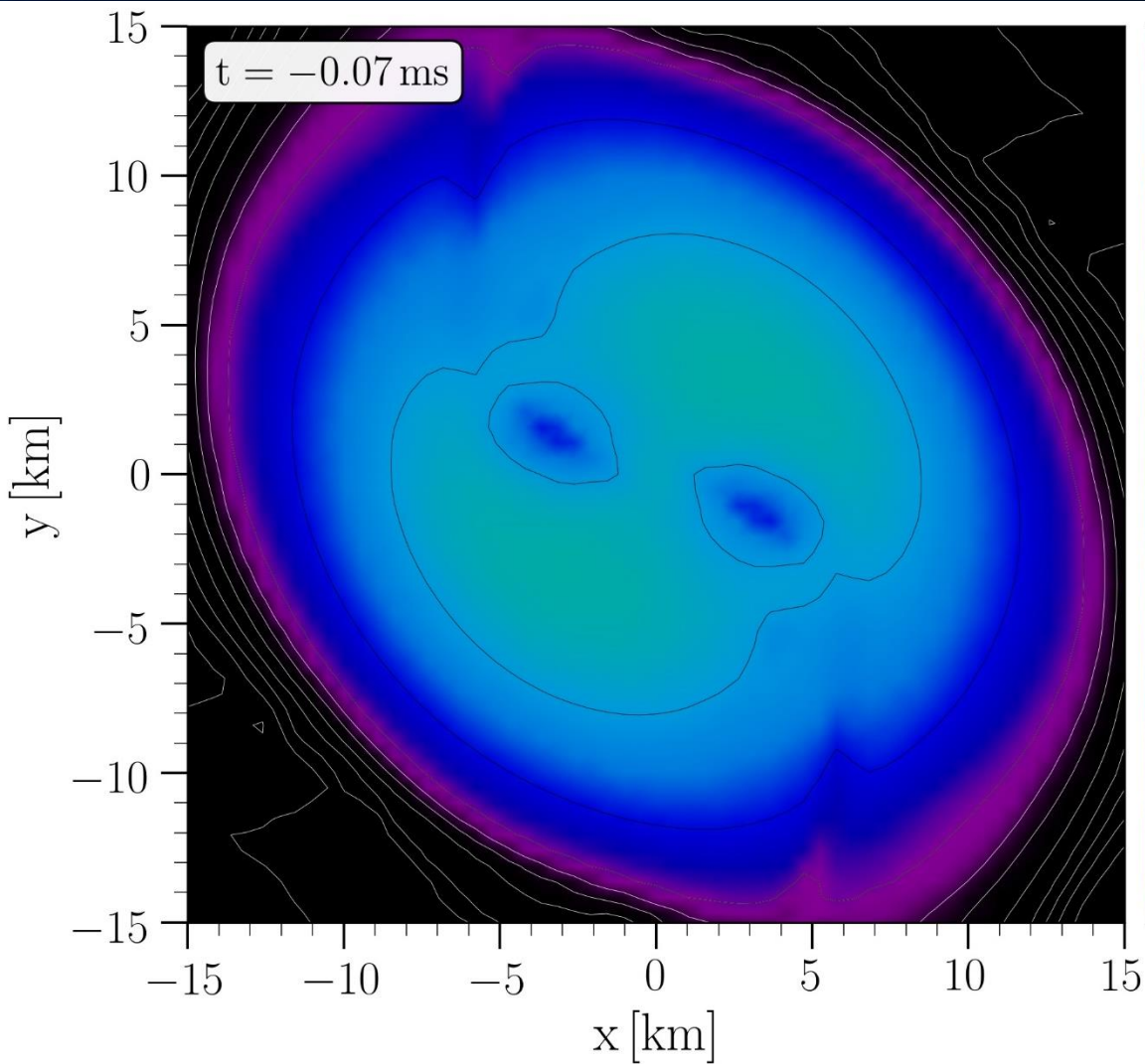
# Late Inspiral Phase



Rest mass density



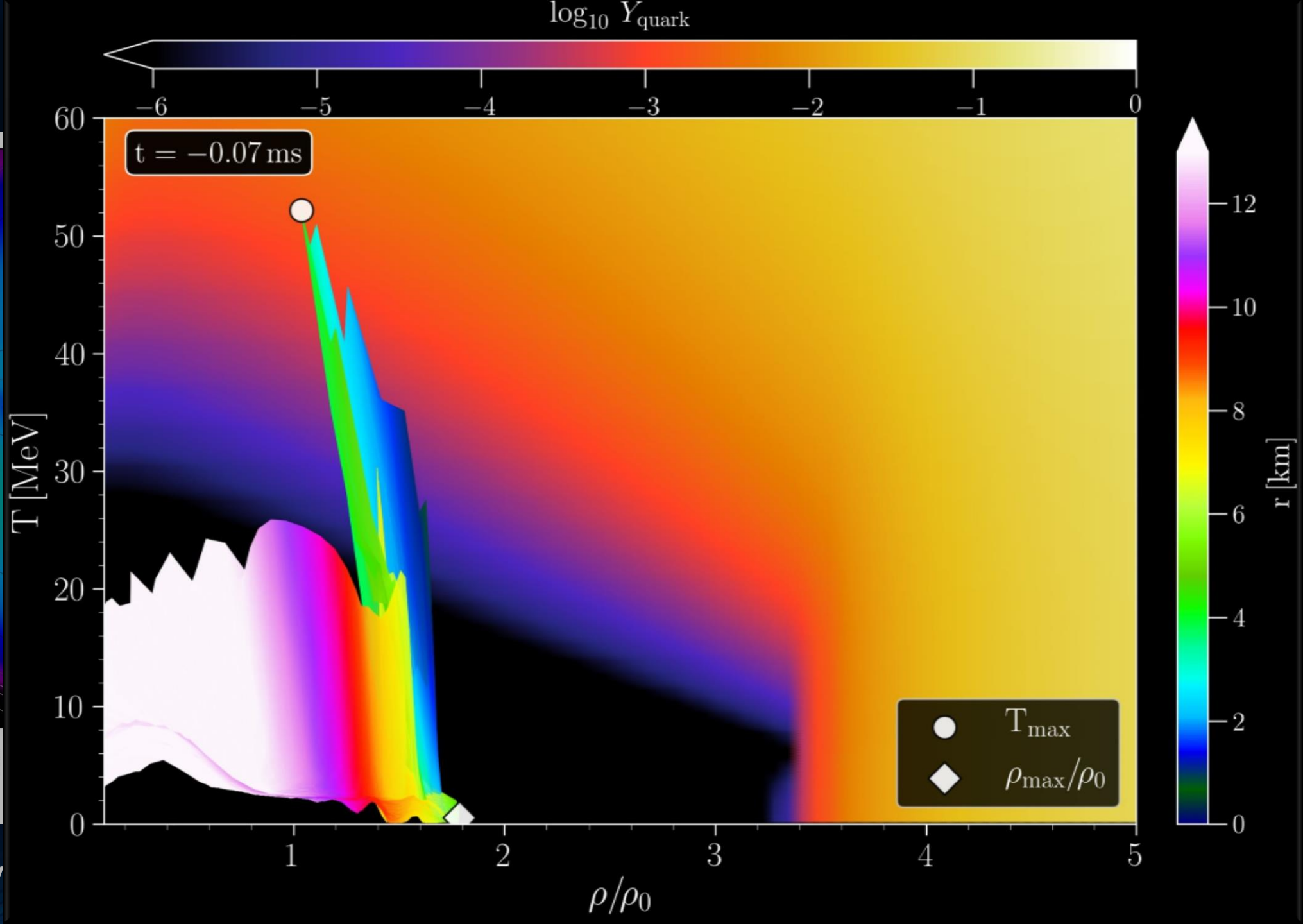
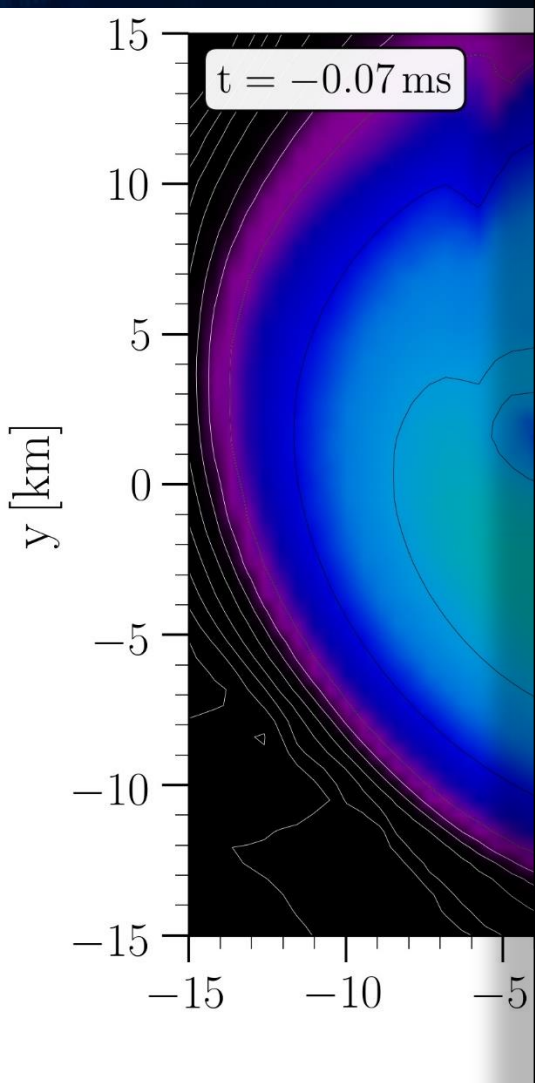
# Merger Phase



Rest mass density on the equatorial plane

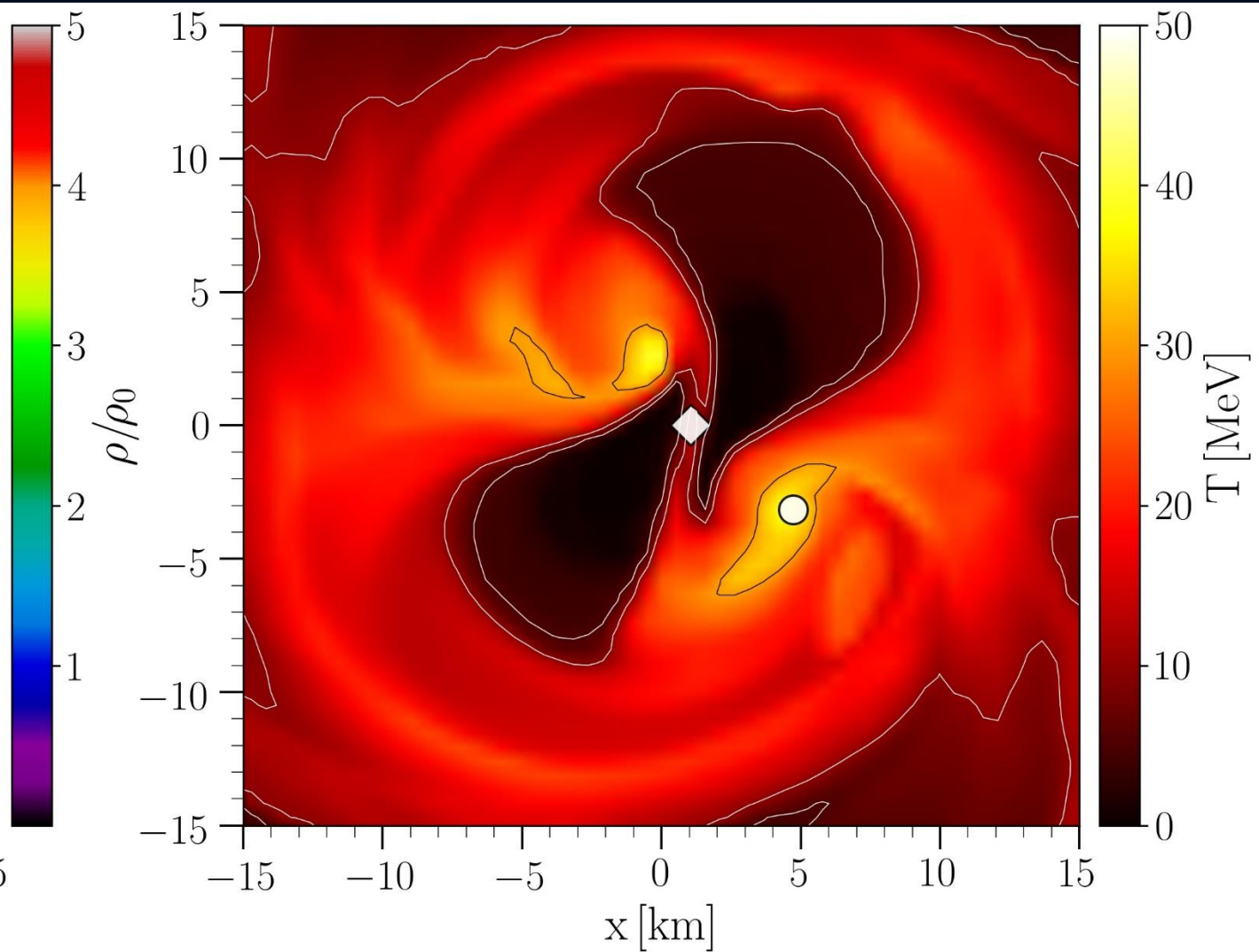
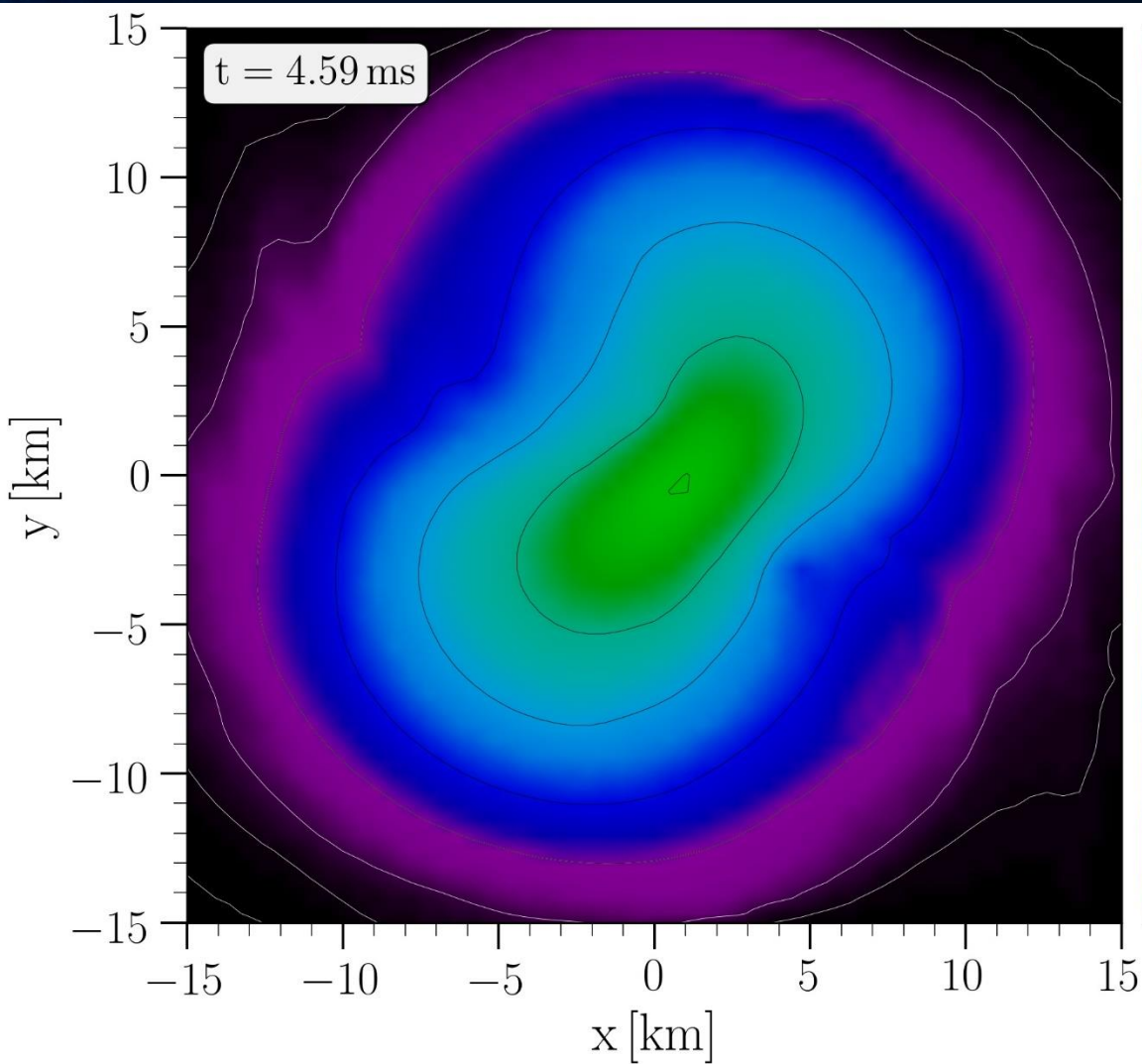
Temperature on the equatorial plane

# Merger Phase

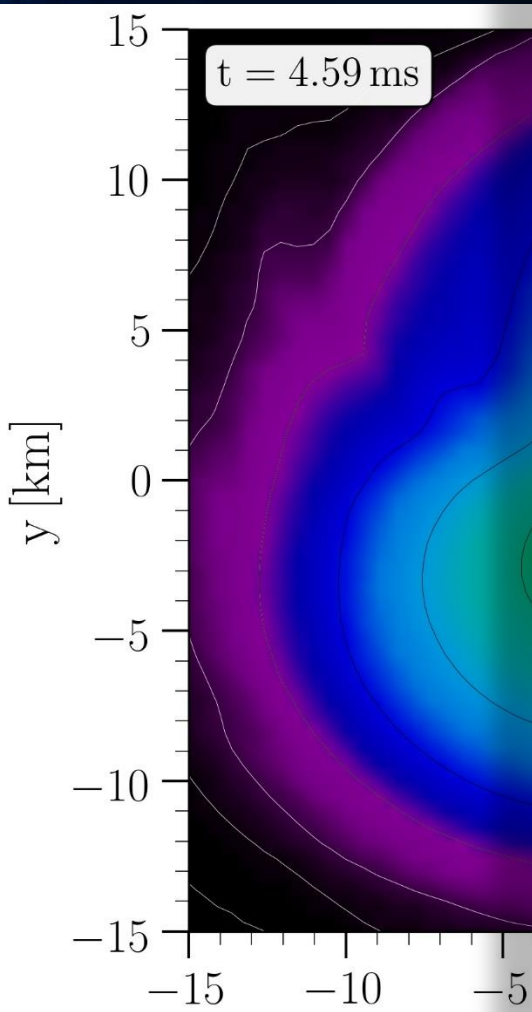


Rest mass density

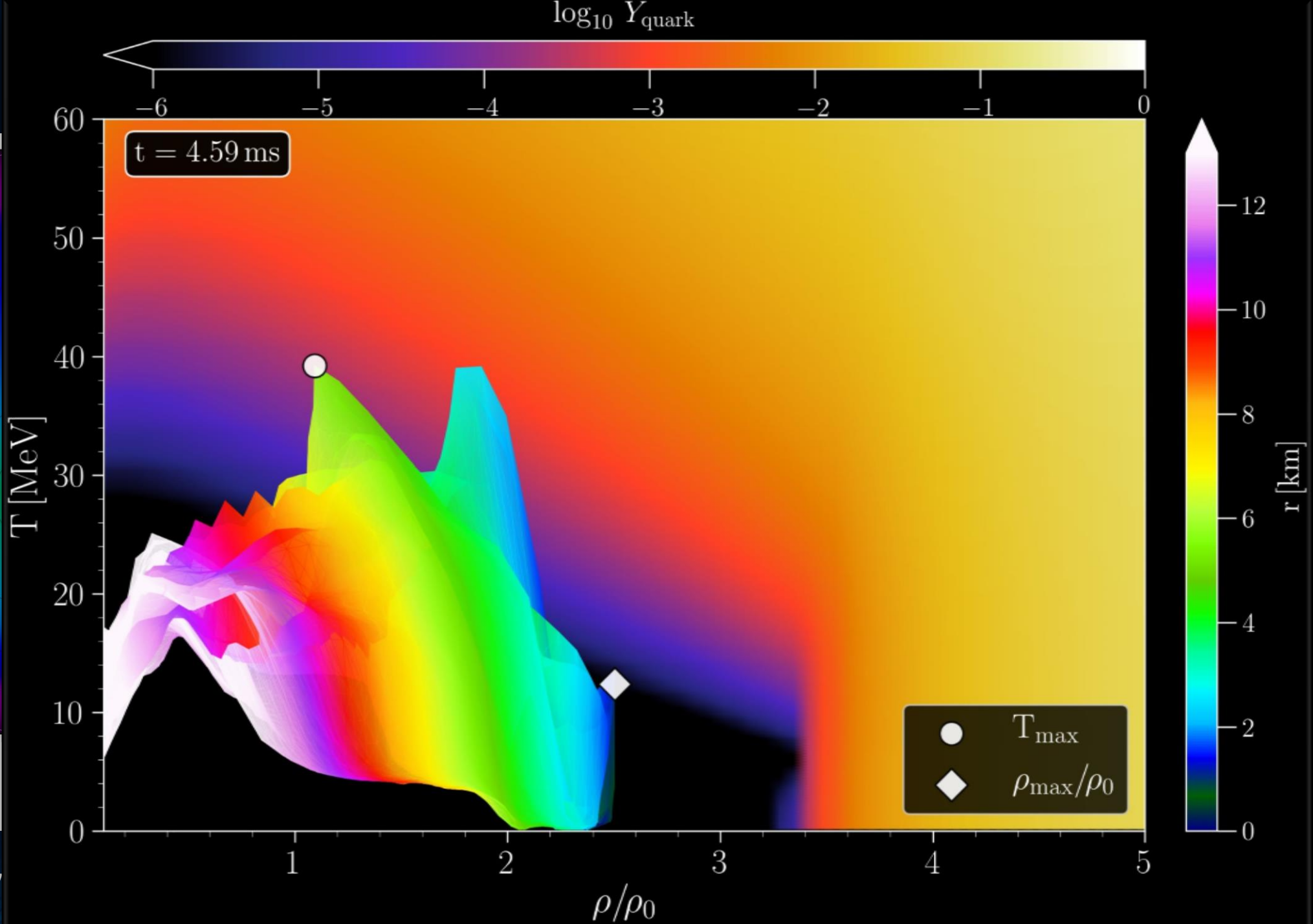
# Post Merger Phase



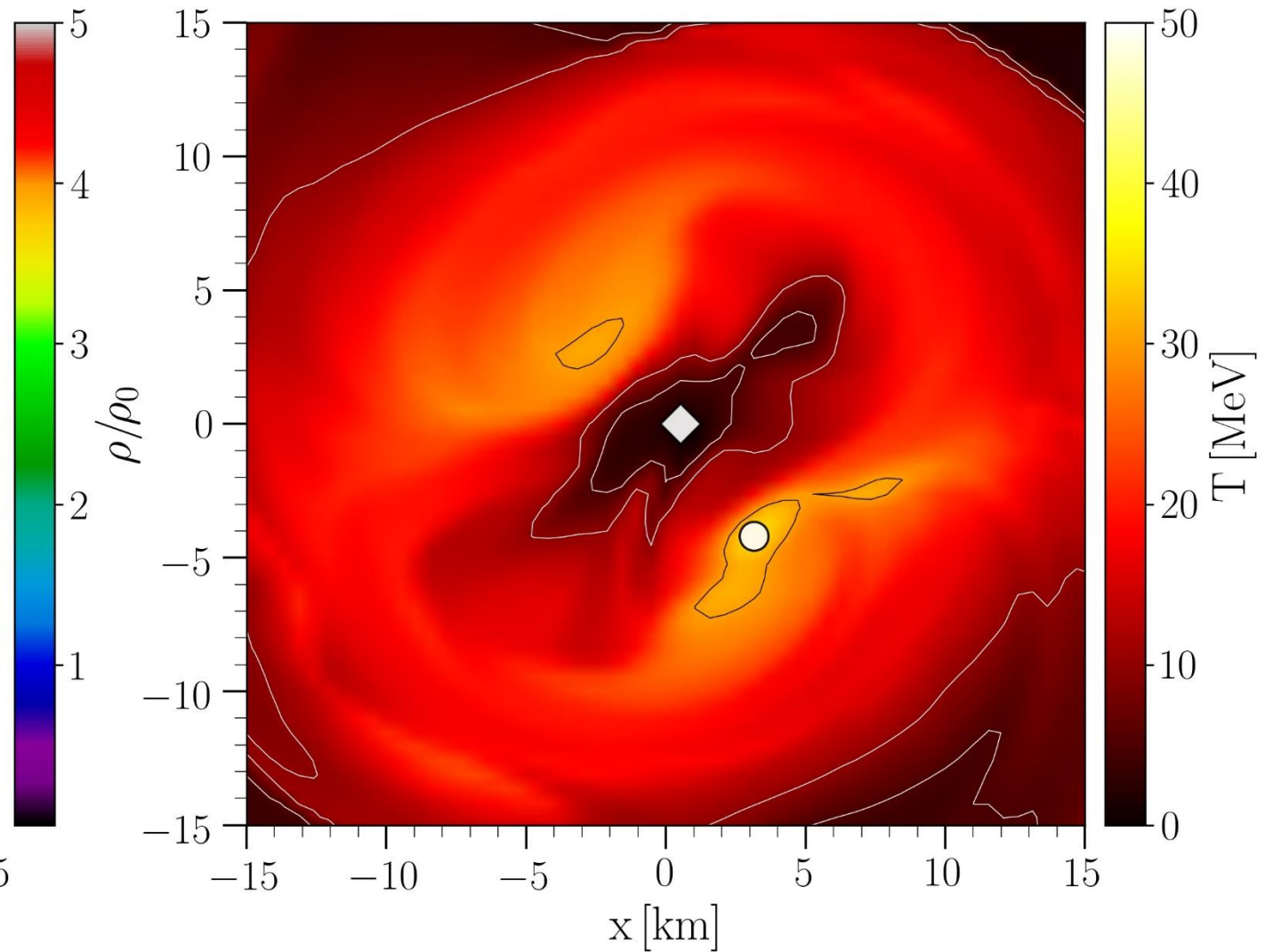
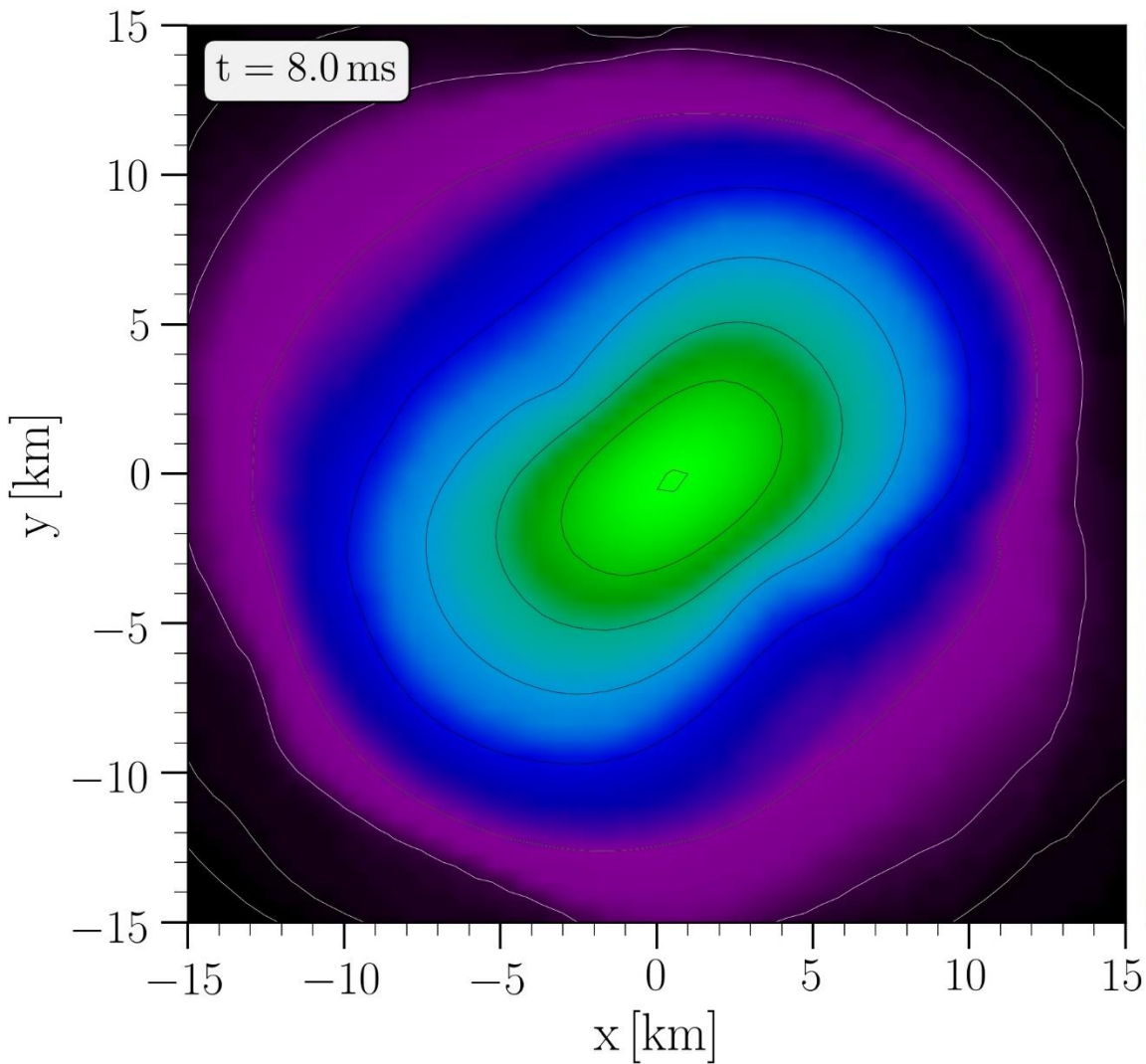
# Post Merger Phase



Rest mass density



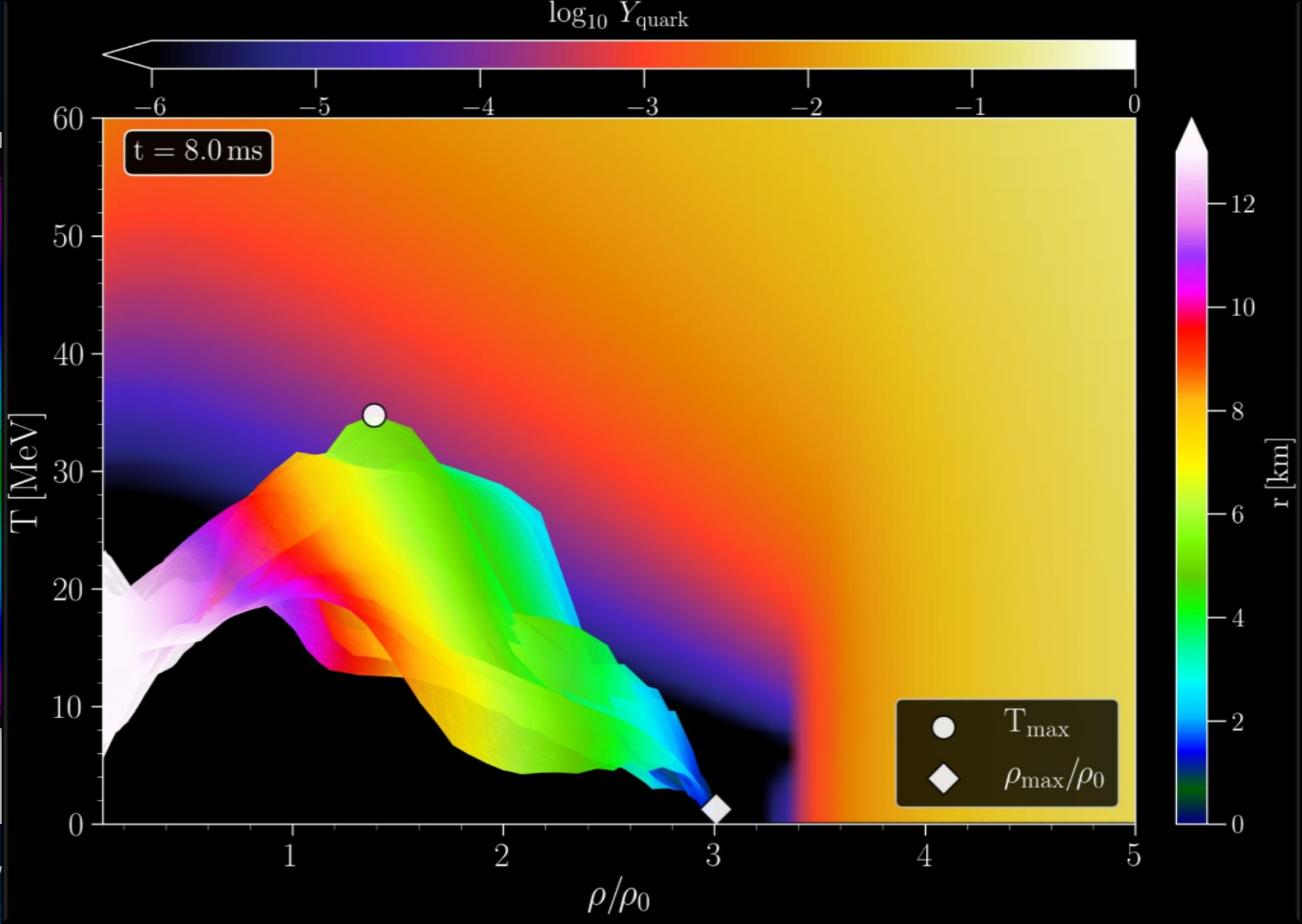
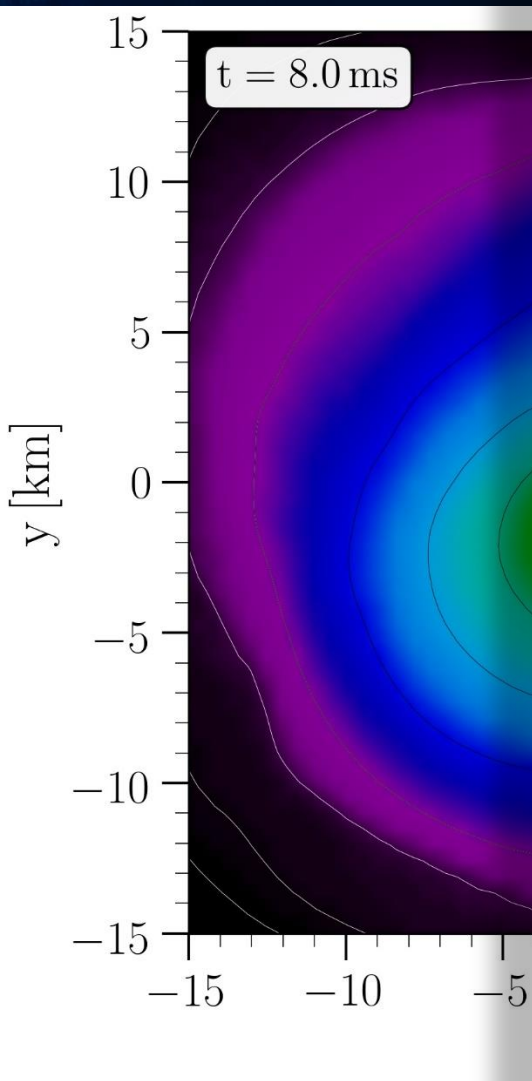
# Merger Phase



Rest mass density on the equatorial plane

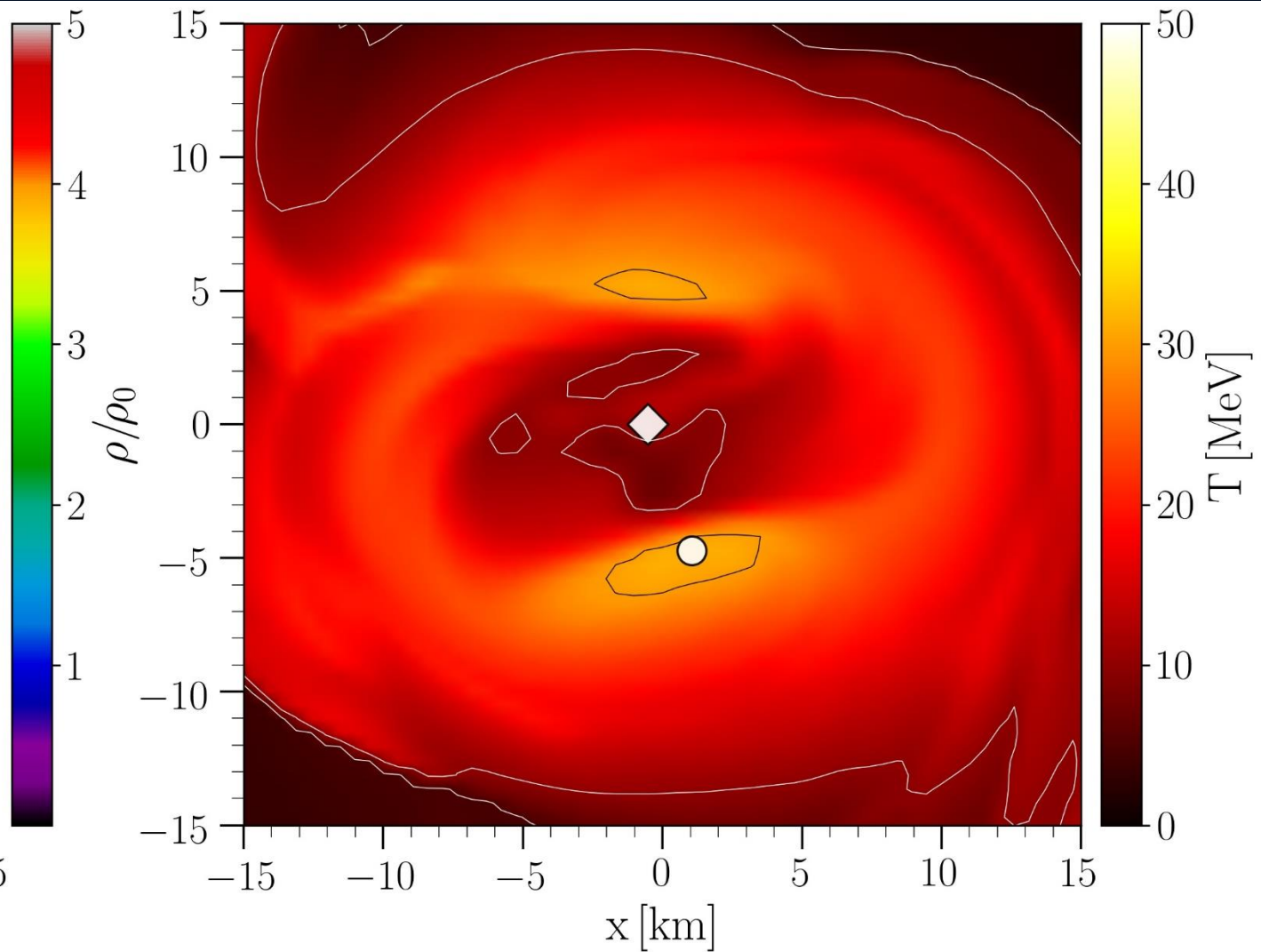
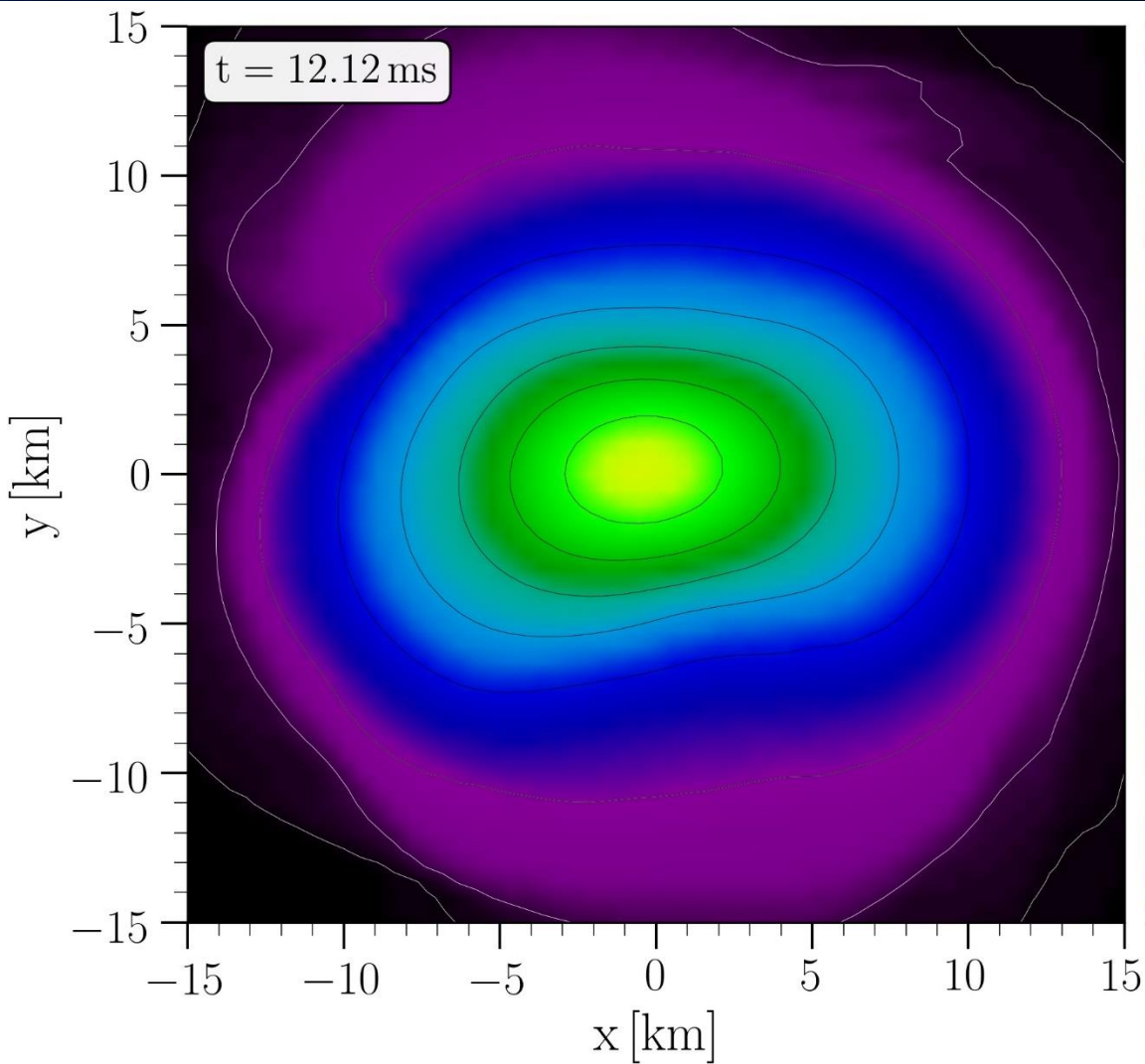
Temperature on the equatorial plane

# Merger Phase



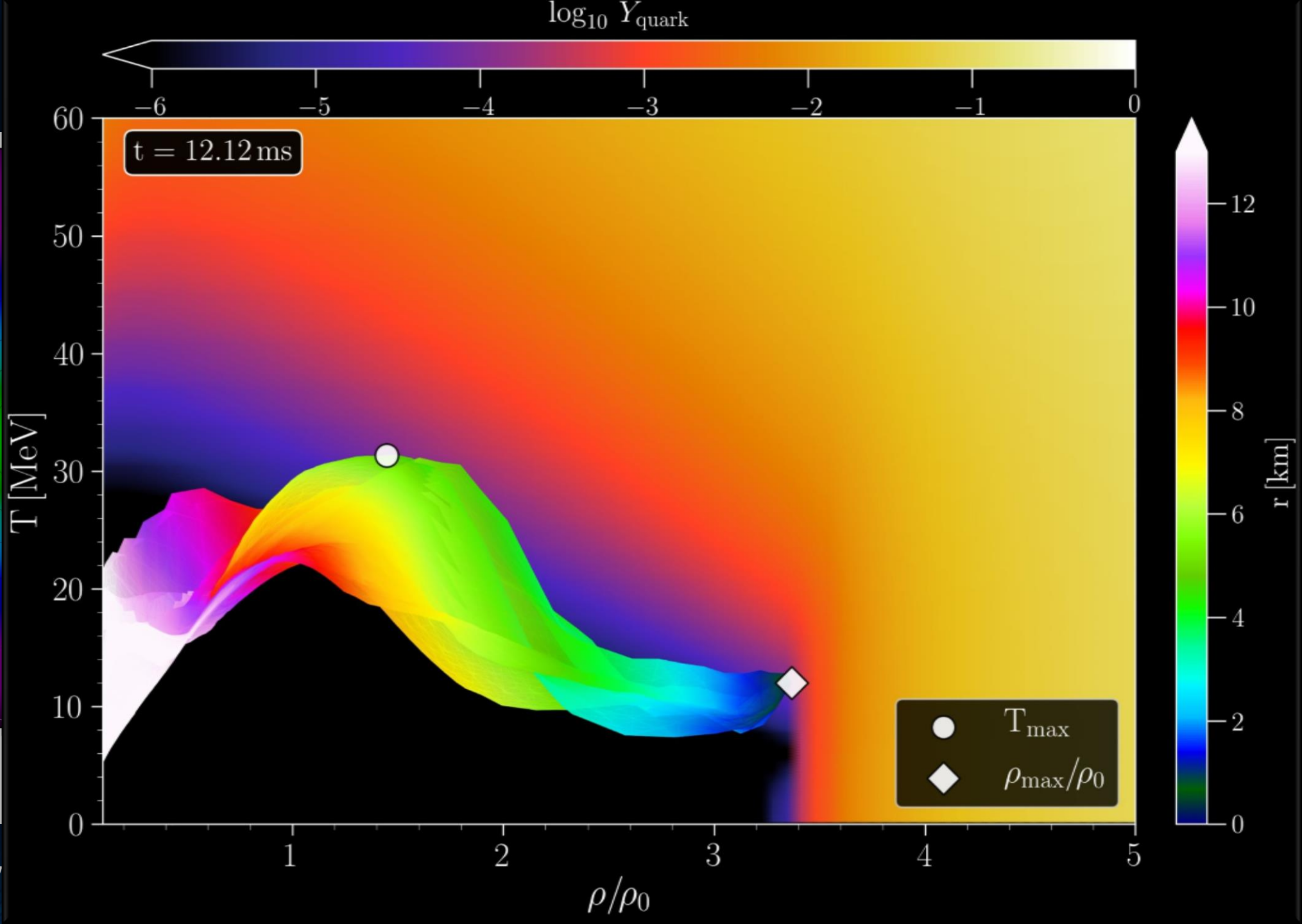
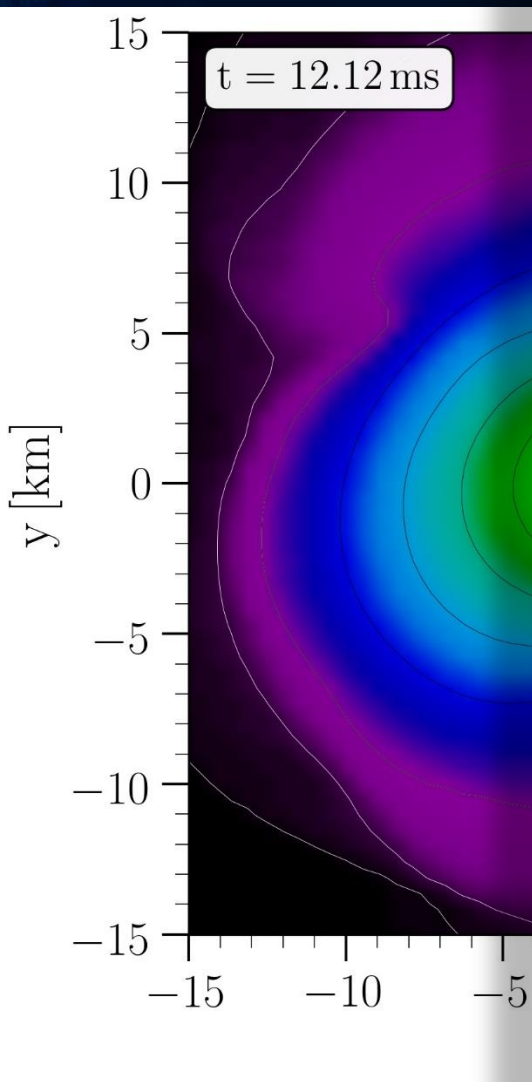
Rest mass density

# Merger Phase



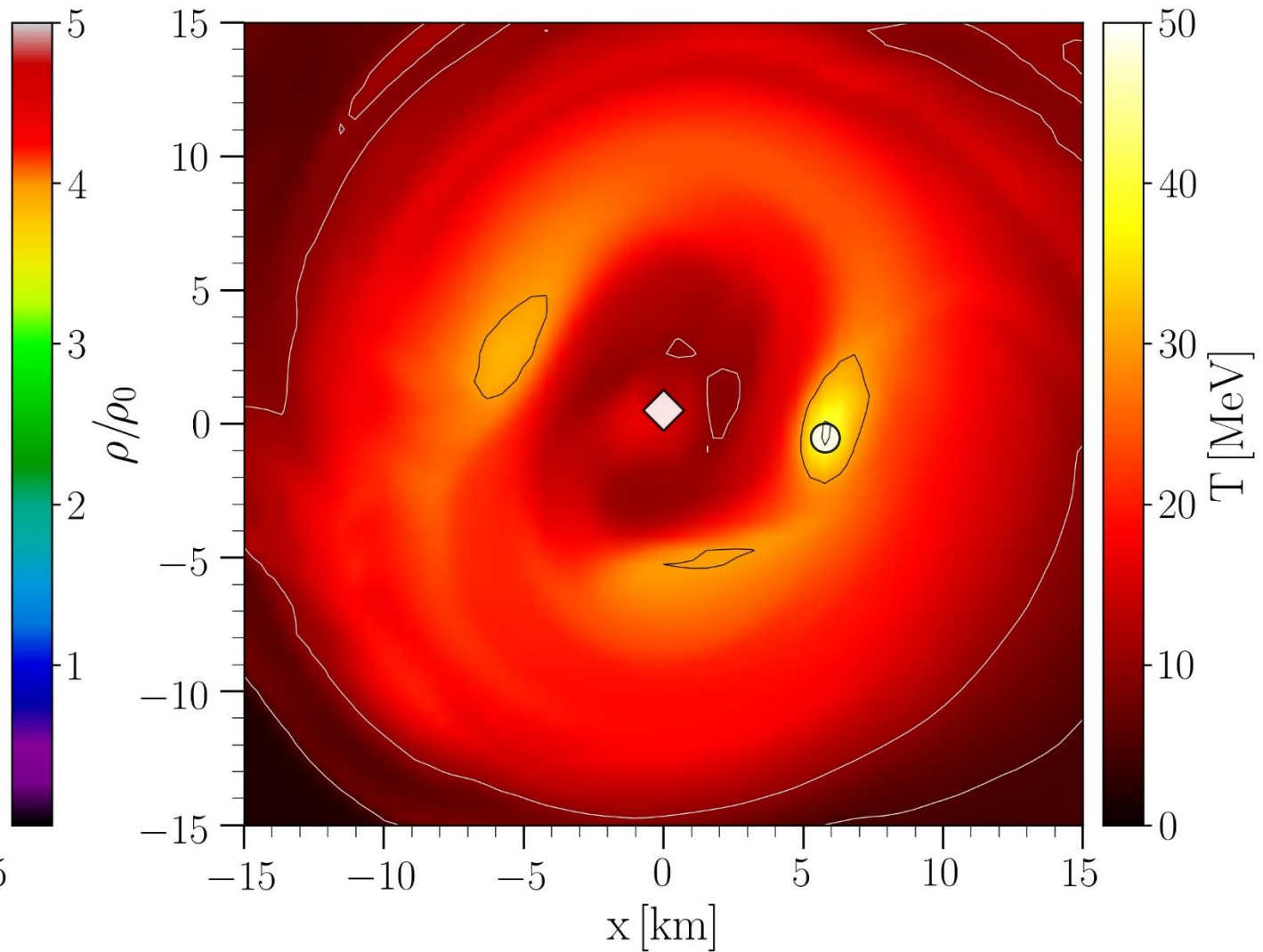
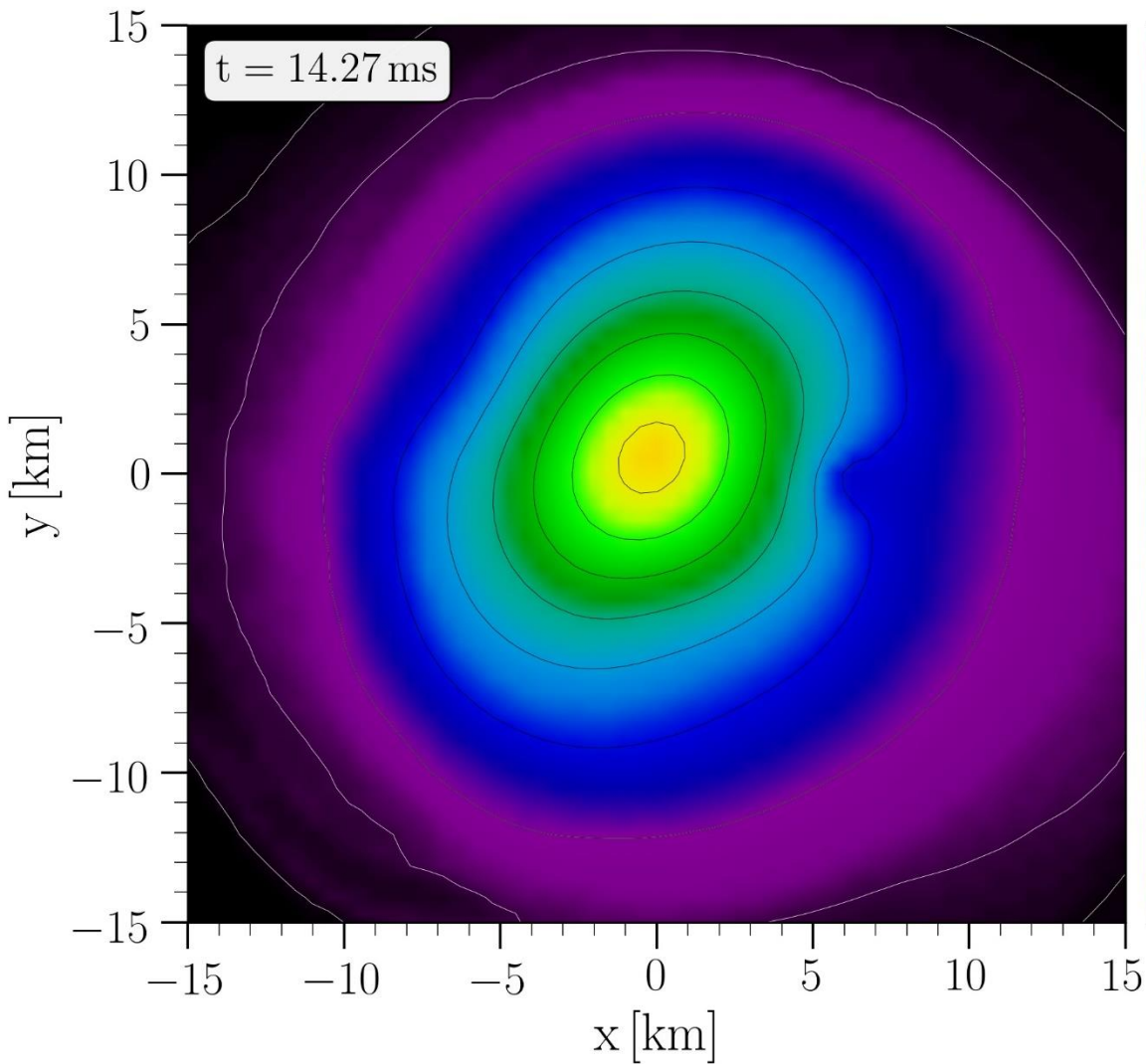


# Merger Phase

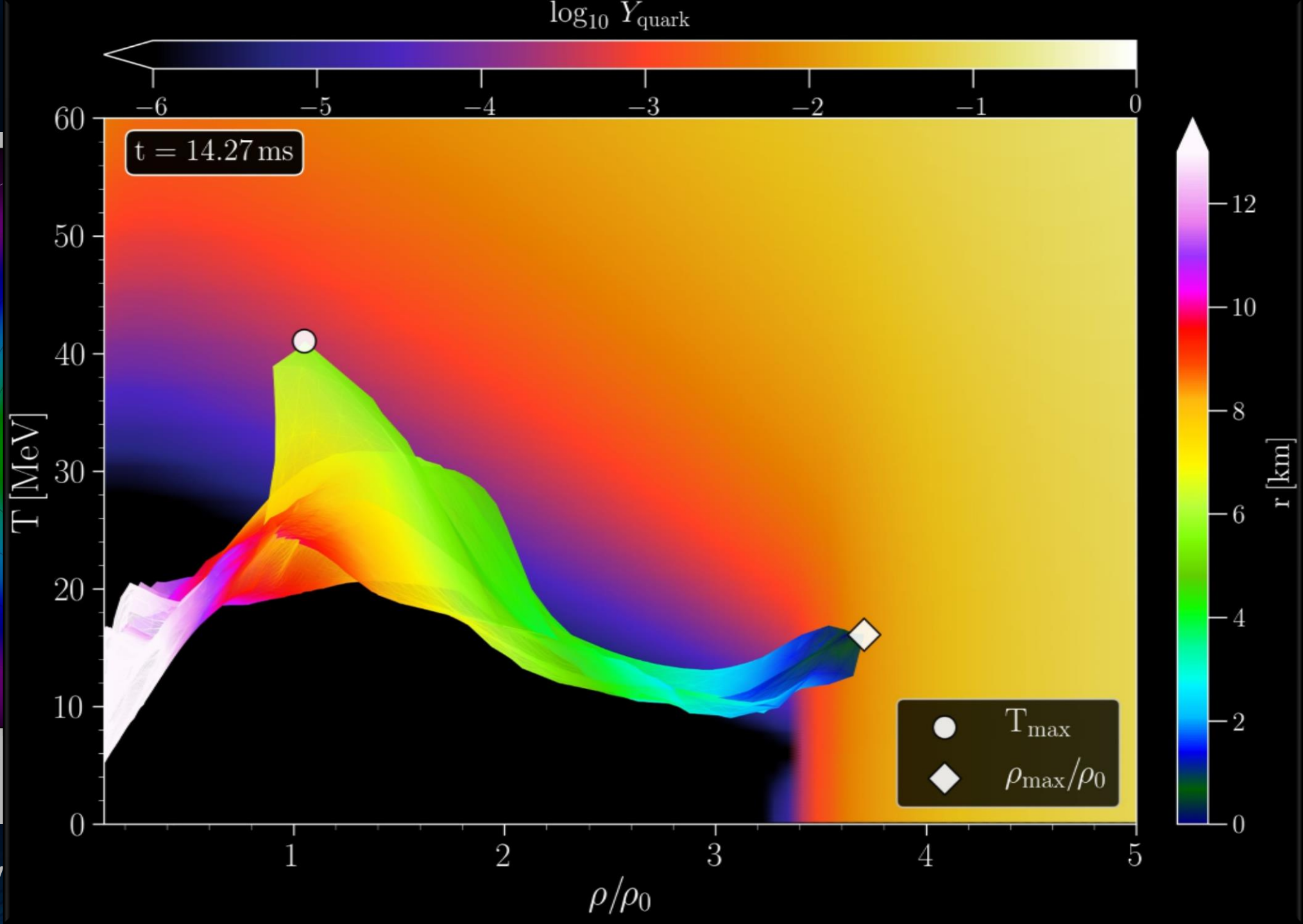
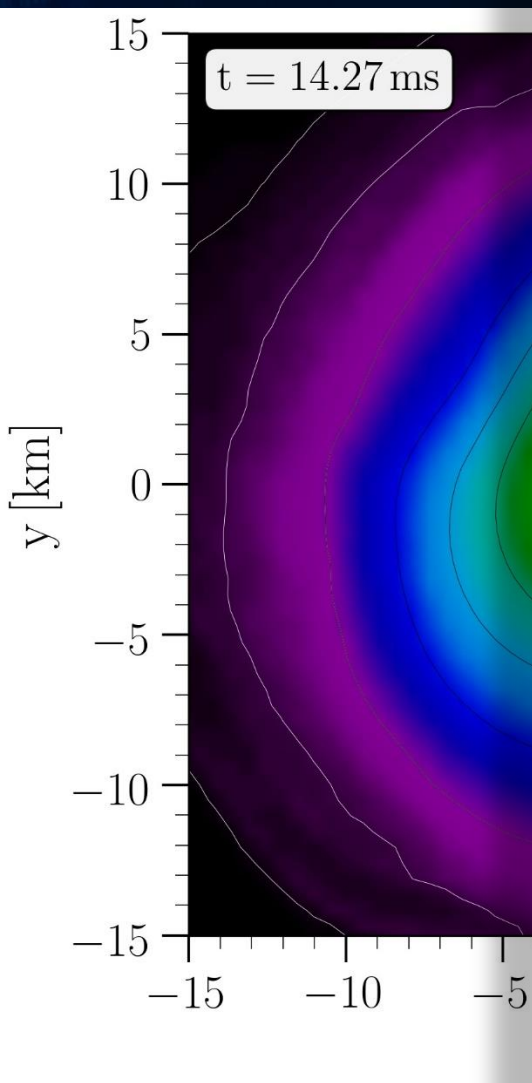


Rest mass density

# Merger Phase

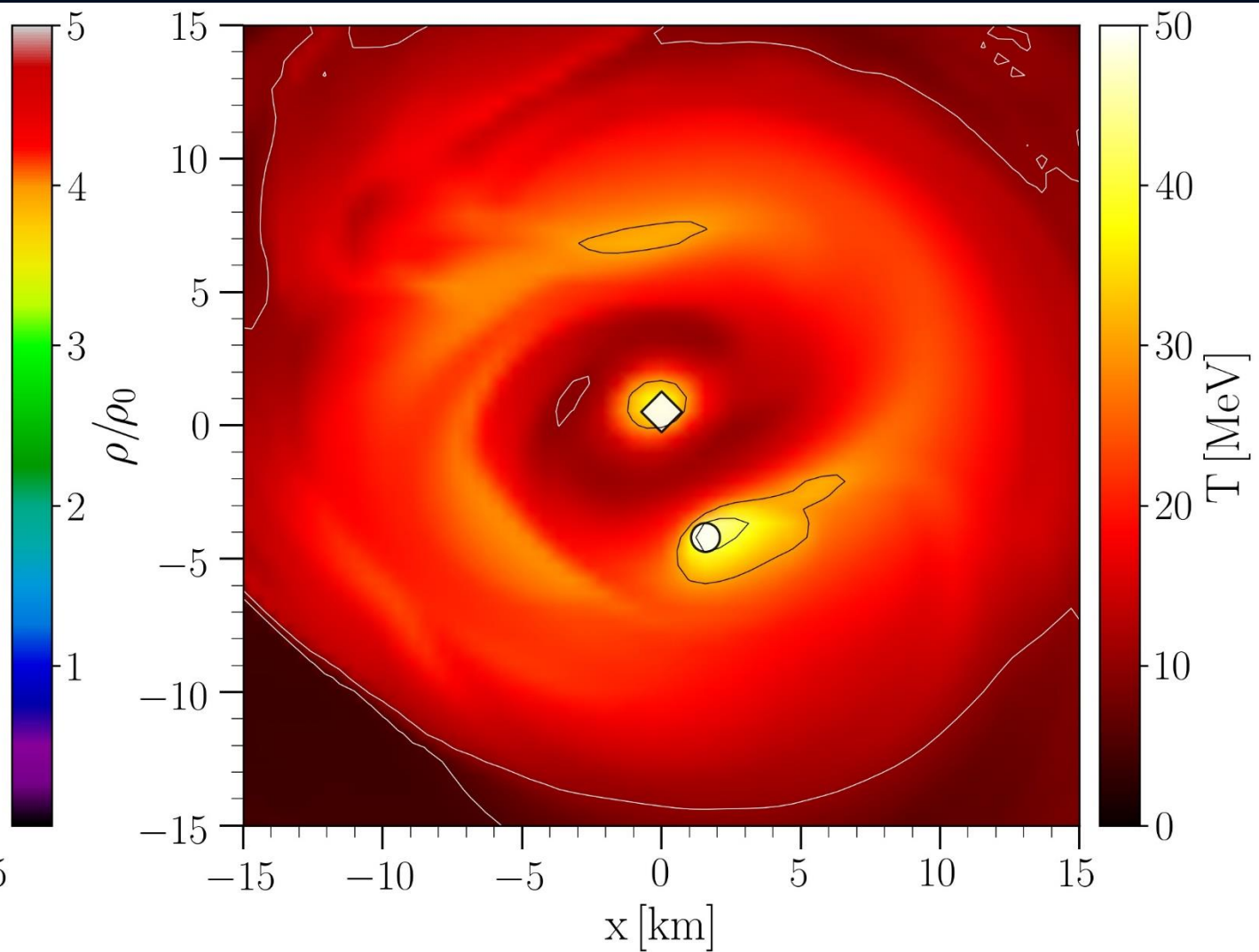
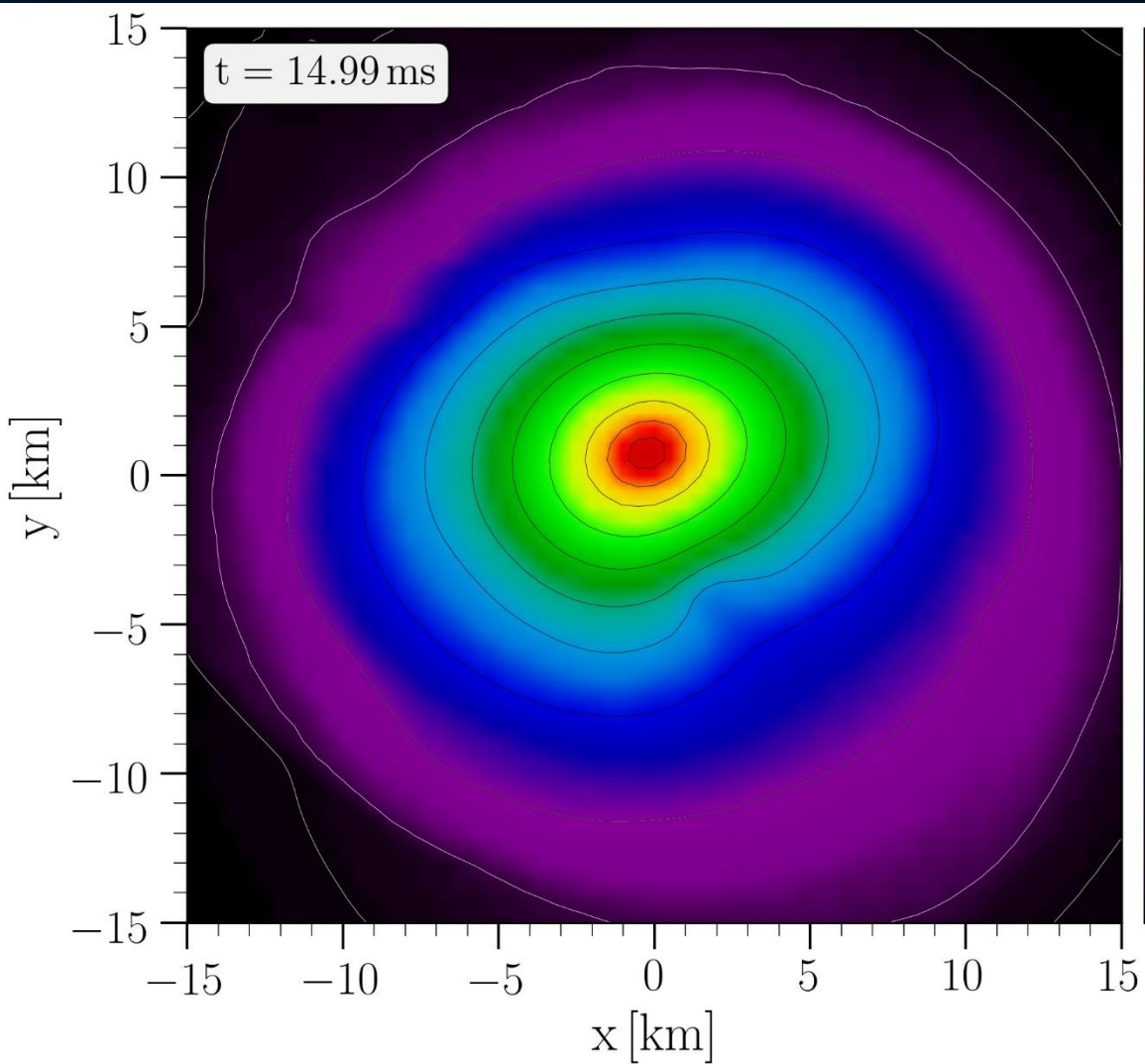


# Merger Phase



Rest mass density

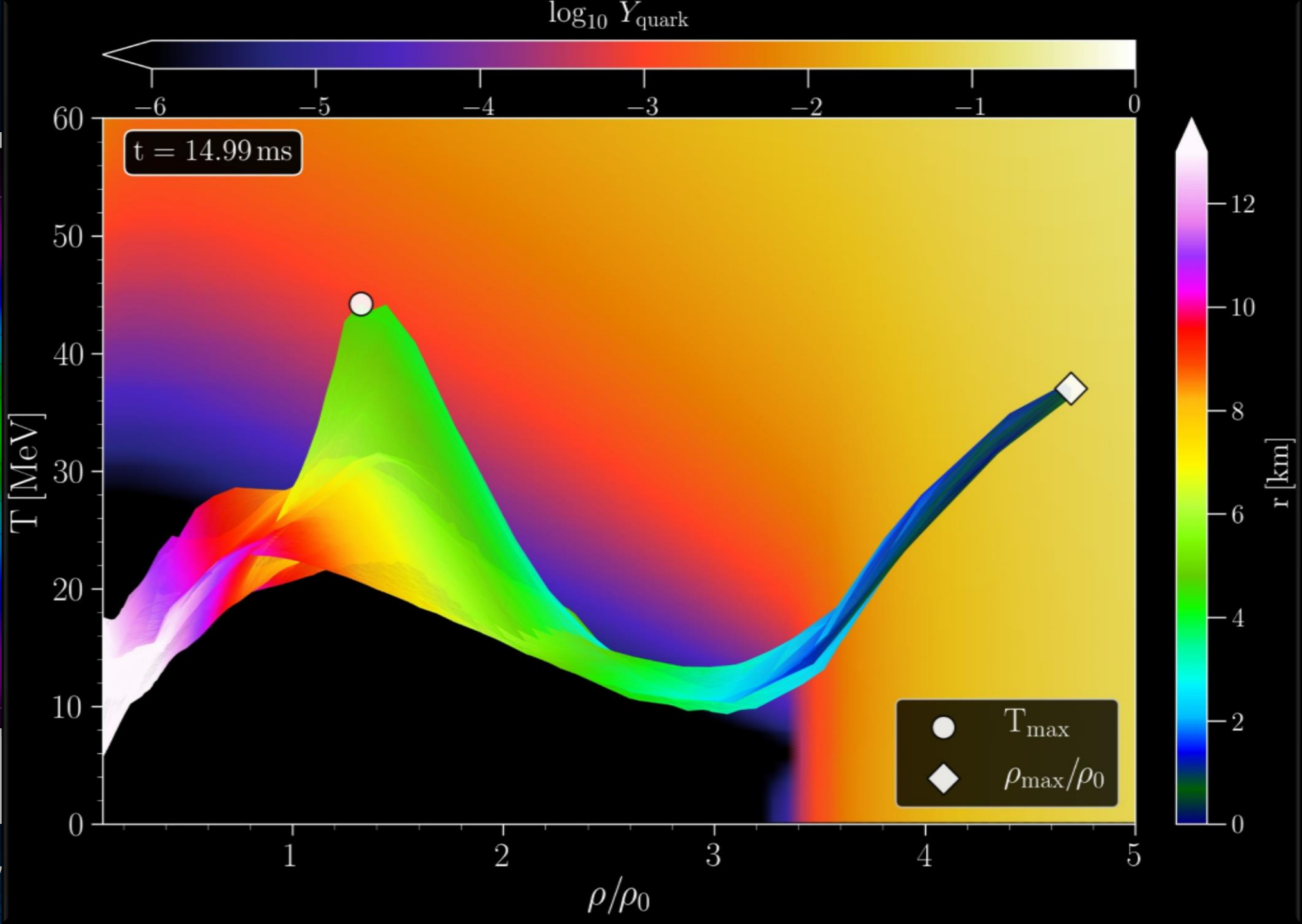
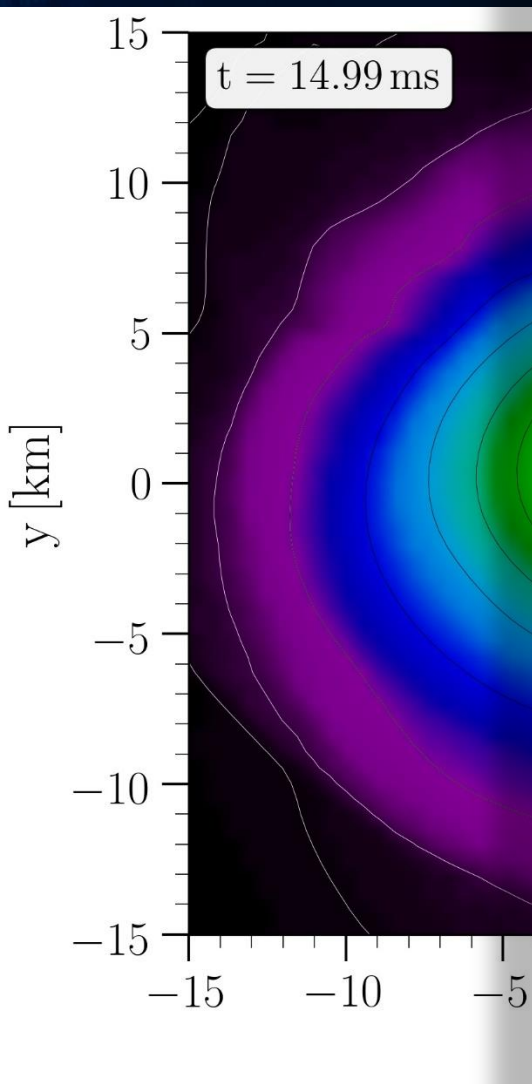
# Merger Phase



Rest mass density on the equatorial plane

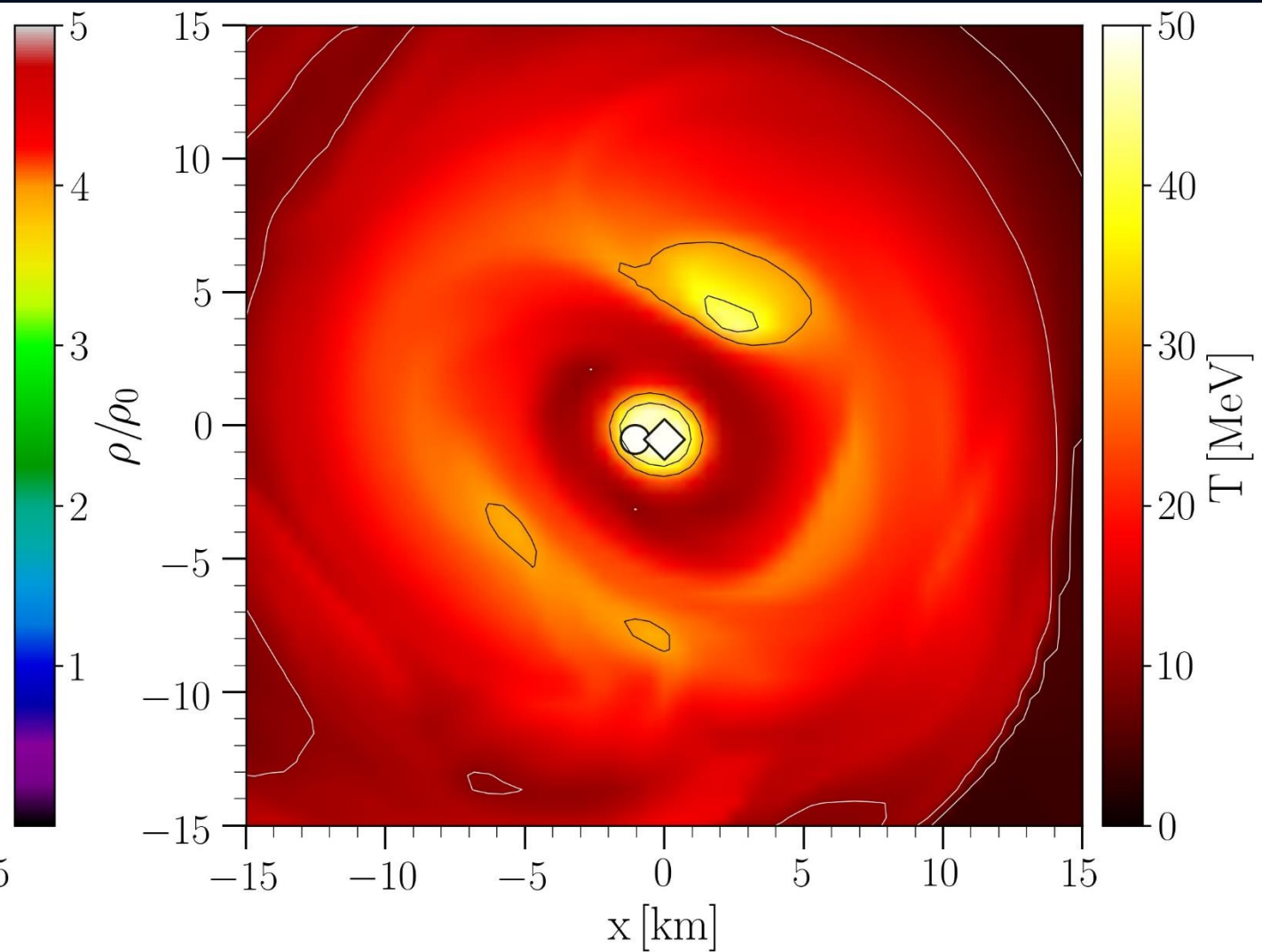
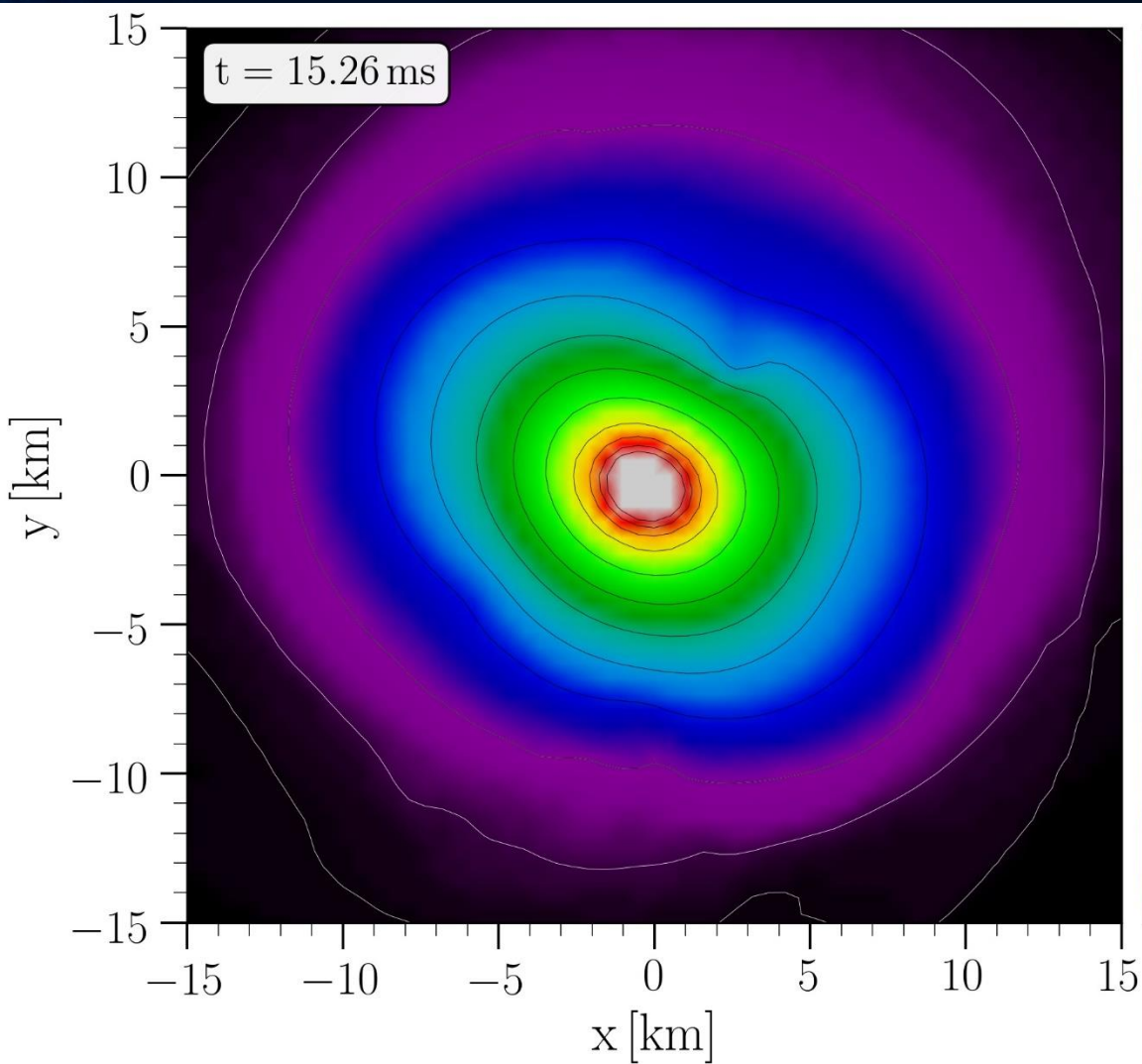
Temperature on the equatorial plane

# Merger Phase



Rest mass density

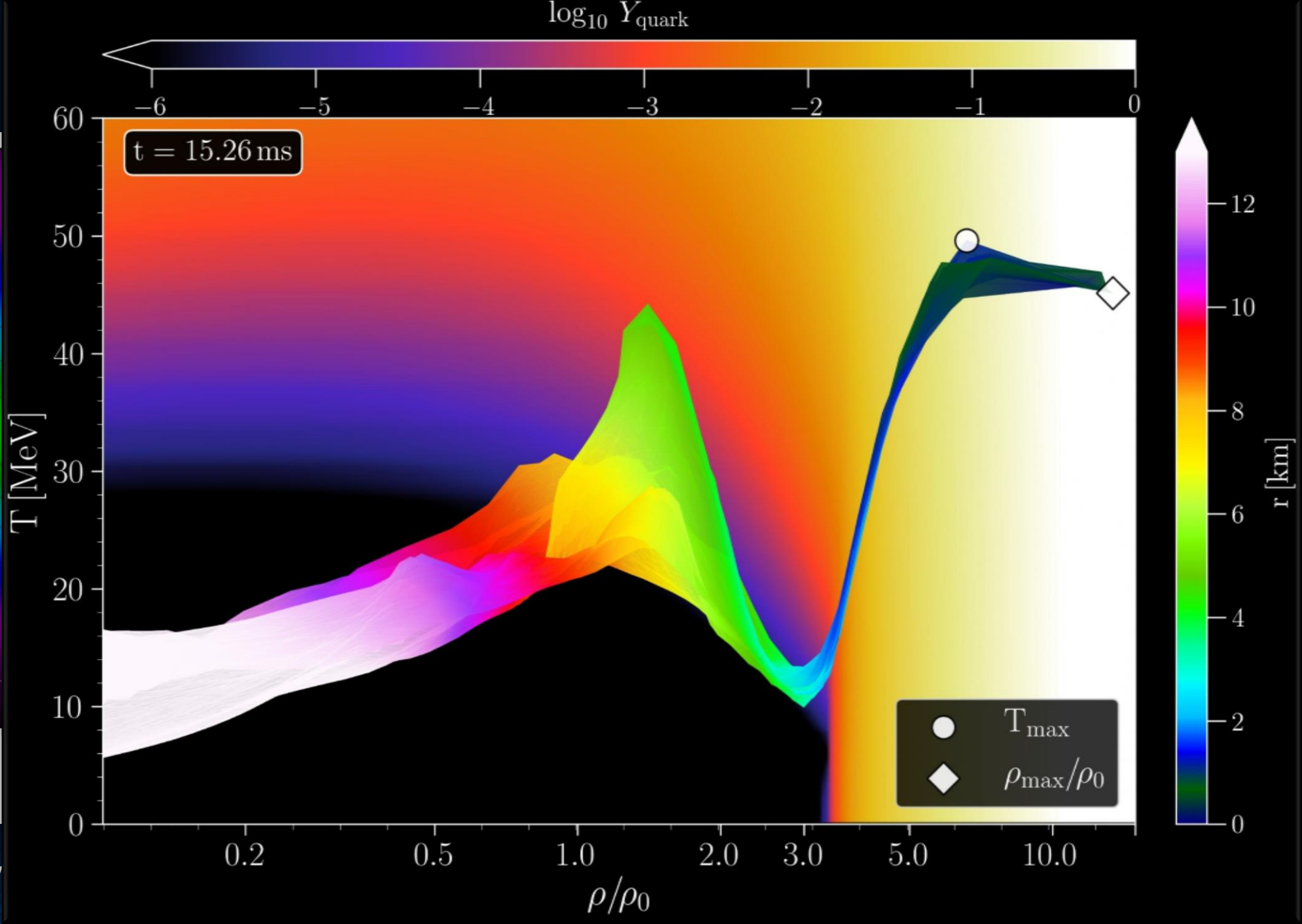
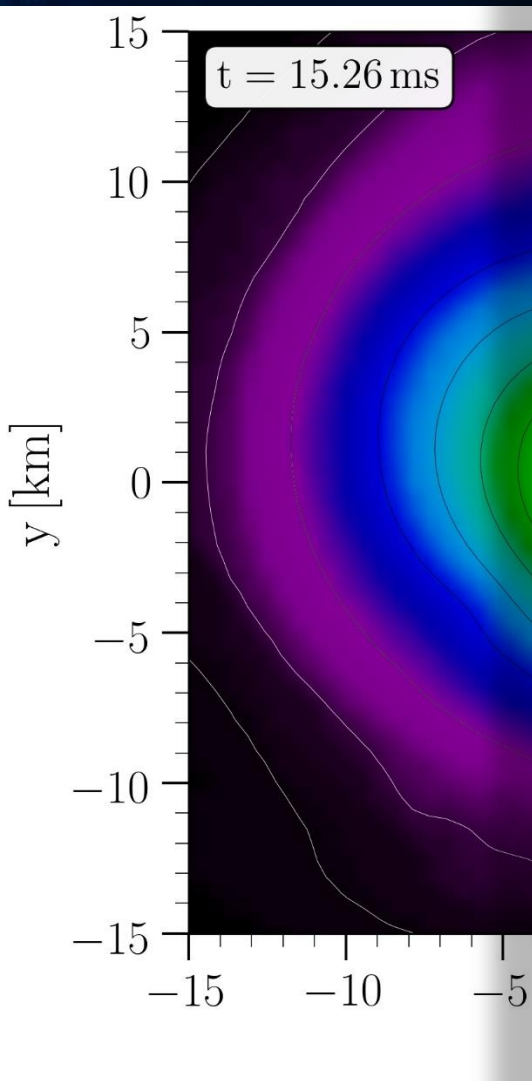
# Merger Phase



Rest mass density on the equatorial plane

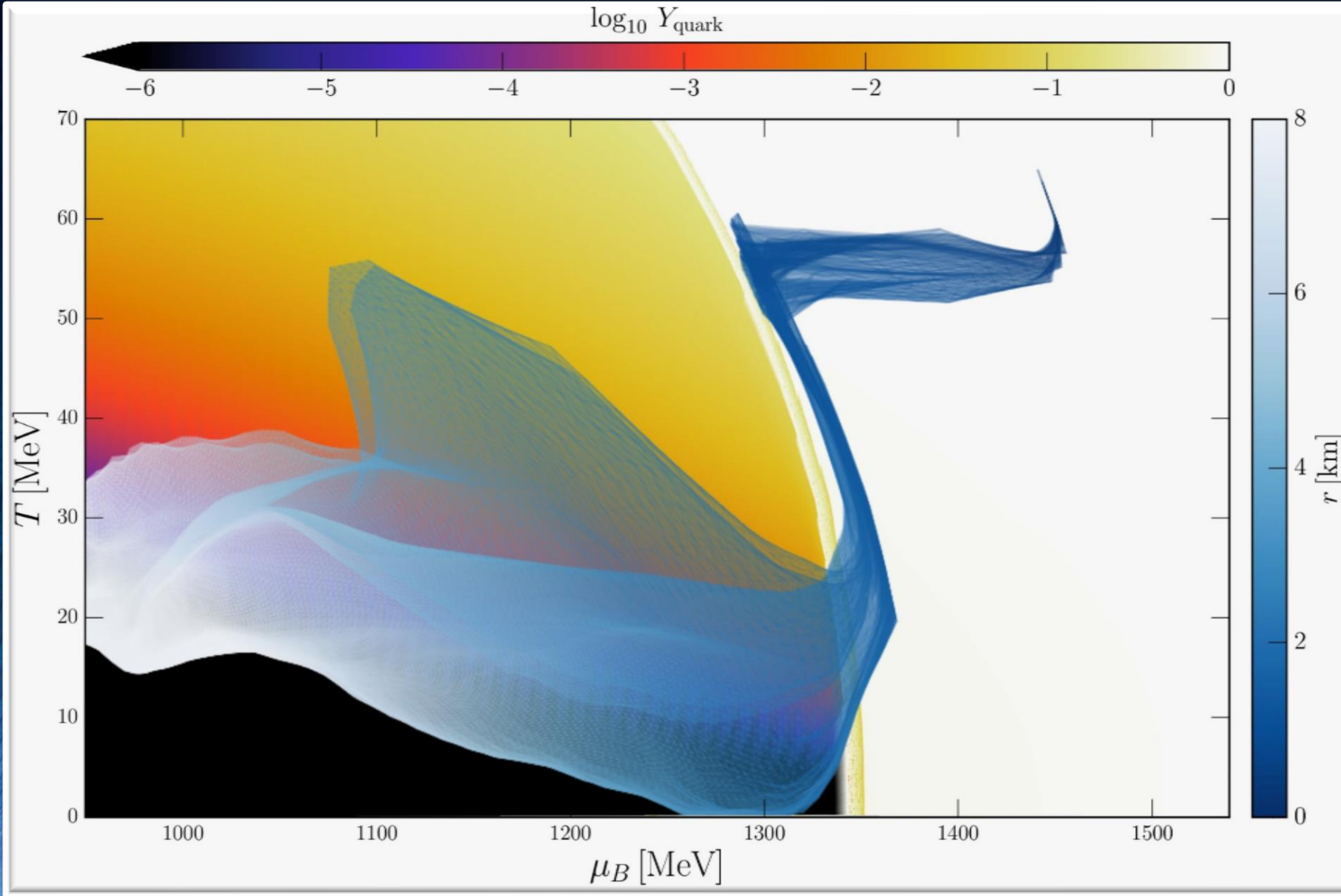
Temperature on the equatorial plane

# Merger Phase



Rest mass density

# The Pelican Plot



The shadowy blue image resembles the shape of a strange bird, e.g. a pelican, wherein the hot head of a pelican contains a high amount of strange quark matter, its thin neck follows the QCD phase boundary, while its hot wings (local temperature maxima) contain mostly hadronic matter at much lower densities.

The maximum temperature and density points correspond to the head of the pelican where pure strange quark is present. Due to the stiffening of the EOS in the pure quark phase, the temperature stops rising and the high pressure in the central region pushes against the huge gravitational force.

E. Most, J. Papenfort, V. Dexheimer, M. Hanauske, H. Stöcker and L. Rezzolla;  
„On the deconfinement phase transition in neutron-star mergers“, arXiv:1910.13893

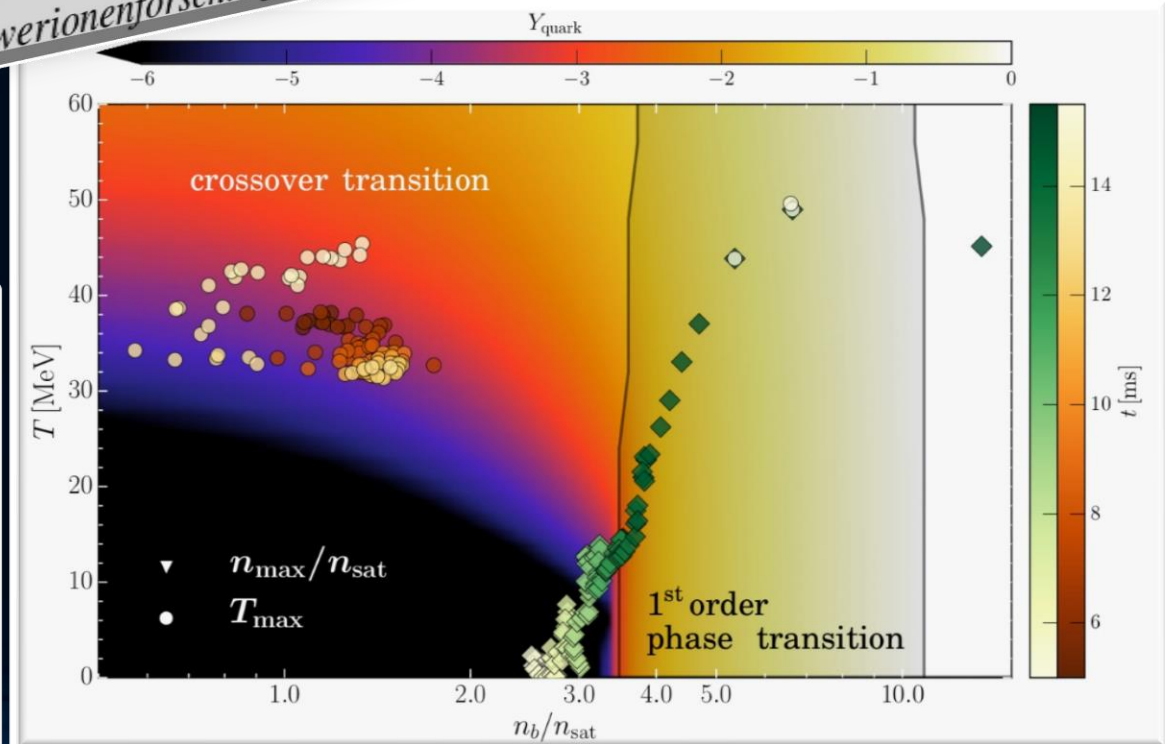
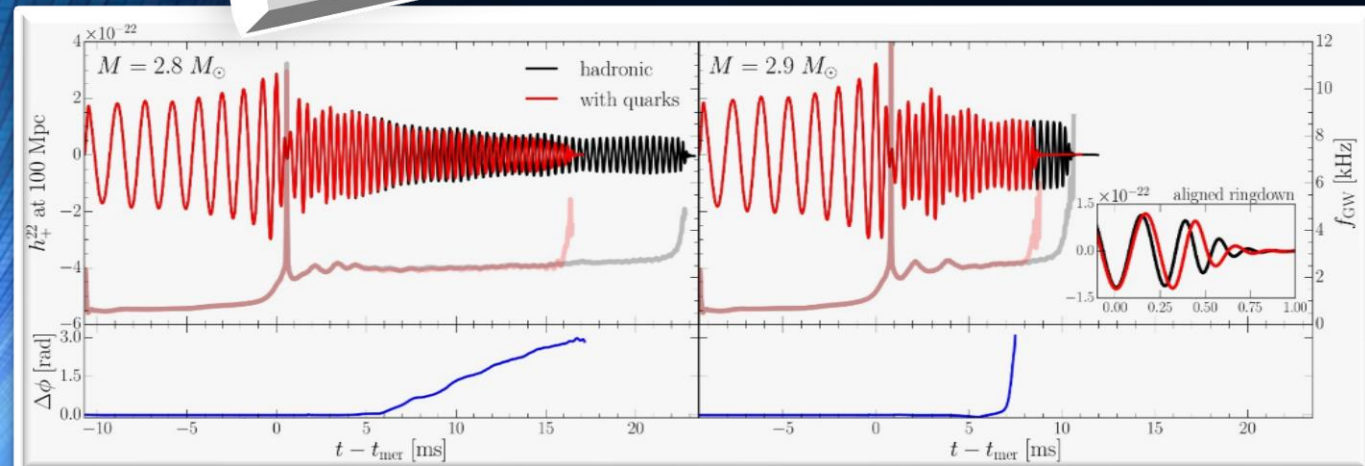
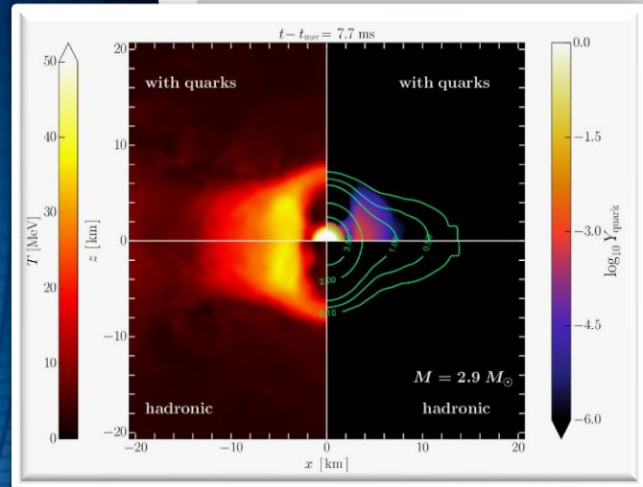


# Hybrid Star Mergers with T-dependent EOS (PRL paper 1)

## Signatures of quark-hadron phase transitions in general-relativistic neutron-star mergers

Elias R. Most,<sup>1</sup> L. Jens Papenfort,<sup>1</sup> Veronica Dexheimer,<sup>2</sup> Matthias Hanauske,<sup>1,3</sup>  
 Stefan Schramm,<sup>1,3</sup> Horst Stöcker,<sup>1,3,4</sup> and Luciano Rezzolla<sup>1,3</sup>

<sup>1</sup>Institut für Theoretische Physik, Max-von-Laue-Straße 1, 60438 Frankfurt, Germany  
<sup>2</sup>Department of Physics, Kent State University, Kent, OH 44243 USA  
<sup>3</sup>Frankfurt Institute for Advanced Studies, Ruth-Moufang-Straße 1, 60438 Frankfurt, Germany  
<sup>4</sup>GSI Helmholtzzentrum für Schwerionenforschung GmbH, 64291 Darmstadt, Germany



# Hybrid Star Mergers with T-dependent EOS (PRL paper 2)

## Identifying a first-order phase transition in neutron star mergers through gravitational waves

Andreas Bauswein,<sup>1,2</sup> Niels-Uwe F. Bastian,<sup>3</sup> David B. Blaschke,<sup>3,4,5</sup> Katerina Chatziioannou,<sup>6</sup> James A. Clark,<sup>7</sup> Tobias Fischer,<sup>3</sup> and Micaela Oertel<sup>8</sup>

<sup>1</sup>GSI Helmholtzzentrum für Schwerionenforschung, Planckstraße 1, 64291 Darmstadt, Germany  
<sup>2</sup>Institute for Theoretical Studies, Schloss-Wolfsbrunnengasse 35, 69118 Heidelberg, Germany  
<sup>3</sup>University of Wrocław, 50-205 Wrocław, Poland  
<sup>4</sup>Institute for Theoretical Physics, 115409 Moscow, Russia  
<sup>5</sup>Institute for Theoretical Physics, 111980 Dubna, Russia  
<sup>6</sup>National Research Center "Kurchatov Institute", Laboratory for Theoretical Physics, P.O. Box 39, 123182 Moscow, Russia  
<sup>7</sup>Center for Nuclear Studies, Georgia Institute of Technology, Atlanta, GA 30332, USA  
<sup>8</sup>Observatoire de Paris, Sorbonne Paris Cité, Sorbonne Université, Université de Paris, 91191 Gif-sur-Yvette, France

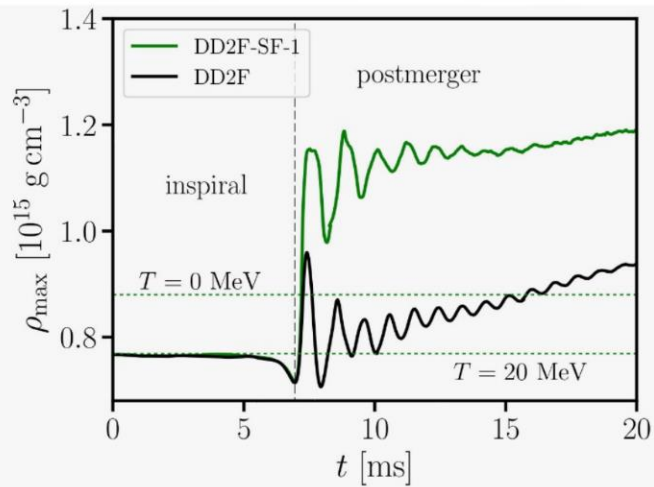


FIG. 1: Evolution of the maximum rest-mass density comparing DD2F-SF-1 (green) and DD2F (black) for  $1.35\text{-}1.35 M_{\odot}$  mergers (solid curves). Horizontal dotted green lines mark the onset density  $\rho_{\text{onset}}$  of the phase transition for DD2F-SF-1 at  $T = 0$  and at  $20$  MeV.

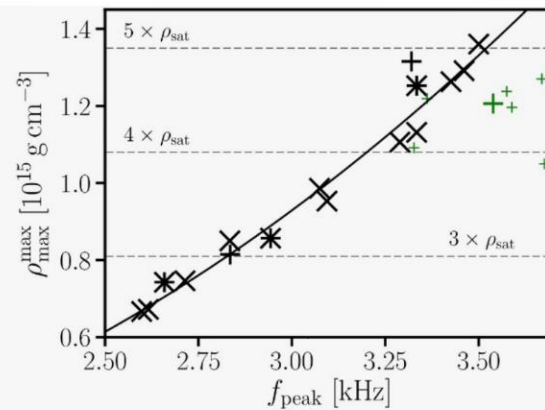


FIG. 4: Maximum rest-mass density  $\rho_{\text{max}}^{\text{max}}$  during the first milliseconds of the postmerger phase as function of the dominant postmerger GW frequency  $f_{\text{peak}}$  for  $1.35\text{-}1.35 M_{\odot}$  mergers. Green symbols display results for DD2F-SF (big symbol for DD2F-SF-1). Asterisks indicate models with hyperons. Black plus signs display ALF2/4. Solid curve is a second order polynomial least square fit to the data excluding hybrid EOSs.

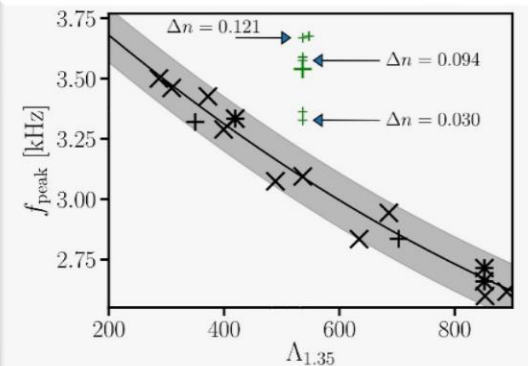


FIG. 3: Dominant postmerger GW frequency  $f_{\text{peak}}$  as function of tidal deformability  $\Lambda$  for  $1.35\text{-}1.35 M_{\odot}$  mergers. The DD2F-SF models with a phase transition to deconfined quark matter (green symbols) appear as clear outliers (big symbol for DD2F-SF-1). Solid curve displays the least square fit to Eq. (1) for all purely hadronic EOSs (including three models with hyperons marked by asterisks). ALF2 and ALF4 are marked by black plus signs. EOSs incompatible with GW170817 are not shown. Arrows mark DD2F-SF models 3, 6 and 7, which feature differently strong density jumps  $\Delta n$  (in  $\text{fm}^{-3}$ ) with roughly the same onset density and stiffness of quark matter.

# Literature

Plenary talk (Tuesday, 09:40) by Luciano Rezzolla:  
"Binary Neutron Stars: Einstein's richest laboratory"

Hanuske, Matthias, and Walter Greiner.

"Neutron star properties in a QCD-motivated model." *General Relativity and Gravitation* 33.5 (2001): 739-755.

Hanuske, Matthias. "How to detect the Quark-Gluon Plasma with Telescopes." *GSI Annual Report* (2003): 96.

Hanuske, M., Takami, K., Bovard, L., Rezzolla, L., Font, J. A., Galeazzi, F., & Stöcker, H. (2017). Rotational properties of hypermassive neutron stars from binary mergers. *Physical Review D*, 96(4), 043004

M. Hanuske, et.al., Connecting Relativistic Heavy Ion Collisions and Neutron Star Mergers by the Equation of State of Dense Hadron-and Quark Matter as signalled by Gravitational Waves, *Journal of Physics: Conference Series*, 878(1), p.012031 (2017)

Hanuske, Matthias, et al. "Gravitational waves from binary compact star mergers in the context of strange matter." *EPJ Web of Conferences*. Vol. 171. EDP Sciences, 2018.

Mark G. Alford, Luke Bovard, Matthias Hanuske, Luciano Rezzolla, and Kai Schwenzer (2018), Viscous Dissipation and Heat Conduction in Binary Neutron-Star Mergers. *Phys. Rev. Lett.* 120, 041101

Hanuske, Matthias, and Luke Bovard. "Neutron star mergers in the context of the hadron-quark phase transition." *Journal of Astrophysics and Astronomy* 39.4 (2018): 45.

Hanuske, Matthias, et al. "Neutron Star Mergers: Probing the EoS of Hot, Dense Matter by Gravitational Waves." *Particles* 2.1 (2019): 44-56.